Identifications of Potential Structural Contributors for Effective Inhibition of HDAC9: An Emerging Target of Cancer and Other Diseases

Submitted by

Totan Das

EXAM ROLL NO: M4PIP24002
CLASS ROLL NO: 002211402052
REG. NO:163692 of 2022-2023
Department of Pharmaceutical Technology

Jadavpur University

Session- 2022-2024

Under The Guidance Of

Dr. Shovanlal Gayen

Laboratory of Drug Design and Discovery
Department of Pharmaceutical Technology
Jadavpur University, Kolkata-700032

Thesis submitted in partial fulfillment of the requirements for the Degree of Master of Pharmacy
Department of Pharmaceutical Technology
Faculty of Engineering and Technology
Jadavpur University, Kolkata

Jadavpur University

Jadavpur, Kolkata-700032

CERTIFICATE OF APPROVAL

This is to certify that ***Totan Das*** (Exam Roll No. M4PIP24002, Reg. No. 163692 of 2023-2024) has sincerely carried out the research work on the subject entitled ***"Identifications of potential structural contributors for effective inhibition of HDAC9, an emerging target of cancer and other diseases"*** under the supervision of **Dr. Shovanlal Gayen**, Laboratory of Drug Design and Discovery, Department of Pharmaceutical Technology of Jadavpur University. He has incorporated his findings in this thesis he submitted in partial fulfillment of the requirements for the degree of **Masters of Pharmacy** (Pharmaceutical Technology) of Jadavpur University. He has carried out the research work independently and sincerely with proper care and attention to our satisfaction.

29/8/24

Head
Dept. of Pharmaceutical Technology
Jadavpur University
Kolkata - 700 032, W.B. India

Head of the Department
Department of Pharmaceutical Technology
Jadavpur University
Kolkata-700032

Shovanlal Gayen 29.8.24

Dr. Shovanlal Gayen
Laboratory of Drug Design and Discovery
Jadavpur University
Kolkata-700032
Department of Pharmaceutical Technology

DR. SHOVANLAL GAYEN
Assistant Professor
Dept. of Pharmaceutical Technology
Jadavpur University
Kolkata - 700 032, INDIA

Dipak Laha 29.8.24

Dean
Faculty of Engineering and Technology
Jadavpur University
Kolkata-700032

DEAN
Faculty of Engineering & Technology
JADAVPUR UNIVERSITY
KOLKATA-700 032

Acknowledgment

The outcome of this thesis required a lot of guidance and assistance from many people. I am extremely fortunate to have had these all along the completion of my work. Whatever I have done is only due to such guidance and assistance and I would not forget to thank them.

I am highly obliged and like to express my deep gratitude and profoundness to my reverend mentor **Dr. Shovanlal Gayen** of the Department of Pharmaceutical Technology, Jadavpur University, Kolkata for his excellent and constant guidance and help, endless encouragement, thoughtful and freedom and stupendous cooperation throughout the term paper till its successful completion. I am greatly indebted to his motivation, fruitful suggestions, and inspiration.

I owe my deep respect to **Prof. Amalesh Samanta**, Head of the Department, Department of Pharmaceutical Technology, Jadavpur University, Kolkata for all the necessary help and encouragement. I would like to convey my sincere gratitude to AICTE and Jadavpur University for their financial and equipment support for my M. Pharm course.

I would like to thank **Prof. Tarun Jha**, Natural Science Laboratory, Jadavpur University, Kolkata for the continuous encouragement, necessary help, and support to perform my work.

I express my sincere thanks to **Prof. Tapan Kumar Maity, Prof. Kunal Roy, Dr. Probir Kumar Ojha, Dr. Emdad Hossain, and Dr. Nilanjan Adhikari** sir for their cooperation, help, and support.

I am extremely grateful to **Ms. Samima Khatun, Mr. Sourav Sardar,** and **Mr. Arijit Bhattacharya** for their guidance and support which assisted me in gathering knowledge about the different aspects of this work. I would express my sincere thanks to my laboratory colleague **Mis. Rinki Prasad Bhagat** and my juniors **Mr. Indrasis Das Gupta** and **Biplab Das** from the Laboratory of Drug Design and Discovery**,** Department of Pharmaceutical Technology, Jadavpur University, Kolkata-700032.

I express my wholehearted thanks to my friends **Sai Satyaprakash Mishra, Abhisek Samal, Souptick Barmon, Mamani Sahoo Barmon**, and **Aniruddha Barik** for always being there and motivating me.

Finally, I would like to express my deep respect to my father **Mr. Shudhanshu Das**, my mother **Mrs. Sadhana Das**, and my friends for their continuous help, love, encouragement, and moral support throughout my work.

Finally, I would like to thank one and all who were directly or indirectly there to help me with the successful completion of my thesis, as well as express my apology that I could not mention personally.

Totan Das.

[Totan Das]

Date: 29.08.2024

Place: Department of Pharmaceutical Technology, Jadavpur University

Kolkata

India.

Declaration of Originality and Compliance of Academic Ethics

I hereby declare that this thesis contains a literature survey and original research work performed by me **(Totan Das)** as a part of my Master of Pharmacy studies. All the information in this document has been obtained and presented according to academic rules and ethical conduct. I also declare that, as required by these rules and conduct, I have cited and referenced the materials and results that are not original to this work.

Name: Totan Das

Exam Roll Number: M4PIP24002

Class Roll Number: 002211402052

Registration Number: 163692 *of 2021-2023*

Thesis Title: "Identifications of potential structural contributors for effective inhibition of HDAC9, an emerging target of cancer and other diseases".

Totan Das
29.08.2024

Signature with Date ***(Totan Das)***

Dedicated to

My Parents, Teachers, Seniors and Friends

Contents **Page No.**

Preface

For several decades, "Cancer" has been a serious human threat to mankind, which is defined as a group of pathological conditions characterized by uncontrolled and abnormal cell proliferation. In recent times, it ranks among the prime reasons for mortality, with an exponentially increasing number of individuals affected globally. Moreover, the expensive and painful treatments required for cancer patients pose a substantial threat to both our society and economy. The onset and proliferation of cancer cells result from both internal and external factors. Numerous external factors, such as pollution, inadequate nutrition, radiation exposure, and lifestyle choices, contribute to alterations in the biological system, alongside internal factors like genetic mutations and irregular hormone regulation.

Histone deacetylase 9 (HDAC9) is a class IIa and stands out as a crucial member of the HDAC family. The activity of HDAC9 primarily depends on tissue-specific gene expression, the recruitment of critical cofactors, and nucleo-cytoplasmic shuttling. It is involved in several pathological and physiological conditions related to various diseases, encompassing HDAC9 as an appealing target for cancer, diabetes, and several other metabolic diseases. By altering histone acetylation at target genes, it has also been linked to lipid metabolism, atherosclerosis development, and macrophage polarisation. Furthermore, HDAC9 has been discovered as a significant risk factor for peripheral artery disease, myocardial infarction, and coronary artery disease.

Additionally, the quantitative structure-activity relationship (QSAR) methodology quantifies the biological activity of molecules about their molecular structure through the development of mathematical correlation to predict the key structural factors influencing the activity of these compounds. As a result, a comparative molecular modeling technique is used in this study to examine a set of reported HDAC9 inhibitors that have a wide range of inhibitory activity and contain the hydroxamate group as the zinc-binding motif.

The goal of this study is to find the significant structural fingerprints of the HDAC9 inhibitors that are essential for controlling inhibitory activity. Bayer's theorem is used in Bayesian classification QSAR studies, that utilize probability function. The recursive partitioning modeling is a non-linear classification-based QSAR approach that employs the chemical properties of compounds to generate a decision tree to differentiate these molecules in a binary fashion. Some of the important fingerprints of HDAC9 inhibitors regulating the activity have been discovered in this work. In addition, the molecular docking study was processed for

generating the protein-ligand complex which identified some potential amino acid residues for the binding interactions. Finally, the molecular dynamics study establishes the compounds' stability inside the core of the HDAC9 receptor.

(Totan Das)

LIST OF FIGURES

LIST OF TABLES

1. Introduction

1. Introduction

Epigenetic alterations affect DNA and histone structures, making them crucial for gene control. HDACs remove acetyl groups from lysine residues at the amino terminus of histones as seen in **Figure 1** (Vaissière *et al*., 2008). HDACs primarily contribute to gene silence by condensing chromatin into a transcriptionally suppressed shape. Recent studies have found non-histone HDAC targets, including cytoplasmic and nuclear proteins (Nicolas *et al*., 2007). HDACs control cellular processes such as proliferation, differentiation, migration, and cell death by targeting both histone and non-histone targets. Recent research indicates that changing HDAC activity can lead to cancer in humans by affecting the acetylation of key oncogenic and tumor suppressor proteins (Clocchiatti *et al*., 2011).

HDACs are classified into five classes based on their similarity to the original yeast enzyme sequences. HDACs are classified into three types: class I (HDAC1, HDAC2, HDAC3, and HDAC8), class IIa (HDAC4, HDAC5, HDAC7, and HDAC9), and class IIb (HDAC6, HDAC10). Class III HDACs consist of sirtuins 1-7, which rely on NAD+. The single HDAC in class IV is HDAC11 (Yang *et al*., 2005).

HDAC9 is a class IIa HDAC and it have a conserved C-terminal catalytic domain with limited deacetylase activity and an N-terminal regulatory region that helps them interact with transcription factors (Yang *et al*., 2005). Class IIb HDACs differ from class IIa HDACs due to the presence of duplicated domains. Class IIa HDACs are larger (120-135 kDa) than other zinc-dependent HDACs and have a unique ability to shuttle nucleo-cytoplasm (Milazzo *et al*., 2020). Class II HDACs have both a nuclear export signal (NES) and a nuclear localization signal (NLS), allowing them to move between the nucleus and cytoplasm (Milazzo *et al*., 2020). Asfaha *et al*. reviewed the structural properties of class IIa HDACs and their regulatory actions (Asfaha *et al*.,2015). Class IIa HDACs' nucleo-cytoplasmic trafficking is mostly determined by their phosphorylation status. Parra and Verdin *et al*. examined the kinases and phosphatases responsible for the nucleocytoplasmic location of class IIa HDACs (Para *et al*.,2010). DiGiorgio *et al*. recently evaluated the significance of posttranslational changes, including as ubiquitination, sumoylation, acetylation, and proteolytic cleavage, in regulating class IIa HDAC activity (Di Giorgio *et al*., 2015).

Class IIa HDACs inhibit gene transcription in several tissues (Di Giorgio *et al*., 2015). Their action relies on tissue-specific gene expression, cofactor recruitment, and nucleo-cytoplasmic shuttling. They also need the development of multiprotein complexes at their respective C-

termini. HDAC3, also known as the nuclear receptor co-repressor (N-CoR), and mammalian SIN3 transcription regulator family member A (SIN3A) is part of a complex that silences retinoid and thyroid receptors (Clark *et al*., 2015). Chromosome 7p21.1 contains the human HDAC9 gene, which encodes many different protein isoforms. Exons 2–26 include a sequence that codes for 1,069 amino acids, which make up the full-length HDAC9 protein (exon 1 is untranslated). One example of a well-characterized shortened splice variant of HDAC9 is an ortholog of Xenopus myocyte enhancer-binding factor 2-interacting transcriptional repressor (MITR), also referred to as histone deacetylase-related protein (HDRP) (Brancolini *et al*., 2021). The length of human MITR is 590 amino acids, and it lacks a catalytic domain. It is mostly made up of the 450–600 amino acid noncatalytic N-terminal region of HDAC9, which is shared by several class IIa HDACs (Brancolini *et al*., 2021).

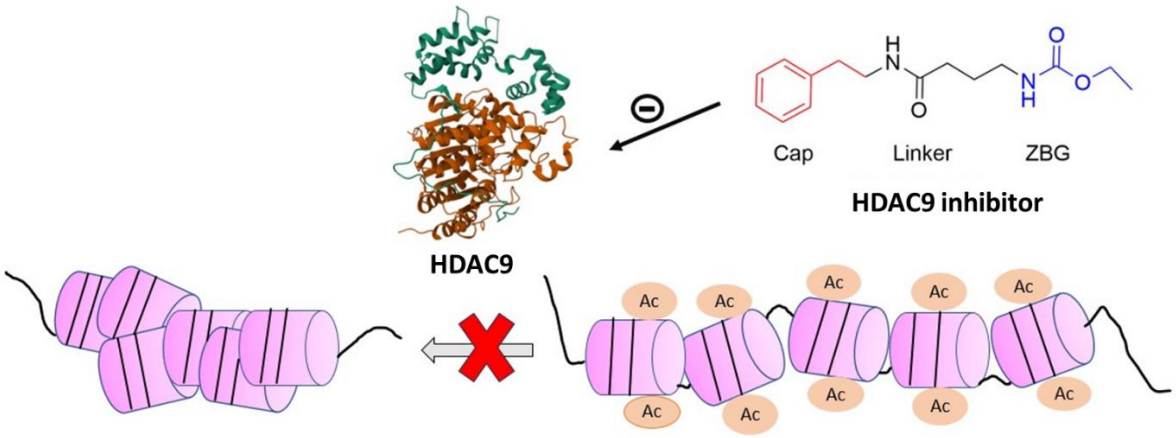

Figure 1: Deacetylation of Histone protein inhibited by HDAC9 inhibitors

There are transcripts encoding HDAC9 in the brain, skeletal muscle, colon, thymus, spleen, kidney, placenta, lung, bone marrow, fetal brain, and fetal liver, and they are expressed at different levels in many normal human tissues and cell lines (Yang *et al*., 2021). Although HDAC9 is abundantly expressed in the brain and skeletal muscles, it is very sometimes or never identified in the heart. In the human heart, brain, and skeletal muscle, the HDAC9 homolog MITR is expressed at similar levels; in the placenta, lung, liver, kidney, and pancreas, it is expressed at extremely low levels (Yang *et al*., 2021). HDAC9 and MITR are specifically expressed in lymphoid and monocytic cells of the hematopoietic system. The mouse brain's hippocampus, cerebral cortex, basolateral amygdaloid nuclei, and choroid plexus all have significant levels of HDAC9 expression. HDAC9 is only expressed in mature and post-mitotic

neurons; it is not present in adult neural stem cells, glia cells, astrocytes, or oligodendrocytes (Lang *et al*., 2012).

The expression of MTR was investigated and the developing embryos and adult tissues of several Xenopus frogs. They discovered that whereas MITR was expressed in mature somite at the neurula stage of early embryogenesis, it was exclusively expressed in muscle tissue in later developmental stages (Xie *et al*., 2019). MITR was found in adult tissues at relatively low concentrations in the heart, lung, skeletal system, stomach, gall bladder, and spleen.

The expression patterns of MTR in mouse tissues differ markedly from those in Xenopus tissues. Particularly, MITR expression is extremely low in the lungs, liver, skeletal muscles, and kidneys of adult mice, but it has been found in the mouse heart, brain, and skeletal muscle during embryogenesis and at high levels in the heart, brain, and spleen of mature mice (Zhang *et al*., 2001).

1.2. Physiological Role and Target of HDAC9

Many studies have shown that HDAC9 controls a broad range of physiological reactions and many targets (shown in **Figure 2**) (Glaser *et al*., 2007). Research using transgenic (TG) and HDAC9 KO (knockout) mice indicates that HDAC9 is essential for myocyte and adipocyte differentiation as well as cardiac muscle development (Zhou *et al*., 2014). HDAC9 has been linked to several functions, including immune system support, metabolic regulation, and nervous system protection. According to a recent study by Hu *et al*. and Brancolini *et al*., HDAC9-mediated immunological and metabolic dysregulations have been related to pathological processes associated with human disorders (Hu *et al*., 2019, Brancolini *et al*., 2021). The discussion that follows will concentrate on how we now understand HDAC9's activity and potential roles in several critical physiological processes.

HDAC9 may be involved in the formation of the heart since it is expressed in the interventricular septum and growing cardiac chambers throughout embryogenesis (Glaser *et al*., 2007). Despite the absence of obvious morphological abnormalities in HDAC9 KO mice (note that homozygous mutants lack functional HDAC9 or MITR proteins), reports of brain and neurological impairments have been made (Volpatti *et al*., 2022). Mice lacking HDAC9 experience cardiac hypertrophy as they become older and in reaction to high heart pressure.

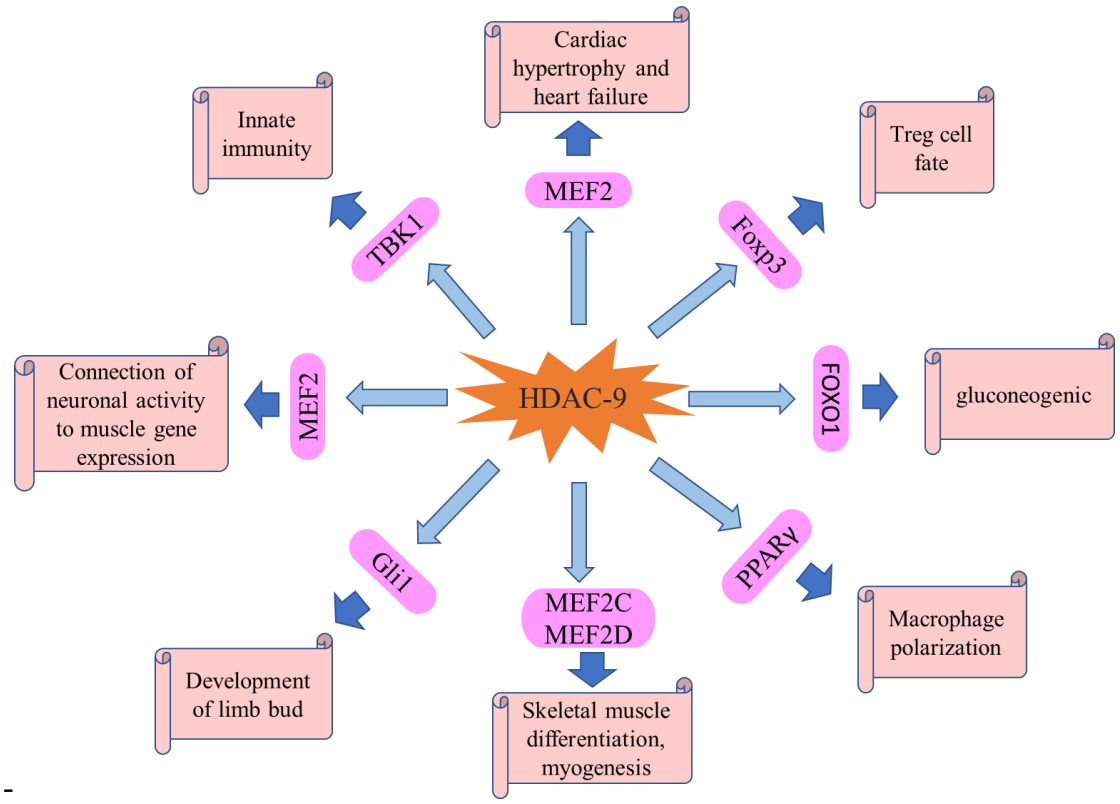

Figure 2: Various targets of HDAC9 and related physiological role

Additionally, they exhibit hypersensitivity to hypertrophy induced by calcineurin. Several cardiovascular illnesses have higher morbidity and death rates when there is cardiac hypertrophy. MITR is the primary form of HDAC9 produced in the heart and can efficiently suppress fetal gene expression (Mejat *et al.*, 2005). Mechanistically, MITR inhibits the acetylation of fetal gene promoters, hence blocking signals that encourage cardiac hypertrophy. The super-activation of MEF2 activity in HDAC9 KO mice, which is calcineurin-mediated, implies that MEF2 is an in vivo downstream target of HDAC9 (Zhang *et al.*, 2001). According to these results, MITR and HDAC9 are essential regulators of the hypertrophic signaling pathways. Maternally expressed gene 3, or MEG3 is a long noncoding RNA (lncRNA) that has been studied by Zhang *et al*. about the development of cardiac hypertrophy (Zhang *et al.*, 2019). They discovered that MEG3 upregulates HDAC9 expression by competing with miR-361-5p binding, which aids in the development of heart hypertrophy. Thus, HDAC9 functions as a negative regulator of the gene expression program in muscles.

Similar to HDAC9, MEF2 factors—most notably MEF2C and MEF2D—have a similar pattern of high expression in skeletal and cardiac muscle (Potthoff *et al.*, 2007). MEF2 is a strong activator of the HDAC9 promoter and can directly increase HDAC9 expression in skeletal muscle. By forming corepressor complexes, HDAC9 interacts with MEF2 proteins to limit

their transcriptional activity (Haberland *et al*., 2009). Thus, HDAC9 functions as a negative regulator of the gene expression program in muscles.

After birth, HDAC9 may suppress activity-dependent genes in skeletal muscle since the denervation of HDAC9 KO mice has been shown to enhance the expression of several genes (Moresi *et al*., 2010). Mejat *et al*. discovered, for instance, that in response to denervation, HDAC9 was downregulated, which raised chromatin acetylation and acetylcholine receptor (AchR) expression (Mejat *et al*., 2005). In mouse skeletal muscle, denervation-induced histone H3 hyperacetylation and inhibition of MEF2 transcriptional activity are mitigated by MITR through interactions with both HDAC1 and HDAC3. In denervated muscle, forced production of MITR inhibits chromatin acetylation and activity-dependent gene repression (Cohen *et al*., 2007). Therefore, through its interaction with MEF2, MITR may be able to influence the activity-dependent regulation of genes related to skeletal muscle by causing histone H3 deacetylation at the promoter of its target genes (Tang *et al*., 2006).

Since HDAC9 is exclusively produced in mature and postmitotic neurons in the adult nervous system, HDAC9 may be essential for preserving neuronal function in the mature brain (Cho *et al*., 2014). Research concentrating on the neuropathology of schizophrenia has particularly linked HDAC9's neuronal protective function (Cho *et al*., 2014). For instance, hemizygous deletions of HDAC9 have been found in a tiny percentage of individuals with schizophrenia. Moreover, decreased expression of MITR and HDAC9 in central nervous system-derived cells causes the death of neurons (Cacabelos *et al*., 2019). Zhang *et al*. showed that MITR participates in direct interactions that enable it to prevent AES-induced neuronal cell death and that AES (amino enhancer of split, a member of the Groucho family of transcriptional repressors) promotes neuronal apoptosis (Zhang *et al*., 2019).

Mice lacking HDAC9 have an additional hallux on their right hind foot in addition to post-axial polydactyly (Morrison *et al*., 2008). A key regulator of digit development is the morphogenic signaling protein Shh (sonic hedgehog), and polydactyly is caused by enhanced Shh-mediated signaling in the developing limb bud (Tickle *et al*., 2017). In tissues taken from the foot of perinatal HDAC9 KO mice, the transcription factor Gli1 (glioma-associated oncogene homolog 1) is significantly expressed and functions as a downstream modulator of Shh signaling. According to Morrison *et al*. MTR controls Gli1 negatively upstream in the Shh-mediated signaling cascade (Morrison *et al*., 2008). Therefore, the hyper-activation of the Shh pathway caused by the lack of HDAC9 may account for the polydactyly seen in these mice.

1.2. Role of HDAC9 in Cancer

HDAC9 may have many functions in carcinogenesis, according to recent research. Upregulated HDAC9 expression is seen in several neoplastic tissues, and it interacts with transcriptional repressors and oncogenic proteins involved in carcinogenesis (shown in **Figure 3**) (Patra *et al*., 2023). HDAC9 may influence anti-tumor immune responses by reducing CD8+ DC and T cell infiltration in the tumor microenvironment. HDAC9's role in cancer has been extensively explored internationally. Research suggests that abnormal HDAC9 expression is associated with certain tumors and transcription factors (Ning *et al*., 2020).

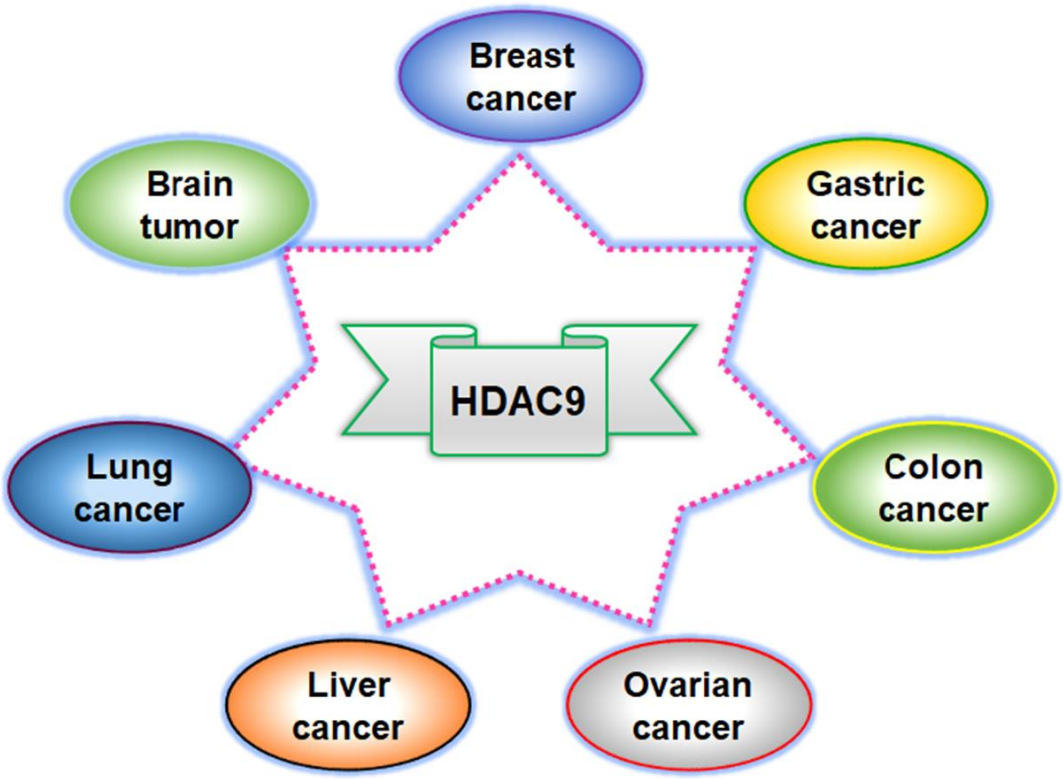

Figure 3: HDAC9 linked with various cancer diseases

❖ **Breast Cancer**

Bera *et al*. discovered that individuals with recurrent triple-negative breast cancer (TNBC) had considerably greater HDAC9 levels in their blood samples compared to nonrecurrent patients (Bera *et al*., 2020). TNBC cells do not express estrogen receptors (ERs), progesterone receptors, or HER2. TNBC is a very aggressive type of breast cancer with a poor prognosis. HDAC9 expression may be a useful diagnostic for detecting recurring cases (Chen *et al*., 2009). TNBC tissues showed higher levels of HDAC9 expression compared to non-TNBC patients. Inhibiting HDAC9 reduces TNBC cell invasiveness and prevents tumor angiogenesis in vivo.

miR-206 is downregulated in both TNBC cell lines and tumor tissues (Chen *et al*., 2009). miR-206 inhibits TNBC cell invasion and angiogenesis by suppressing the expression of VEGF, MAPK3, and SOX9. Inhibiting HDAC9 in TNBC cells leads to higher expression of miR-206 and lower levels of VEGF and MAPK3. HDAC9 suppresses miR-206 expression, potentially contributing to TNBC invasiveness and angiogenesis (Salgado *et al*., 2018). Human BC cell lines, including MCF-7 and BT474, showed increased HDAC9 expression. A study indicated that high levels of HDAC9 were linked to a poor prognosis in Chinese female breast cancer patients (Rahmani *et al*., 2021). This study found a correlation between HDAC9 expression levels, lymph node metastases, and TNM stage. In vitro investigations show that downregulating HDAC9 in BC cells reduces proliferation, migration, and invasion (Garmpis *et al*., 2022).

HDAC9 is overexpressed in both aggressive human BC cell lines and basal cells, including HCC1937, SUM149, MDA231, MDA436, Hs578T, BT549, and HBL100, compared to luminal cells (Yang *et al*., 2021). Lapierre *et al*. analyzed a cDNA array dataset encompassing mRNA profiles from 184 cancer patients, with findings presented in a public dataset (GSE2250). Their findings indicated higher HDAC9 expression in basal tumor cells (Lapierre *et al*., 2016). HDAC9 expression connected with SOX9 expression and predicted a bad prognosis. Exogenous HDAC9 expression in MCF-7 cells led to enhanced proliferation and reduced apoptosis. This was associated with dysregulated expression of cell cycle and apoptosis regulators such as cyclin-dependent kinase inhibitor 1A, BAX, and TNF receptor superfamily member 10a (Sher *et al*., 2022).

Paclitaxel, a microtubule inhibitor, is presently the most commonly used therapy for TNBC. Lian *et al*. found MITR enrichment in paclitaxel-resistant cells, indicating that MITR may play a crucial role in paclitaxel resistance in TNBC MDA-MB-231 cells (Lian *et al*., 2020). MITR inhibits the transcription of interleukin 11 and activates the JAK/STAT3 signaling pathway by interacting with and repressing MEF2A. JAK/STAT signaling is crucial for breast cancer development, progression, and metastasis (Dinakar *et al*., 2022). MITR may be a viable biomarker for paclitaxel response in TNBC tumors.

Estrogens play a significant part in the etiology of BC, and anti-estrogen treatments are widely utilized to treat ER-positive cases. Anti-estrogen-resistant MCF-7 and ERα-negative BC cell lines, such as MDA-MB231 and MDA-MB436, have high levels of HDAC9 expression (Lumachi *et al*., 2015). HDAC9 expression leads to lower ERα expression and transcriptional activity in MCF-7 cells. Additionally, HDAC9-overexpressing BC cells are less responsive to anti-estrogens. High HDAC9 expression is linked to gene upregulation and a worse prognosis

in endocrine therapy-resistant breast cancer compared to antiestrogen-responsive individuals. The link between HDAC9 and ERα signaling in BC cells may lead to hormone treatment resistance (Hervouet *et al*., 2013).

❖ **Gastric Cancer**

GC, or gastric adenocarcinoma, is a malignant epithelial tumor (Huang *et al*., 2015). Xiong *et al*. found increased HDAC9 expression in several human GC cell lines, including SGC-7901, BGC-823, and MKN-45 (Xiong *et al*., 2012). HDAC9 expression in primary tumor tissues from GC patients is associated with a worse survival rate. HDAC9 appears to play a pro-oncogenic function in GC, as evidenced by in vitro and in vivo investigations (Yang *et al*., 2021). Knocking down HDAC9 decreased tumor development and induced GC cell death and proliferation. Xu *et al*. discovered that miR-383-5p reduces GC progression by decreasing HDAC9 expression and promoting apoptosis (Xu *et al*., 2022).

❖ **Lung Cancer**

Lung Cancers are uncommon, extremely aggressive mesenchymal tumors originating from smooth muscle cells (Hashimoto *et al*., 2019). The HDAC9 SNP rs10248565 on chromosome 7p21.1 may be a biomarker for lung cancer in non-smoking women. Okudela *et al*. investigated the expression of immunoreactive HDAC9 in surgically resected primary lung adenocarcinoma (Okudela *et al*., 2014). HDAC9 expression was lower in lung cancer cells compared to non-tumor epithelial cells, and even lower in adenocarcinomas. Exogenous HDAC9 expression decreased clonogenicity and proliferation in the immortalized airway epithelial NHBE-T and NSCLC cell lines A549 and H2087, respectively (Yang *et al*., 2021). These findings imply that HDAC9 may act as a tumor suppressor, particularly in lung adenocarcinomas. Another study indicated that HDAC9 expression was elevated in NSCLC. Ma *et al.* analyzed 337 tumor samples from NSCLC patients and discovered that high levels of HDAC9 expression were associated with worse survival rates and poor clinical outcomes (Ma *et al*., 2012).

In vivo and in vitro studies show that HDAC9 promotes proliferation and reduces apoptosis in NSCLC cells. Guan *et al*. studied the role of CBR3AS1, a lncRNA, in the development of NSCLC. LncRNAs commonly operate as miRNA inhibitors, sequestering them or competing with miRNAs for particular mRNA binding sites (Guan *et al*., 2009). CBR3AS1 is significantly expressed in NSCLC tissues and cell lines, indicating a pro-tumorigenic impact. Research demonstrated that CBR3AS1 competed with endogenous miR5093p, a known tumor suppressor in NSCLC cells. miR5093p directly targets HDAC9. The CBR3AS1/miR5093p/HDAC9 pathway likely contributes to the development and progression of NSCLC (Duan *et al*., 2021).

❖ **Bladder Cancer**

Bladder Cancer is a malignant tumor with high incidence and recurrence rates (Lenis *et al*., 2020). Lucca *et al*. used a gene array-based study to assess HDAC9 expression in RNA samples from individuals with asymptomatic microscopic haematuria who were diagnosed with urothelial BCa (Lucca *et al*., 2019). HDAC9 mRNA was shown to be increased in patients with urothelial BCa. Wang *et al*. discovered that HDAC9 was increased in BCa tumor tissues and cell lines, including 5637 and T24. miR-211-5p decreased HDAC9 expression (Wang *et al*., 2022). Overexpressing miR-211-5p or downregulating HDAC9 in cell studies reduced BCa cell growth, migration, and apoptosis. Wang *et al*. found that HDAC9 may act as an oncogene, promoting BCa formation (Wang *et al*., 2022).

❖ **Glioblastoma (GBM)**

Glioblastoma (grade IV glioma) is the most prevalent and fatal primary brain tumor (Omuro *et al*., 2013). Yang *et al*. analyzed HDAC9 expression in a large cohort of GBM patients and found high levels in 472 out of 504 cases (Yang *et al*., 2021). Additionally, 33 out of 88 instances in the TCGA dataset were linked with a poor prognosis. HDAC9 is expressed in both human GBM cell lines (e.g., U87 and LN229) and freshly cultured patient-derived GBM cells (Kumari *et al*., 2023). HDAC9 is required for GBM cell development in vitro and increases the formation of U87 tumors in immune-deficient animals. In GBM cells, HDAC9 enhances its expression by interacting with a transcriptional co-activator containing a PDZ binding motif (TAZ). TAZ is an oncogene that increases the activity of the epidermal growth factor receptor (EGFR), a critical signaling protein that promotes cell proliferation and cancer (Strepkos *et al*., 2022). HDAC9 may stimulate the TAZ-mediated EGFR signaling pathway, leading to GBM development.

❖ **Hepatocellular carcinoma (HCC)**

HCC is the most commonly diagnosed aggressive primary liver cancer and the top cause of cancer-related mortality globally (Yang *et al*., 2019). HDAC9 has been linked to both the development of HCC and its prognosis, according to many independent investigations. Freese *et al*. showed higher levels of HDAC9 expression in HCC tissues compared to tumor-free liver **(**Freese *et.al.,* 2019). An examination of the TCGA dataset found that increased HDAC9 expression was associated with poor patient survival (Yang *et al*., 2021).

Hu *et al*. examined HDAC9 expression in tumors and para-cancerous tissues from 37 HCC patients. HDAC9 mRNA levels were elevated in HCC tissues, and individuals with greater levels had a worse prognosis (Hu *et al*., 2019). According to Zheng *et al*., HDAC9 was found to be overexpressed in 41 HCC specimens at levels that showed an inverse correlation with

miR-376a (Zheng *et al*., 2015). They also showed that HDAC9 directly reduces the expression of miR-376a in human HCC Huh7 cells through a mechanism that involves site-specific deacetylation of H3K18 in its upstream region. It's interesting to note that miR-376a downregulates HDAC9 expression in this cell line directly and that miR-376a overexpression suppresses HCC cell growth and encourages apoptosis. Due to the frequent downregulation of miR-376a in primary tissues and HCC cell lines, autoregulation of HDAC9 through a miR-376a/HDAC9 regulatory circuit may play a significant role in the formation of HCC (Zhao *et al*., 2019). HDAC9 is preferentially expressed in undifferentiated HCC, including HLE and HLF cell. In vitro tests and TCGA dataset analysis results point to the possibility that HDAC9 controls HCC cell differentiation and stemness acquisition. By regulating aldehyde dehydrogenase 1A3 (ALDH1A3), a gene linked to stemness, HDAC9 also contributes to anchorage-independent growth. Clinical trials have shown that oxaliplatin (OXA)-based systemic chemotherapy is beneficial for treating advanced HCC; nevertheless, resistance reduces this treatment's ability to prolong patient survival (Kanki *et al*., 2020). According to Liang *et al*. HDAC9 is significantly expressed in HCC cells and is associated with OXA resistance, indicating that HDAC9 may be crucial for regulation in this context (Liang *et al*., 2017).

❖ **Acute myeloid leukemia (AML)**

Adults with AML are afflicted with an aggressive malignancy that mostly starts in their bone marrow stem cells. As with other malignancies, high expression of HDAC9 in AML is strongly associated with a worse overall survival rate (Greim *et al*., 2014). In their investigation of HDAC9 expression in primary AML blasts, Bradbury *et al.* also examined HDAC9 levels in four other cell types: quiescent or cycling CD34+ progenitor cells from umbilical cord blood, as well as cycling CD34+ progenitors extracted from peripheral mononuclear cells obtained from adult donors, stimulated with granulocyte colony-stimulating factor (GCSF) (Bradbury *et al*., 2005). Between these cell types, there were no discernible variations in HDAC9 expression. While human AML HL60 cells exposed to the histone deacetylase inhibitor (HDI) sodium valproate in tissue culture showed a strong and selective increase in HDAC9 expression, this response was not seen in AML blasts, the human KG1 AML cell line, or in response to treatment with other HDIs (Breccia *et al*., 2010). To completely comprehend clinical responses and drug resistance, greater research on alterations in HDAC9 expression in AML is necessary, particularly in response to the treatment of one or more HDIs (Yang *et al*., 2021).

❖ **Retinoblastoma**

In youngsters, Rb is the most common malignant intraocular tumor. Rb tissues express HDAC9, and an increased level of HDAC9 has been linked to a worse prognosis in Rb patients (Lee *et al*., 2021). The levels of HDAC9 expression were positively correlated. the expansion of human Rb cells, such as Y79 and WERI-Rb-1. According to Zhang *et al*., in vitro, downregulation of HDAC9 caused cell cycle arrest at the G1 phase and significant reductions in the levels of CDK2 and cyclin E2. In a mouse xenograft model, Rb tumor development was likewise reduced by HDAC9 (Zheng *et al*., 2015). Xu *et al*. investigated the pro-oncogenic effects of HDAC9 in Rb further and discovered that HDAC9 is a direct target of miR-936. HDAC9 inhibited the tumor-suppressive effects of miR-936 in Rb cells in these assays (Xu *et al*., 2022). Similar findings were made by Jin *et al*., who showed that the tumor suppressor miR-101-3p directly inhibits HDAC9 production, which in turn inhibits the proliferation of Rb cells (Jin *et al*., 2018).

1.3. Role of HDAC9 in Other Diseases

It has been demonstrated that HDAC9 is a desirable target for diabetes, cancer, and several other metabolic disorders. It has also been connected to lipid metabolism, the onset of atherosclerosis, and macrophage polarisation by modifying histone acetylation at target genes (Hu *et al*., 2020). Moreover, it has been found that HDAC9 significantly increases the risk of coronary artery disease, myocardial infarction, and peripheral artery disease. **Figure 4** illustrates the role of HDAC9 and the related pathways in several illnesses. We will go into great detail in the following sections regarding HDAC9's role in the etiology of bone diseases like osteoporosis and osteonecrosis, cancer, inflammation and immune responses, diabetes mellitus (DM), atherosclerosis and cardiovascular disease (CVD), kidney disease, liver fibrosis, and obesity.

❖ **Alzheimer's disease (AD)**

Dementia is the result of a brain disorder called Alzheimer's disease (AD). In the population over 65, a prevalence of 10–30% is anticipated. The initial clinical manifestations of AD include synaptic impairment and abnormal processing of the amyloid precursor protein (APP) (Masters *et al*., 2015). MiR-138 in APP/PS1 (presenilin-1) mice increased with age, according to Lu *et al*. As per the report, ADAM10, a protein that contains a disintegrin and metalloproteinase domain, is not expressed as much when MiR-138, a microRNA precursor involved in the pathogenesis of AD, is present. This leads to an accelerated formation of amyloid beta (Aβ) and consequent impairments in synaptic and memory functions in APP/PS1

mice. This group hypothesized that HDAC9 has a miR-138 binding site. Its expression and miR-138 have an inverse relationship (Lu *et al*., 2019).

As a miR-138 sponge, HDAC9 reduces miR-138 expression and rectifies increased Aβ generation brought on by miR-138. Furthermore, it was discovered that individuals with moderate cognitive impairment and AD patients had reduced blood levels of HDAC9. These results indicate that HDAC9 regulates synaptic function and APP processing in AD, pointing to a potential therapeutic target for the disease's management (Lu *et al*., 2019).

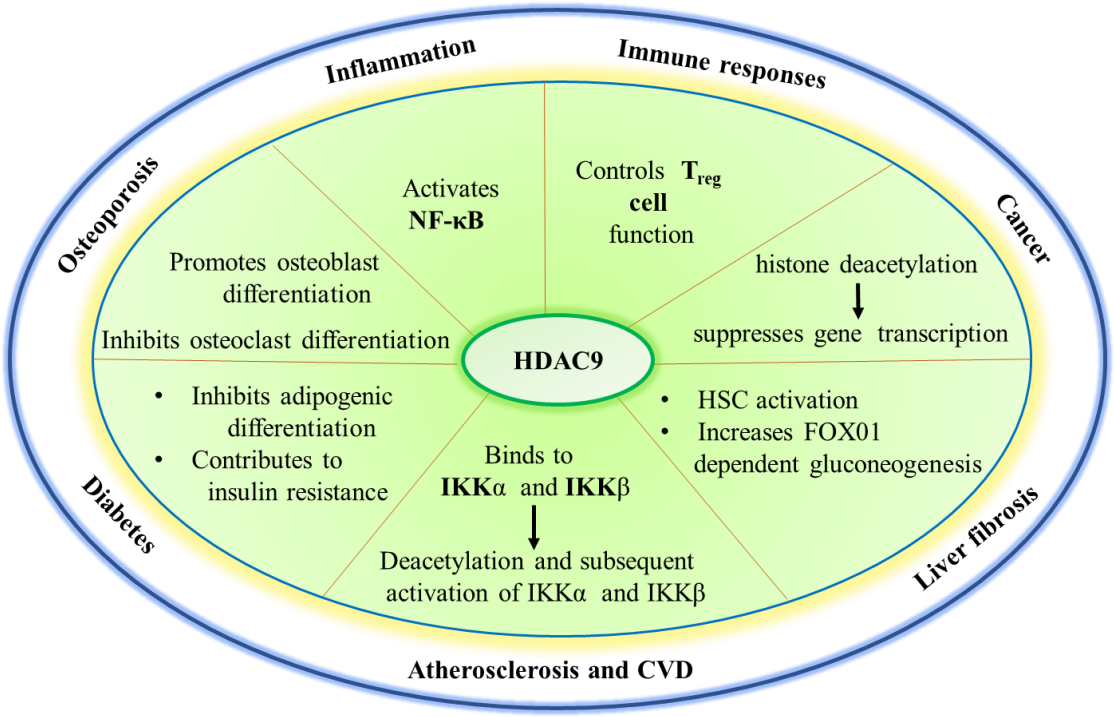

Figure 4: HDAC9 involvement in different diseases other than cancers

❖ Atherosclerosis and CVD

Atherosclerosis, or arterial inflammation, is a basic component of the pathogenesis of CVD. Numerous innate and adaptive immune response mediators control the inflammatory disease known as atherosclerosis (Asare *et al*., 2020). HDAC9 is a noteworthy regulator of vascular inflammation and has been found to have remarkable associations with atherosclerosis. HDAC9 is expressed by vascular cells and tissues. Human vascular HDAC9 expression has been associated with aortic and femoral atherosclerosis, large vessel ischaemic stroke, and carotid artery disease (Markus *et al*., 2013). Smooth muscle cells in the human aorta vascular system that have high levels of HDAC9 expression show reduced contractility and increased vascular calcification. CVD may be mediated by HDAC9's effects on atherosclerotic plaques and the genes it controls (Azghandi *et al*., 2015).

According to Asare *et al*., HDAC9 increases the vasculature's vulnerability to atherosclerotic plaque by inducing proinflammatory responses. This can lead to rupture-prone lesions that increase the risk of myocardial infarction and ischaemic stroke (Das *et al*., 2020). Additionally, this study found the mechanism by which HDAC9 controls vascular inflammation, which might act as a mediator for CVD. The regulation of IKK deacetylation by HDAC9 was shown to promote the activation of NF-κB signaling (Cao *et al*., 2014). Plaque stability and athero protection are further benefits of TMP195, a specific inhibitor of this HDAC9-dependent mechanism. According to studies on mice and isolated cells, HDAC9 is also implicated in human atherosclerosis and may be a target for future interventional research (Zhang *et al*., 2002).

❖ **Diabetes Mellitus (DM)**

A chronic metabolic disease called diabetes mellitus (DM) is identified by insufficiency in either the amount of insulin released its mechanism of action, or both. In individuals with type 2 diabetes mellitus, hepatic gluconeogenesis plays a significant role in the development of hyperglycemia (Wong *et al*., 2009). HDAC9 is important in managing glucose metabolism because it controls glucose homeostasis. HDAC9 is responsible for modulating hepatic gluconeogenesis (Chen *et al*., 2017). This is achieved through deacetylating the transcription factor forkhead box O1 (FoxO1), which in turn regulates the expression of PGC-1α (peroxisome proliferator-activated receptor-γ) and CREB (cyclic AMP-responsive element-binding protein) (Chatterjee *et al*., 2014). New FoxO1 regulatory targets have been found, including glucocorticoid receptor (GR), PGC-1α, and CREB. Given that HDAC9 knockdown raises FOXO1 acetylation, the beneficial effects of HDAC9 on gluconeogenesis may be attributed to the FOXO1-HDAC9 axis (Dehghani *et al*., 2023). The control of blood levels of adiponectin, which is released by adipocytes, has been proposed as another mechanism linking HDAC9 to diabetes. The control of blood levels of adiponectin, which is released by adipocytes, has been proposed as another mechanism linking HDAC9 to diabetes (Damić *et al*., 2022). It has been demonstrated that HDAC9 is specifically down-regulated before adipogenic differentiation occurs. The researchers found that HDAC9 and USF1 are recruited in preadipocytes near the E-box region of the C/EBPα gene promoter. Here, HDAC9 inhibits the transcription of C/EBPα. Additionally, the transcription of ABCG1, a gene involved in cholesterol efflux, is inhibited by HDAC9 overexpression. ABCG1 silencing inhibits key genes involved in insulin signaling, glucose absorption, and adipocyte development (Zou *et al*., 2015).

❖ **Kidney Fibrosis**

The most prevalent cause of chronic kidney disease (CKD) is assumed to be renal fibrosis, which is brought on by aberrant extracellular matrix (ECM) deposition in the kidney tissue (Li *et al*., 2022). Tubular epithelial cells (TECs) are the main component of the kidney and a major target in the development of chronic kidney disease (CKD). It is yet uncertain which HDAC isoforms cause renal fibrosis and the underlying mechanism (Liu *et al*., 2006). Zhang *et al*. reported in 2023 that HDAC9 expression is markedly increased in the kidneys of fibrotic mice, especially in the proximal tubules. HDAC9 deacetylates STAT1 and enhances its reactivation, which results in TECs being arrested at the G2/M stage and tubulointerstitial fibrosis in the end. Thus, by preventing epithelial cell cycle arrest in the G2/M phase, in vitro inhibition of HDAC9 may mitigate fibroblast activation and keep TECs from losing their epithelial character. HDAC9 may thus be a viable therapeutic target for renal fibrosis, according to this research (Zhang *et al*., 2023).

❖ **Liver Fibrosis**

The aberrant accumulation of fibrous connective tissue surrounding the liver's damaged region is referred to as hepatic fibrosis. There are many different causes of chronic liver disease (CLD), such as metabolic abnormalities, viral infections, and alcoholism (Puche *et al*., 2013). They all result in liver fibrosis, which is almost always the case with CLD. Hepatic stellate cell stimulation is thought to be the most important mechanism for hepatic fibrogenesis (HSCs).

HDAC9 is essential for liver fibrosis and HSC stimulation. The main source of myofibroblasts that produce ECM is HSCs. These cells control the contraction of the sinusoids and the ECM turnover in a healthy liver (Yang *et al*., 2017). HSCs get activated and undergo trans-differentiation to become myofibroblasts, which create an extracellular matrix (ECM) when the liver is wounded. HDAC9 mRNA and protein levels are elevated in human livers with primary biliary cirrhosis, alcoholic cirrhosis, and non-alcoholic liver disease in comparison to healthy livers (Claveria-Cabello *et al*., 2020). According to reports, the expression of genes involved in the creation of fibrous tissue is drastically reduced in LX-2 cell lines when HDAC9 is knocked down. Furthermore, in LX2 cells treated with HDAC9 siRNA, it was shown that HDAC9 knockdown suppresses the production of TGFβ-target genes (α-SMA and COL1A1). As a result, it may be concluded that HDAC9 is necessary for HSC activation and that blocking it may prevent liver fibrosis from progressing. The transdifferentiation of HSCs is associated with downregulated HDAC9 expression (Mannaerts *et al*., 2013). In a different study, it was found that fibrosis raises the levels of most HDACs (HDAC1, 2, 4, 5, 6, 8) including HDAC9. Primary biliary cirrhosis (PBC) and alcoholic cirrhosis are two examples of human liver

illnesses where HDAC9 expression is noticeably higher. Owing to these differences, further investigation is required to ascertain the alterations in HDAC9 expression during hepatic fibrogenesis (Yang *et al.*, 2021, Rippe *et al*., 2004).

❖ **Obesity**

Decreased adipose tissue function, which is brought on by changed gene expression, has a major impact on obesity. Research using in vitro and animal models indicates that HDAC9 is a novel epigenetic factor in the etiology of obesity (Jannat *et al.*, 2020). It is still unclear, nevertheless, what role HDAC9 plays clinically in the study of obesity and insulin resistance. The mRNA expression of HDAC9 in the visceral adipose tissue (VAT) of 19 women who were normal weight and 20 obese women (Li *et al*., 2022). Compared to controls, obese individuals had significantly decreased VAT mRNA levels of HDAC9. Therefore, obesity may be related to the reduced expression of HDAC9 mRNA in adipose tissue. However additional investigation is needed to support this theory. HDAC9 has been linked to obesity and insulin resistance in recent studies (Chatterjee *et al*., 2011). Human pre-adipocytes have been shown to express less HDAC9 before developing into adipocytes, suggesting that HDAC9 is a negative regulator of adipogenic growth. Insulin sensitivity is enhanced by HDAC9 deletion, which also lessens the negative effects of a high-fat diet on fatty tissue malfunction, weight gain, and hepatic steatosis. Insulin resistance brought on by weight gain activates the transcription factor FOXO1, which controls the enzymes phosphoenolpyruvate carboxykinase (PEPCK) and glucose 6-phosphatase (G6PC), resulting in the production of glucose. While HDAC9 knockdown has the opposite impact on Huh7 cells, overexpression of HDAC9 leads to FOXO1 deacetylation, which increases transcriptional activity (Chatterjee *et al*., 2014).

❖ **Bone Disease**

The regulation of osteogenic differentiation and autophagic activity by HDAC9 renders it a desirable target for the treatment of many bone disorders. Osteocytes and bone marrow apoptosis are hallmarks of the progressive, refractory illness osteonecrosis, and mesenchymal stem cells (MSCs) from human bone marrow function as osteonecrosis seed cells (Zhang *et al*., 2020). According to research by Wang *et al*., HDAC9 controls osteogenic differentiation in MSCs through the MAPK signaling pathway, which causes osteonecrosis. Human bone marrow MSCs that are not differentiated into osteoblasts may produce less phosphorylated extracellular signal-regulated kinase 1/2 (pERK1/2) when HDAC9 is inhibited (Wang *et al*., 2022). For this reason, HDAC9 could be a target for osteonecrosis therapy. Furthermore, HDAC9 has also been linked to osteoporosis. By restricting bone resorption, HDAC9 appears to inhibit osteoclast formation, potentially preventing bone loss. There is a connection between

HDAC9 activity and PPAR-γ, which is a crucial modulator of osteoclast development. Age-related bone loss may be less common if HDAC9 stimulates MSC bone marrow growth (Jin *et al*., 2015). Li *et al*. report that microRNA-188 (miR-188) targets the mRNA of the gene Hdac9 exclusively. In contrast, miR-188 deletion in mice decreased age-related loss of bone mass, increased bone formation in the osteoblast, and reduced the accumulation of fat in the bone marrow. MiR-188 overexpression suppresses HDAC9 expression in bone marrow. In general, it seems that HDAC9 inhibits osteoclastogenesis and promotes osteogenesis to prevent osteoporosis (Li *et al*.,2015).

❖ **Inflammation and Immune Responses**

An important part of inflammatory processes is played by HDAC9. It is unclear if and how HDAC9 is regulated during inflammation, despite its importance (Li *et al*., 2018). The reduction of many inflammatory chemokines and cytokines, such as IL-12, IFN-γ, MCP1, inducer of NOS, etc., is most likely due to PPAR-γ activation. Bacterial materials stimulate the production of cytokines and histone acetylation in human sebocytes. In these cells, inhibiting HDAC9 increases the synthesis of inflammatory cytokines such as IL1B and CXCL8 (Sanford *et al*., 2016). In human sebocytes, HDAC9 depletion increases the inflammatory response overall. HDAC9 thereby opposes the inflammatory response epigenetically. HDAC9 is necessary for many different cell types, including regulatory T-cells, to proliferate and differentiate. HDAC9's biological significance in T-effector cells remains unclear, though (Sanford *et al*., 2019). The HDAC9 deficiency is the reason for the decrease in lymphoproliferation and autoantibody production. Furthermore, reduced BCL6 gene expression and increased GATA3 and roquin are linked to HDAC9 deficiency. It also plays a unique part in autoimmune diseases and the flexibility of CD4+ T-cells (Yan *et al*., 2011). Histone acetylation, nonhistone acetylation, and protein-protein interaction are some of the ways that HDAC9 modifies gene expression; these processes are not necessarily mutually exclusive, though. Higher HDAC9 expression in Treg cells reduces their suppressive ability (Tao *et al*., 2007). Treg cells lacking in HDAC9 proliferate more quickly, suppressing the immune system more severely. HDAC9 thus functions as a strong immunological enhancer (Wakabayashi *et al*., 2009).

2. Literature Review of HDAC9

2. Literature Review of HDAC9

- **Xu *et al.*, 2007**. reports that, in GC tissues and cell lines, miR-383-5p was downregulated and functioned as a tumor suppressor by blocking HDAC9 production, hence averting the development of gastric cancer. According to our findings, miR-383-5p is a key player in the development of gastric cancer and is a key regulator of oncogenic HDAC9 in GC. This information may be useful in the creation of new therapeutic approaches for the treatment of GC.
- **Guan *et al.*, 2011**. reports that the CBR3-AS1-induced cancer-promoting properties in NSCLC cells, both in vivo and in vitro. It was discovered that CBR3-AS1 works mechanistically as a ceRNA that absorbs miR-509-3p and increases HDAC9 expression. These results might have a beneficial effect on the creation of new targeted medications and the improvement of NSCLC treatment approaches.
- **Jin *et al.*, 2018**. demonstrated that MiR-101-3p is downregulated in retinoblastoma. Additionally, by directly targeting EZH2 and HDAC9, miR-101-3p overexpression inhibits the growth of retinoblastoma cells. These findings suggest that miR-101-3p plays a significant role in the carcinogenesis of retinoblastoma and might guide the creation of new treatment approaches.
- **Freese *et al.*, 2019**. confirms the possible advantages of using HDACi alone or in conjunction with sorafenib for the treatment of HCC. Crucially, even at subtoxic levels, HDACi seem to reduce several aspects of the tumorigenicity of HCC cells in addition to encouraging cell death. Although HDAC expression is generally elevated in HCC, individual patients and HDAC classes seem to differ from one another. Additionally, HDACi demonstrated a variety of inhibitory effects on HCC cells in vitro, both qualitatively and quantitatively. All things considered, the cause of these differences as well as how they affect the onset and course of HCC require additional research in the future and may be used to create more specialized treatment modalities.
- **Zheng *et al.*, 2019.** report the regulatory pathway between miR-376a and HDAC9 in HCC and propose that epigenetic changes facilitated the silencing of the miR-376 cluster through HDAC9, a direct target of miR-376a.
- **Xu *et al.*, 2019**. reported that In TNBC cells, there is an inverse relationship between greater HDAC9 expression levels and miR-206 expression. Moreover, the selective inhibition of HDAC9 specifically blocked TNBC invasion and angiogenesis in addition to modifying the expression of miR-206, VEGF, and MAPK3. According to our research, VEGF and

MAPK3 by regulating miR-206 enable invasion and angiogenesis in TNBC cells when HDAC9 is overexpressed. These findings might help in the development of tailored treatments for people with breast cancer and a better knowledge of TNBC regulation.

- **Bera *et al.*, 2020**. suggested that Epigenetic regulation plays a crucial function in the recurrence of breast cancer and helps to regulate inflammatory processes. The discovered proteins may serve as building blocks for the creation of a serum-based test for the detection of breast cancer recurrence. An earlier and more precise diagnosis, better information for patient-specific treatment, enhanced monitoring of therapeutic responses, and the discovery of new therapeutic targets for treatment would all be made possible by the development of a more predictive, noninvasive biomarker panel for recurrence-type breast cancer.
- **Wang *et al.*, 2020**. reported that MiR-211-5p expression in BCa tumor tissues was negatively correlated with HDAC9 expression. Through its inhibition of HDAC9 production, miR-211-5p, a post-transcriptional regulator, contributed to growth retardation and apoptosis in BCa cells. About treating BCa, this mechanism offers a potential treatment regimen for precision medicine.
- **Guan *et al.*, 2020**. reported that the Cancer Genome Atlas (TCGA) database's CBR3-AS1 and miR-509-3p expression data in non-small cell lung cancer (NSCLC) were not examined. Second, data from the TCGA database was not used to analyze the link between CBR3-AS1 and miR-509-3p expression in NSCLC; these limitations will be resolved soon. To the best of our knowledge, however, our work is the first to emphasize CBR3-AS1's carcinogenic effects in NSCLC cells, both in vitro and in vivo. It was discovered that CBR3-AS1 works mechanistically as a ceRNA that absorbs miR-509-3p and increases HDAC9 expression. These results might have a beneficial effect on the creation of new targeted medications and the improvement of NSCLC treatment approaches.
- **Lee *et al.*, 2021.** demonstrate that the HDAC 9 expression levels were greater in PDAC patients. HDAC 9 could also be connected to RFS and DSS in PDAC. According to the current univariate and multivariate study, DSS in PDAC was independently predicted by high HDAC 9 expression level and clinical stage, and poor prognosis was associated with both. Consequently, HDAC 9 could be a novel target for diagnosis and help with PDAC therapy.

3. Rationale behind the study

3. Rationale behind the Study

Excess HDACs (Histone Deacetylases) are one of the primary factors contributing to the development of cancer. It actively participates in chromatin remodeling through the deacetylation of histone protein. It includes the formation of several tiny blood vessels in hypoxic cancer cells, increasing the oxygen supply to the rapidly proliferating malignant cells. Performs a critical role in the epithelial-mesenchymal transition that triggers cancer cell invasion and metastasis. According to recent research, a large number of HDACs are elevated in malignant cells and linked to several malignancies, including multiple myeloma, leukemias, solid tumors, colon cancer, pancreatic cancer, and cutaneous T-cell lymphoma (CTCL). HDACs have been linked to several other illnesses, including liver fibrosis, kidney fibrosis, diabetes mellitus, and cardiovascular disease.

Because of its capacity to alter gene expression and epigenetic regulation, a family of medications known as histone deacetylase (HDAC) inhibitors has drawn a lot of interest from researchers studying cancer as well as other diseases. A few FDA-approved medications are now on the market, including Belinostat, Pacinopstat, Chidamide, Romidepsin, and Panobinostat. It is crucial to remember that although preclinical and early clinical trials have demonstrated the potential of HDAC inhibitors, research is still needed to determine their safety and efficacy in many cancer types. As such, these inhibitors may not be a conventional treatment for every sort of malignancy. Their precise function in cancer therapy may vary based on the kind of cancer and unique patient characteristics, and they are frequently used in conjunction with other cancer therapies. Since most HDAC inhibitors are synthetic or semi-synthetic, there is a risk of various toxicities that need to be carefully examined and treated. The goal of ongoing research is to create HDAC inhibitors that are less harmful and more selective.

Researchers are interested in HDAC9 (Histone Deacetylase 9) because of its important function in many biological processes and possible implications in a wide range of disorders. Here are some explanations for why HDAC9 is a topic of interest for

- HDAC9 removes acetyl groups from histones to control the expression of genes. This mechanism is essential for gene silencing and chromatin remodeling, which affect several biological processes.
- Because it plays a crucial part in epigenetic regulation, HDAC9 regulates the expression of genes related to cell division, proliferation, and apoptosis.

- HDAC9 has been linked to gliomas, leukaemia, and breast cancer, among other cancers. It may be a target for cancer treatment as it may modify gene expression patterns, which can promote oncogenesis.
- Because HDAC9 is involved in synaptic plasticity and neuronal survival, it has been connected to neurodegenerative illnesses including Alzheimer's and Huntington's.
- One of the main areas of study is the development of HDAC inhibitors as possible medications. It may be possible to treat neurological problems, cardiovascular ailments, and cancer by inhibiting HDAC9.
- Knowing the unique functions that HDAC9 plays in various illnesses may help develop more individualised treatment plans, wherein HDAC9 inhibition is customised to meet the needs of each patient.
- HDAC9 may have an effect on immune cell activity and differentiation in the immune system, according to recent research. This might be relevant for immunotherapy and autoimmune illnesses.
- HDAC9 affects a number of physiological functions through interactions with different proteins and signalling pathways. This positions it as a key node in cellular networks, providing a wide range of research opportunities.

Consequently, a collection of 406 HDAC9 inhibitors has been the subject of a Classification-based quantitative structure-activity relationship (QSAR) analysis in this work. Important signatures for strong HDAC9 inhibitory activity have been identified via the use of Machine learning (ML), Bayesian classification, recursive partitioning, SARpy analysis, Docking studies, and Molecular dynamics analysis (MD). The current investigation identified the necessary amino acids for HDAC9 inhibitor binding. The study of the chosen inhibitors' molecular docking will benefit from this research. Some of the lead compounds are then chosen for molecular dynamics after these phases. Molecular dynamics is used to assess the chemicals' stability within the receptor.

4. Materials and Method

4. Materials and method

4.1 Dataset Preparation and Dataset Division

A set of 705 unique compounds with a broad spectrum of HDAC9 inhibitory activity in nM concentration have been found using Binding DB (https://www.bindingdb.org/). Using the program Discovery Studio 3.0 (DS 3.0) (Discovery Studio 3.0 DS 3.0, 2015)., 216 duplicate molecules were eliminated as the first step in the creation of the dataset. For the remaining 489 compounds, the Lipinski rule and Veber's rule were applied to filter them. Using this method, only 406 drug-like molecules that meet Lipinski and Veber's criteria were chosen for the final data set. To do the classification-based QSAR modeling, the HDAC9 inhibitory potency (IC_{50}) values of these drugs were also converted into a binary format. The chemicals were separated into two classes: 1 (active) and 0 (inactive). The 406 chemicals that comprised the whole dataset were used to produce the training set and the test set (Moinul *et al*., 2022). The dataset was split using the "Random splitting" method. The molecules were divided in a 3:1 ratio to create the training sets (NTrain = 284) and the test sets (NTest = 122). The training sets were used to generate the QSAR models, and the corresponding test sets were used to confirm them.

4.2 Development of other machine learning models

4.2.1 Calculation of descriptors and data pre-treatment

Utilizing the training set of 284 and the test set of 122 HDAC9 inhibitors, further machine-learning models were created and examined. Several classes of 2D descriptors were built using PaDEL-Descriptor. The data pre-treatment tool used Data Pre-TreatmentGUI 1.2 from the DTC laboratory, Jadavpur University, deleted the intercorrelated descriptors (intercorrelation cut off >0.90) and the descriptors with a modest level of value variability (variance cut off <0.0001) (Ambure *et al*., 2015).

4.2.2 Feature selection

Finding the bare minimum of significant features or variables in the descriptor form is an important step in evaluating an ML model. The present study employed the most discriminating features (MDF) selection technique, which can be accessed at https://dtclab.webs.com/software-tools, to ascertain the minimum number of features required for the classification of HDAC9 enzyme inhibitors as either active or inactive (Banerjee *et al*., 2023).

4.2.3 ML model development and analysis

Three classification-based machine learning models—logistic regression (LR), random forest classifier (RFC), linear discriminant analysis (LDA) were created for this work (Pandey *et al*.,

2023). These models were made using the Scikit Learn module, which was written in Python and has optimized hyperparameters. The ML models were created using the ML classifier tool (https://sites.google.com/jadavpuruniversity.in/dtc-lab-software/home/machine-learning-model-development-guis). For the application domain study, the leverages of the training and test set compounds were calculated.

Bayesian classification study

Bayesian modeling is a well-known molecular modeling approach that heavily relies on the classical probability function and the naïve Bayes' theorem in classification-based analysis. The numerous HDAC9 inhibitors were classed as active or inactive based on the excellent and bad Bayesian fingerprints found during the molecular modeling investigation. The following molecular properties (MPs) were calculated using the Discovery Studio version 3.0 (DS 3.0) (Discovery Studio 3.0 DS 3.0, 2015) software: lipophilicity (AlogP), molecular weight (MW), number of hydrogen bond donors (nHBD), number of hydrogen bond acceptors (nHBA), number of rings (nR), molecular fractional polar surface area (MFPSA), and number of aromatic rings (nAR) (Sardar *et al*., 2024). Furthermore, the extended connectivity fingerprint of diameter 6 (ECFP_6) was created as a fingerprint descriptor. The training set molecules were used to create the model in Discovery Studio version 3.0 (DS 3.0), and the test set molecules were utilized to validate the model (Rogers *et al*., 2010). The statistical properties of the proposed model were evaluated using fivefold cross-validation (5-CV) techniques. Furthermore, different true positives (TP), true negatives (TN), false positives (FP), and false negatives (FN) were computed. Additionally, statistical validation metrics such as sensitivity (Sen), specificity (Spe), and concordance (Conc) were employed to assess the models' robustness and dependability (Khatun *et al*., 2023).

4.3 Recursive partitioning study

The Recursive partitioning (RP) modeling technique creates the final decision tree by using the dataset compounds' most relevant chemical features. It's a quantitative statistical approach (Ramani *et al*., 2022). It is frequently used to categorize individual molecules as active or inactive in a variety of molecular populations. The RP models were created using Discovery Studio (DS) Version 3.0 and verified with cross-validation procedures (Amin *et al*., 2022). Based on the model's capacity to differentiate between several kinds of inhibitors, the most effective RP model for HDAC9 inhibitors was determined. The following parameters were provided for the addition model construction: The minimum number of samples per node is ten (absolute), the maximum tree depth is twenty, Gini is the splitting algorithm, and there is only

one tree. Bagging is the ensemble voting method; Euclidean is the numerical distance function; and FCFP_2 is the model domain fingerprint (Yang *et al.*, 2023).

Table 1: Brief description of the selected descriptors for model development (Das *et al.*,2024)

S. No.	Descriptors	Type	Definition
1.	Number of hydrogen bond acceptors (*nHBA*)	Functional group counts	The hydrogen acceptor is an electronegative atom of a neighboring molecule or ion that contains a lone pair that participates in the hydrogen bond.
2.	Number of hydrogen bond donors (*nHBD*)	Functional group counts	It is a fundamental descriptor to predict the oral bioavailability of small molecules. Based on Lipinski's rule of five, the majority of orally active drugs have not more than five hydrogen bond donors and fewer than ten hydrogen bond acceptors.
3.	Molecular weight (*MW*)	Constitutional indices	The molecular weight of a substance is the weight in atomic mas units of all the atoms.
4.	Lipophilicity *(ALogP)*	Molecular properties	Ghose-Crippen octanol-water partition coefficient (logP).
5.	Number of rotatable bonds (*nRB*)	Constitutional indices	A rotatable bond is defined as any single non-ring bond, attached to a non-terminal, non-hydrogen atom.
6.	Number of aromatic rings (*nAR*)	Constitutional indices	Aromatic rings (also known as aromatic compounds or arenes) are hydrocarbons that contain benzene, or some other related ring structure.
7.	Molecular fractional polar surface area (*MFPSA*)	Molecular properties	The sum of surface contributions of polar atoms (usually oxygens, nitrogen and attached hydrogens) in a molecule.
8.	centric circular fingerprint descriptor, *ECFP_6*	Molecular fingerprint descriptor	Extended connectivity fingerprint with a bond diameter of 6.
9.	Molecular function class fingerprints of maximum diameter 6 (*FCFP_6*)	Molecular Fingerprint descriptors	sometimes referred to as circular or Morgan fingerprints. the chemical structure is evaluated for all subgraphs with a diameter of up to size of 6.

4.4 Statistical analysis and model evaluation of Bayesian and RP study

The efficacy and quality of the QSAR models developed were evaluated using Receiver Operating Characteristics (ROC) statistical analysis. Equations 2–5 generated the statistical parameters that were used to validate the model's performance (Marzo *et al*., 2016). These measures comprised prediction accuracy (Acc), sensitivity (Se), specificity (Sp), and accuracy (Acc) for both the training and test sets of chemicals. Equations 6-11 were utilized to yield measures such as the F1-measure (F1), area under the balanced accuracy ROC curve (AUCb), Matthew's correlation coefficient (MCC), Youden's index (γ), positive (ρ+), and negative probability (ρ-) for both the training and test set compounds.

4.5 SARpy

SARpy, a Python-based program, employs the likelihood ratio (LR) of structural fingerprints (structural alarms) to assess if they are present and contribute to a certain biological feature or activity (Banerjee *et al*., 2022). The model is built by fragmenting the training set chemicals based on their SMILES strings and experimental activity in binary labels (Activity: 0-1). It creates rules in various stages, including ruleset extraction, evaluation, and ruleset fragmentation, utilizing a recursive algorithm approach for substructures. The test set may be used to verify the resultant model based on the ruleset generated by the training set chemicals (Chen *et al*., 2018).

4.6 Molecular Docking Study

The human X-ray crystallographic structure of HDAC9 remains unknown. In our investigation, we used MODELLER version 10.2 (https://salilab.org/modeller/) to create a homology-modeled structure of HDAC9 (Elmezayen *et al*., 2021). For the homology modeling, the hydroxamate-bound human crystal structure of HDAC4 (PDB ID: 2VQM_A), which has 72% sequence similarity to the FASTA sequence of HDAC9, was used. The MODELLER software's "model-single.py" module produced five distinct homology structures (Soltani *et al*., 2024; Valanciute, *et al*., 2023). ChemDraw version 3.0 was used to create the 2D structure of the bioactive compounds for the molecular docking investigation. Chem3D version 3.0 was then used to transform the 2D structure to an energy-minimized (MMF94 type) 3D structure. The selected compounds from the recursive partitioning and Bayesian classification experiments were used in a LeDock molecular docking investigation utilizing the constructed homology model of HDAC9 (Liu *et al*., 2023). LeDock is a GUI-based docking program that is accurate, user-friendly, and semi-flexible (meaning that ligand complexes attach flexibly

towards the active site whereas proteins are thought to be stiff). The homology protein for HDAC9 was chosen from the LeDock "LePro" module. The grid box parameters were then automatically selected by covering the geometric pattern in the PDB crystal structure that the prototype in-bound ligand occupied, 2VQM_A (where xmin = 13.023, xmax = 25.023, ymin = -16.358, ymax = -0.909, zmin = -15.194, zmax = 7.16; with an RMSD cut-off range of 0.5 to reduce the redundancy of docking poses). The docking process was then initiated. PyMOL provided the final docking data with a docking score expressed in terms of binding affinity (kcal/mol), and Discovery Studio Visualiser version 3.0 produced 2D binding interaction graphs based on the compounds' docked postures (Discovery Studio 3.0 DS 3.0, 2015).

4.7 Molecular Dynamics Simulation

By evaluating the stability of the ligand inside the binding site under simulated human body conditions using GROMACS 2020.3 (Abraham *et al*., 2015) the compound that had the highest docking score was taken into consideration for the MD simulation investigation. The charm-gui web server's "Solution Builder" function (https://www.charmm-gui.org/) was used to prepare the input parameters files. A rectangular TIP3P water box covered the protein-ligand combination (Lee *et al*., 2016). To prevent steric overlapping situations, each system was subjected to 5000 steps of steepest descent energy minimization after being sufficiently neutralized with sodium chloride ions using the Monte-Carlo technique. NVT equilibration was carried out at a constant coupling of 1 picosecond at 310.15 K (for 125000 steps using the V-rescale temperature coupling technique) (Hess *et al*., 2006). Using a CHARMM36m forcefield, the MD simulation of the best-docked complex was run for 100 ns Root mean square deviation (RMSD), root mean square fluctuation (RMSF), and radius of gyration (Rg) trajectory analysis were used to assess the results of the MD simulation.

5. Result and Discussion

5. Result and Discussion

In the current work, 406 HDAC9 inhibitors were used as a dataset for developing the classification-based model. The dataset was split into a training (n_{Train} = 284) and test set (n_{Test} = 122) using the "Random splitting" method for the Bayesian and RP analysis. Before the model (Bayesian and RP) was generated, eight different types of molecular descriptors were computed, including lipophilicity, nR, nAR, nRB, AlogP, MW, nHBA, nHBD, M_FPSA, ECFP_6, and FCFP_6. **Figure 5** displays bin plots for physicochemical parameters for both the active and inactive molecules, including AlogP, molecular weight, and molecular fractional polar surface area (M_FPSA). Plotting AlogP against molecular weight further illustrates the chemical diversity study.

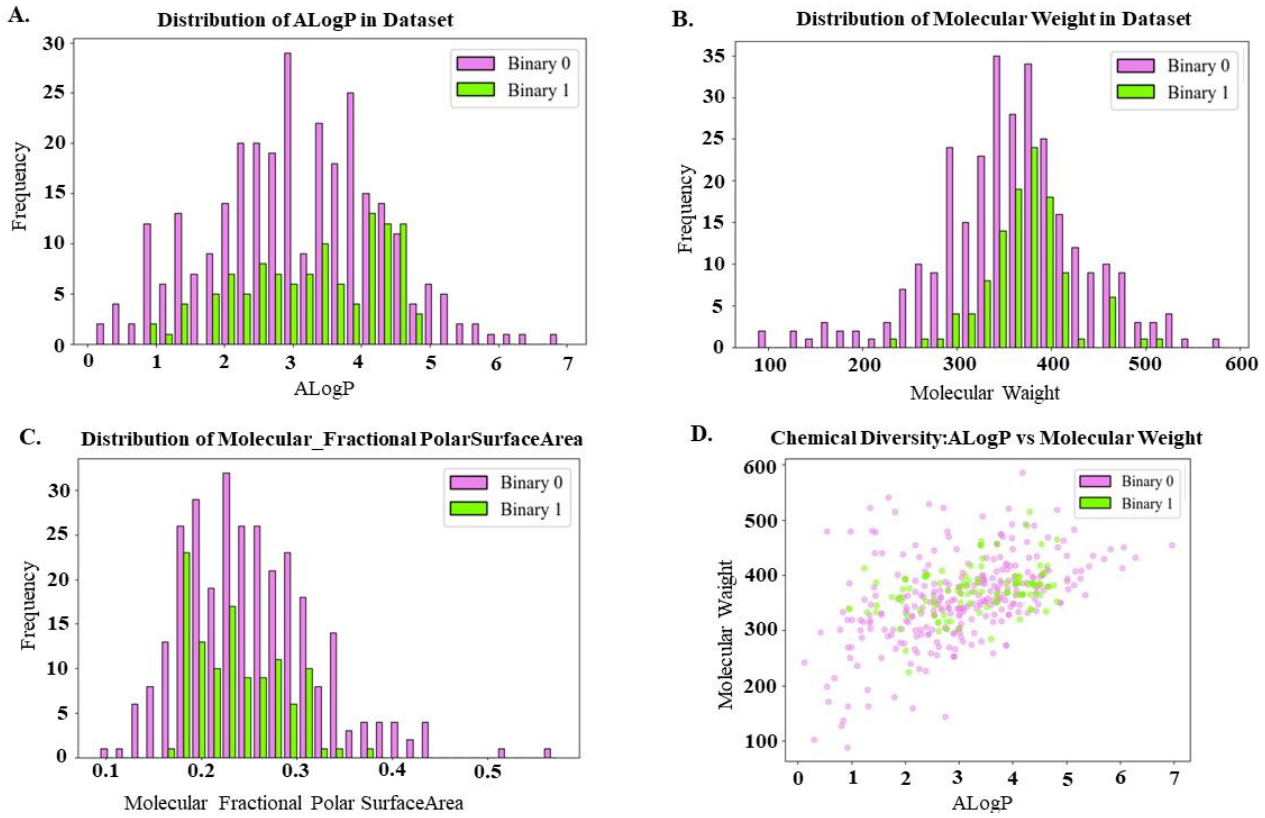

Figure 5: Distribution of HDAC9 inhibitory activity, (A) AlogP, (B) molecular weight, (C) molecular fractional polar surface area along with (D) the chemical diversity analysis of AlogP vs molecular weight

5.1 Machine Learning Models

A further three classification-based machine learning models (LR, LDA, and RFC) have been developed for the 406 HDAC9 inhibitors. Several statistical parameters were utilised to choose

the best machine learning (ML) model, such as accuracy, precision, recall, F1 score, Matthews correlation coefficient (MCC), Cohen's kappa coefficient, and so on. In terms of various classification-based validation measures **Table 2**, it was observed that the Linear Discriminant Analysis (LDA) model is the best model for the HDAC9 inhibitors. The best model (LDA) has a 5-fold cross-validated ROC of 0.927 for the training set and 0.861 for the test set. The detailed statistical analysis is presented in **Table 2.**

Table 2: Validation parameters of the classification-based ML models for HDAC9

Model Type	Set	Accuracy	Precision	Recall	F1 score	MCC	Cohen's k	AUC-ROC	Hyperparameters
RFC	Train	0.828	0.826	0.481	0.608	0.538	0.507	0.876	{'criterion': 'gini', 'max_depth': 2, 'min_samples_leaf': 4, 'min_samples_split': 2, 'n_estimators': 150}
	Test	0.819	0.867	0.394	0.542	0.503	0.448	0.758	
LDA	Train	0.849	0.743	0.696	0.719	0.616	0.616	0.927	{'solver': 'svd'}
	Test	0.828	0.714	0.606	0.656	0.545	0.542	0.861	
LR	Train	0.849	0.773	0.646	0.703	0.607	0.603	0.899	{'C': 1.0, 'penalty': 'l1', 'solver': 'liblinear'}
	Test	0.836	0.783	0.546	0.643	0.556	0.541	0.912	

5.2 Interpretation of The Descriptor of the best ML-based classification Models

Providing a mechanical understanding of the descriptors that significantly impact the model output is crucial, as per OECD Principle 5. The best-identified models were used in the current study's SHAP (SHapley Additive exPlanations) analysis on the HDAC9 inhibitor training datasets. This is done to comprehend how significant descriptors contribute to the model's final output. The most significant descriptors in the SHAP summary plot are indicated by an elevated value with a larger spreading from the mean.

From the SHAP plot, we can infer that features that contribute most to the prediction of the model output include *VPC-4, VC-3, ATSC0e, nssssC, VC-4, SCH-7, GATS2v, ATSC0i, MATS4s, SpMint4_Bhs, ATS4s, ATSC4s, and AlogP* descriptors. Among the highest-ranked descriptors, *VPC-4* contributes positively to the model output whereas *VC-3* contributes negatively as observed from the SHAP plot (shown in **Figure 6**). The *VPC-4* descriptor stands for Valence Path Cluster of order 4. It is a topological descriptor used in cheminformatics and molecular modeling to capture information about the connectivity and valence of atoms in a molecule.

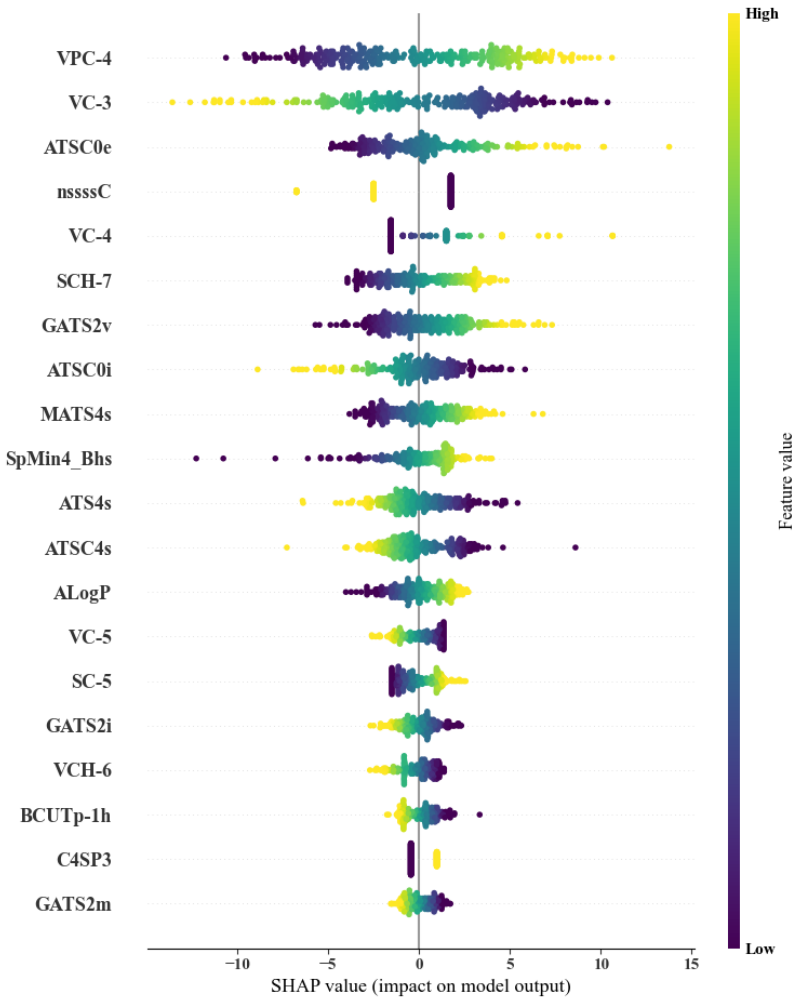

Figure 6. SHAP summary plot for the ML-based RFC model (training set) of HDAC9 inhibitor

This above observation can be justified by examining compounds **241** and **267** where an increase in the value of the descriptor VPC-4 causes the active inhibition of HDAC 9. The next negatively contributing *VC-3* descriptor is the Valence Cluster of order 3. It is also a topological descriptor used in cheminformatics to describe the connectivity and valence of atoms within a molecule, focusing on clusters of atoms connected in a specific way. The above observation can be justified by compound **22**, where it is noted that the low value of the *VC-3* descriptor contributes to its activity as an HDAC-9 inhibitor. The third positively contributing ATSC0e descriptor is Centered Broto-Moreau Autocorrelation - lag 0, weighted by Sanderson electronegativities. It is a descriptor used in cheminformatics to capture information about the distribution of atomic properties (in this case, electronegativities) within a molecule.

Table 3: The details of different descriptors used in this study along with their contributions

Descriptor Java Class	Descriptor	Description
Chi Cluster Descriptor	VC-3	Valence cluster, order 3
	VC-4	Valence cluster, order 4
	VC-5	Valence cluster, order 5
	SC-5	Simple cluster, order 5
Chi Chain Descriptor	SCH-7	Simple chain, order 7
	VCH-6	Valence chain, order 6
Chi Path Cluster Descriptor	VPC-4	Valence path cluster, order 4
Autocorrelation Descriptor	ATSC0e	Centered Broto-Moreau autocorrelation - lag 0 / weighted by Sanderson electronegativities
	GATS2v	Geary autocorrelation - lag 2 / weighted by van der Waals volumes
	ATSC0i	Centered Broto-Moreau autocorrelation - lag 0 / weighted by first ionization potential
	MATS4s	Moran autocorrelation - lag 4 / weighted by I-state
	ATS4s	Broto-Moreau autocorrelation - lag 4 / weighted by I-state
	ATSC4s	Centered Broto-Moreau autocorrelation - lag 4 / weighted by I-state
	GATS2i	Geary autocorrelation - lag 2 / weighted by first ionization potential
	GATS2m	Geary autocorrelation - lag 2 / weighted by mass
Burden Modified Eigenvalues Descriptor	SpMin4_Bhs	Smallest absolute eigenvalue of Burden modified matrix - n 4 / weighted by relative I-state
ALOGP Descriptor	ALogP	Ghose-Crippen LogKow
PaDEL Carbon Types Descriptor	C4SP3	Singly bound carbon bound to four other carbons
Electrotopological State Atom Type Descriptor	nssssC	Count of atom-type E-State: >C<

Autocorrelation refers to the correlation of a property with itself across the molecular structure. The Broto-Moreau autocorrelation specifically measures how a certain atomic property (here, electronegativity) is distributed relative to the positions of atoms in the molecule. The descriptor is weighted by Sanderson electronegativities, a specific scale of electronegativity values assigned to atoms. Electronegativity refers to an atom's ability to attract and hold electrons. By weighting the autocorrelation by electronegativity, the descriptor gives more importance to atoms with higher or lower electronegativity values, depending on their contribution to the overall molecular property. The positive contribution of the *ATSC0e* descriptor is further confirmed by examining compounds **12**, **16**, and **225**, where an increase in the value of this descriptor actively contributes to the inhibition of HDAC9. The next negatively contributing descriptor is nssssC which denotes the number of tetrahedral carbon atoms present in a molecule. The above observation can be justified by examining compounds **214** and **249**, where it is noted that the absence of tetrahedral carbon atoms in their structure contributes to their activity as HDAC9 inhibitors. From the SHAP summary plot, the next positively contributing descriptor is *VC-4* which stands for Valence cluster of order 4. The positive contribution of the *VC-4* descriptor is confirmed by observing compounds **6**, **16**, and **206**, where a high value of this descriptor is associated with active HDAC9 inhibition. The next positively contributing descriptor is *SCH-7* which stands for Simple chain of order 7. In the case of compounds **223**,**252** and **254**, the value of the descriptor is high and they actively contribute to the HDAC9 inhibition. The next positively contributing descriptor *GATS2v* is Geary autocorrelation - lag 2, weighted by van der Waals volumes. The above observation can be justified with the help of the following compounds **22** and **234** where it is observed that an increase in the descriptor value causes active inhibition of the HDAC9. From the SHAP summary plot, the next negatively contributing descriptor is *ATSC0i* which denotes Centered Broto-Moreau autocorrelation - lag 0, weighted by the first ionization potential. The above observation can be verified with the help of compound **263** where it is observed that a decrease in the descriptor value causes active inhibition of the HDAC9. The next positively contributing descriptor is *MATS4s* which denotes Moran autocorrelation - lag 4, weighted by ionization state. The above observation can be further validated by examining compounds **222** and **227**, where an increase in the descriptor value is associated with a more significant contribution to HDAC9 inhibition. The next positively contributing descriptor is SpMin4_Bhs which stands for the Smallest Absolute Eigenvalue of the Burden Modified Matrix - Order 4, weighted by Relative I-State. It is a molecular descriptor used to quantify aspects of a molecule's structure based on its graph representation. The positive contribution of this descriptor can be confirmed

by examining compounds **255** and **280**. It is evident that an increase in this descriptor's value correlates with enhanced activity as an HDAC9 inhibitors.

5.3 Bayesian classification study

By using the molecular descriptors and ECFP_6 fingerprint on the compounds in the training set, the Bayesian classification model was developed. **Table 4.** provides the statistical parameters of the developed Bayesian model. **Figure 7.** provides the receiver operating characteristic curves (ROC curves) for the compounds in the training and test sets. The developed Bayesian model has a 5-fold cross-validated ROC of 0.879, which indicates the accuracy of the model that was built. The test set's ROC score is 0.837, which indicates a strong external validation result.

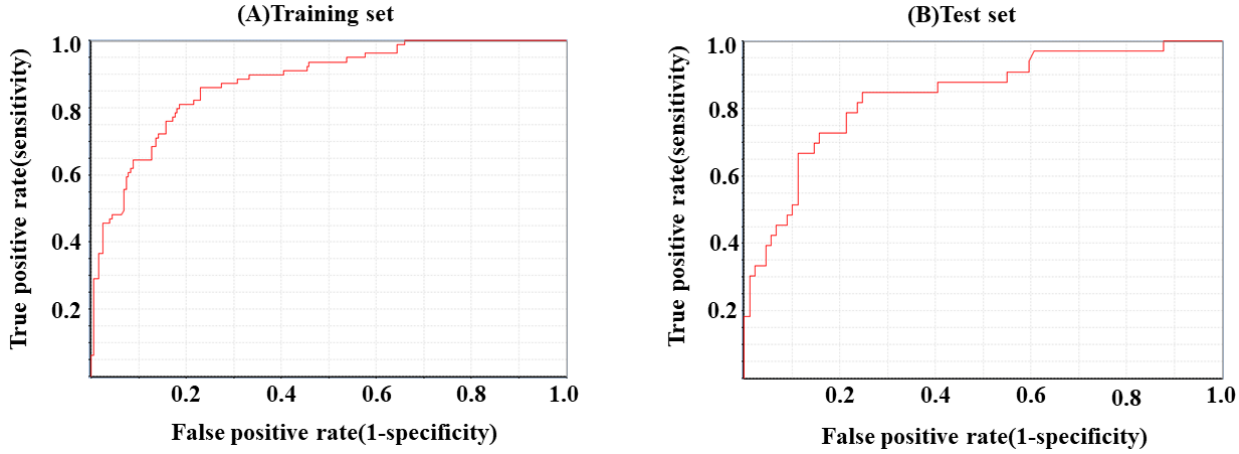

Figure 7. ROC curve for the Bayesian model of (A) training and (B) test set of compounds

Table 4: Statistical parameters of the generated Bayesian model

Set	*ROC score*	*ROC rating*	*TP*	*FP*	*TN*	*FN*	*Se*	*Sp*	*Acc*	*Pr*	*F1*	AUC_b	γ
Training[a]	0.879	Good	71	30	175	8	0.899	0.854	0.866	0.703	0.789	0.876	0.753
Test	0.840	Good	24	14	75	9	0.727	0.849	0.811	0.676	0.676	0.785	0.576

Note: [a]five fold cross-validation result.

The top twenty good fingerprints (G1-G20) and the top twenty bad fingerprints (B1-B20) are presented in **Figure 8.** And **Figure 10.** respectively, based on this Bayesian score. It is evident from **Figure 9.** and **Figure 11.** that the good and bad fingerprints may be combined into fewer structural feature groups, as described below.

For G3, G4, and G12 good fingerprints, N-hydroxy-3,4-dimethyl-1-(4-methylpenta-1,3-dien-3-yl) cyclopentene with carboxamide group is very important for HDAC9 inhibitory activity. Compound **A015** having the G3, G4, and G12 fingerprint possess good HDAC9 inhibition (IC_{50} = 15nM). Similarly, G1 and G13 fingerprints contain 1-(3-fluoro-2-methylphenyl)-N-hydroxy-3,4-dimethylcyclopentene with carboxamide group and 5-isopropyl-1-methyl-5-(prop-1-en-2-yl)-1,4,5,6-tetrahydrocyclopenta[b]pyrrole group containing G2 fingerprint responsible for higher potency in the compound **A210** with IC_{50} value of 39nM. The structural similarities are observed in G6, G16 and G20 fingerprints having 1,5,5-tri(prop-1-en-2-yl)-1,4,5,6-tetrahydrocyclopenta[b]pyrrole group that present in the compound **A217**(IC50 = 44nM).

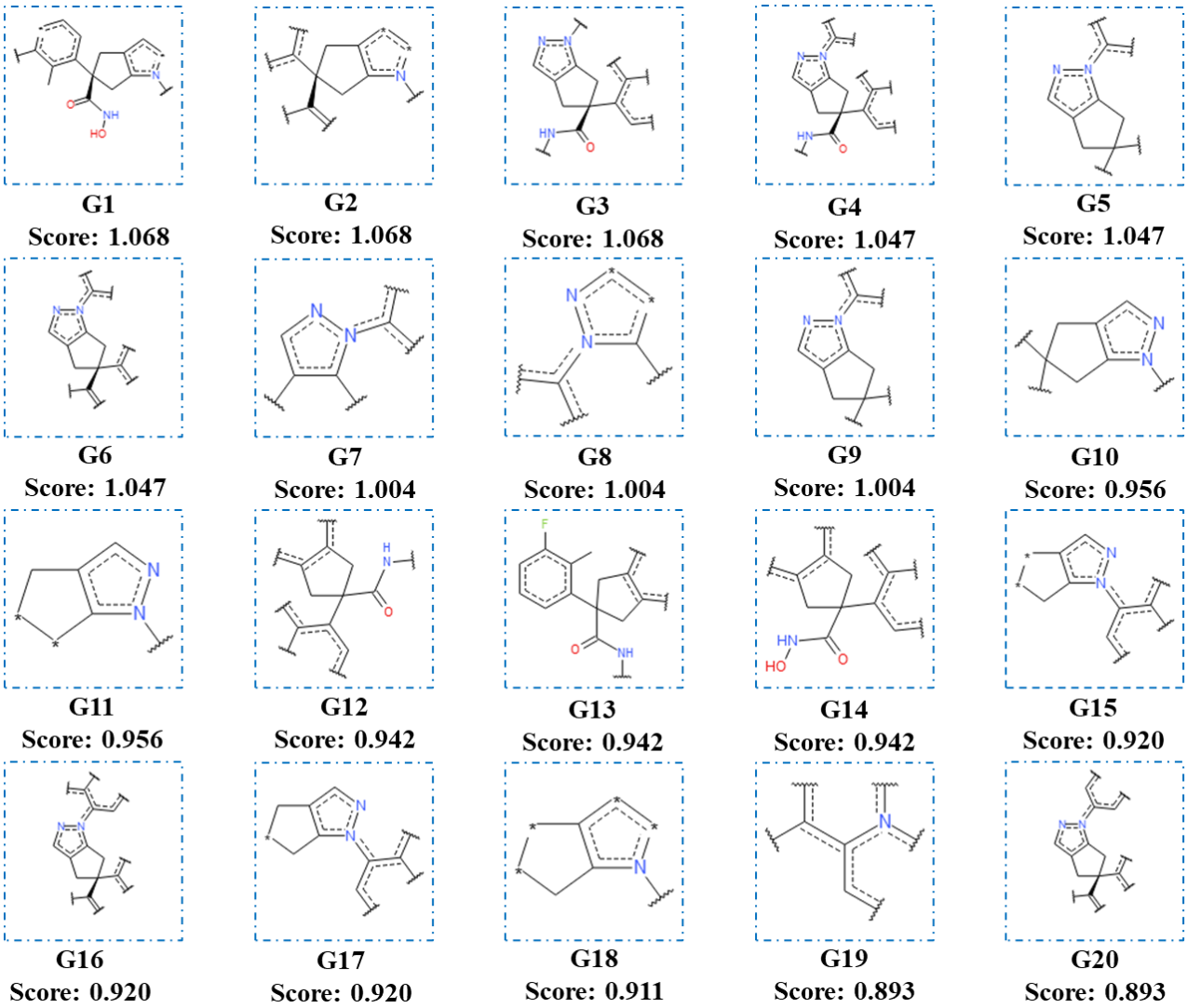

Figure 8. Top twenty good (G1–G20) fingerprints for HDAC9 generated by Bayesian classification study.

The fingerprints G11, G15 and G17 contain 1,4,5,6-tetrahydrocyclopenta[c]pyrazole ring. This is an important ring for showing better HDAC9 inhibitory activity to the compound **A026** (IC_{50} = 27nM). Similarly, for G9 and G10 fingerprints 5,5-dimethyl-1,4,5,6-tetrahydrocyclopenta[c]pyrazole is the most important scaffold for better activity present in compound **A013**(IC_{50} = 12nM).

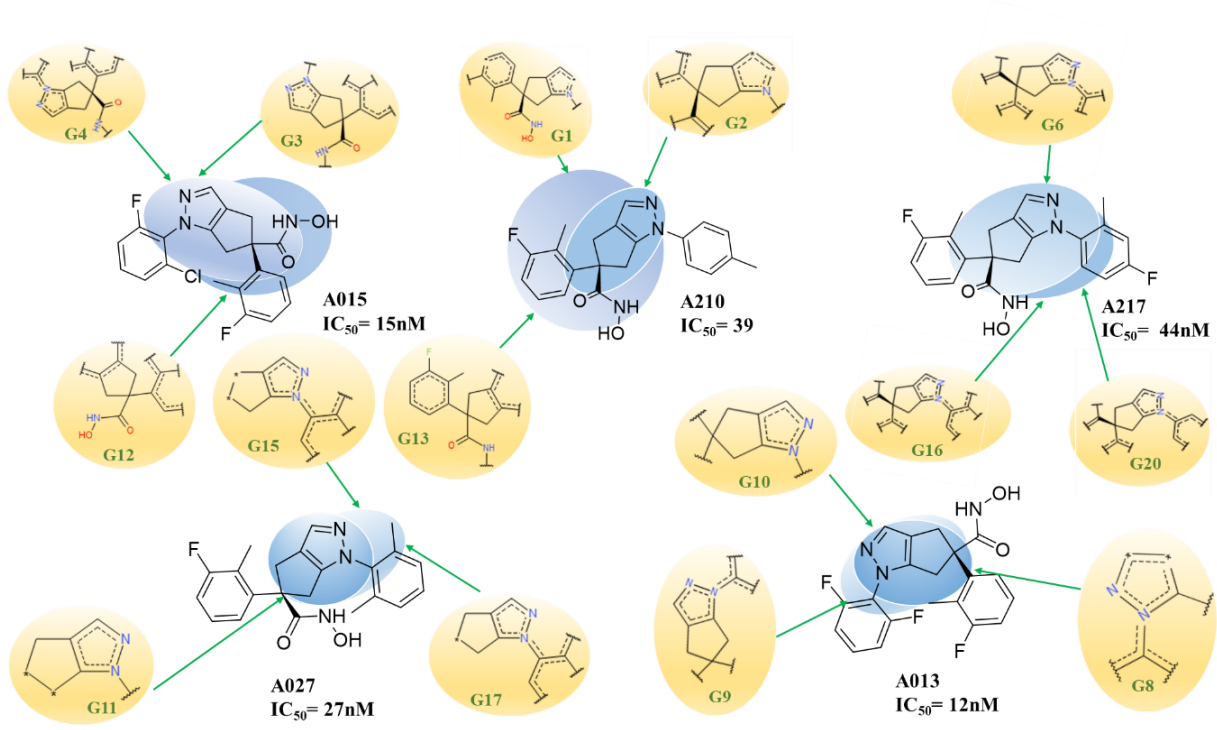

Figure 9. Some common inhibitors as HDAC9 interacting agents contain good fingerprints in their structure

The developed Bayesian model of HDAC9 inhibitors also exports twenty bad (B1-B20) sub-structural fragments, as seen in **Figure 10**. Bad fingerprint B16 indicates that the 1,2-diamine benzene ring is responsible for lower HDAC9 inhibitory activity of the compound **A118** (IC_{50} > 3.33e+4nM).

Similarly, fingerprints B2 and B10 represent carbon chains with amine groups also responsible for bad HDAC9 inhibition. For fingerprints B14, B18 and B20 having the pyrimidine-4 (3H)-one scaffold (for example compound **A051** with IC_{50} >100000nM) that promotes the lower inhibition against HDAC9 enzyme. Some fingerprints containing aromatic rings with multiple substitutions in meta, para and ortho positions (like fingerprints B12, B15 and B19) are responsible for bad inhibitory activity against the HDAC9 enzyme.

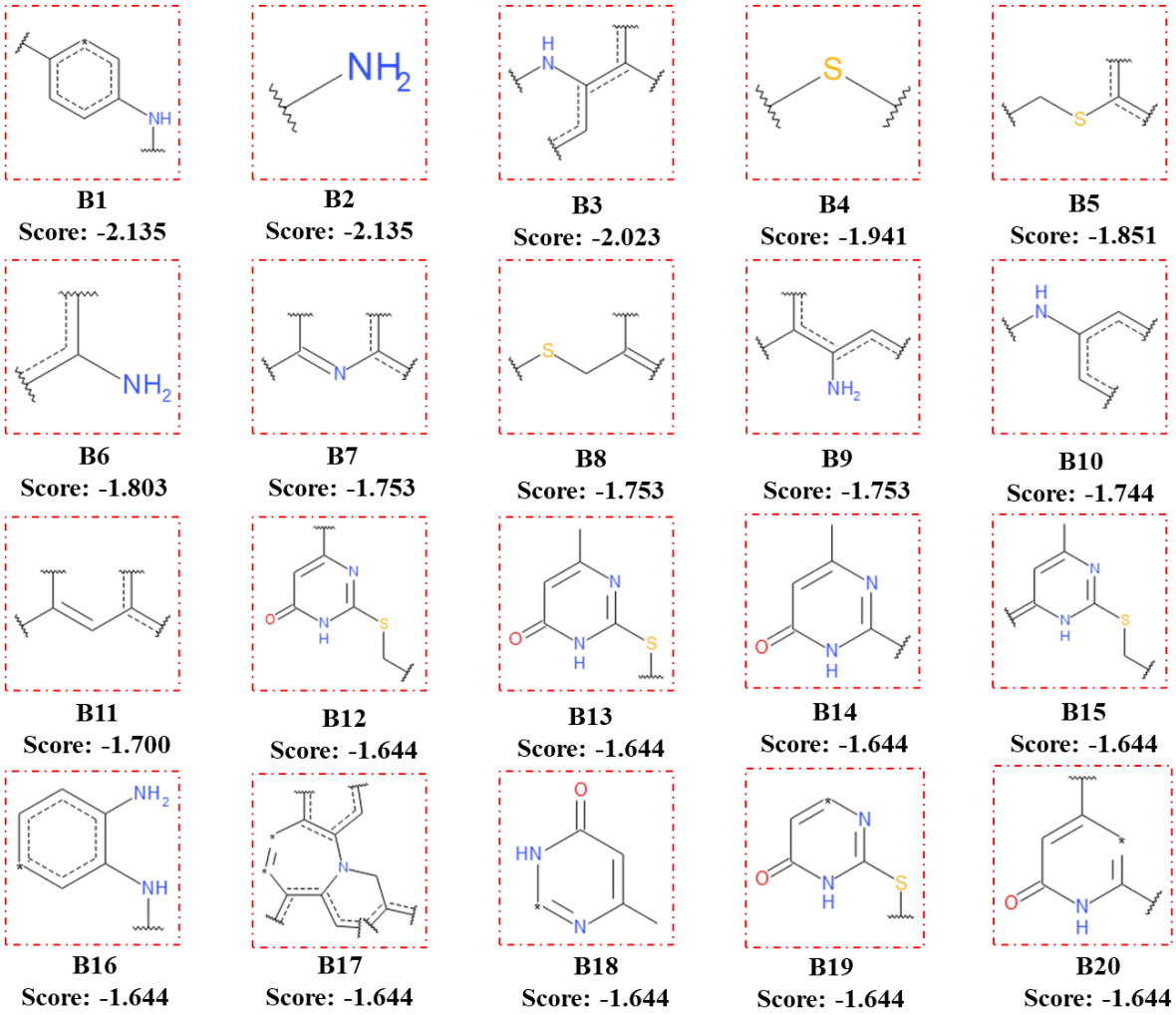

Figure 10. Top twenty bad (B1–B20) fingerprints for HDAC9 generated by Bayesian classification study

Compound **A152**(IC_{50} = 74100nM) consists of such type of fingerprints and shows lower activity. Similarly, some bad fingerprints (B4 and B5) containing carbon chains with the Sulphur group are also responsible for bad HDAC9 inhibition. B1 fingerprint contains an aromatic ring with an amine group attached in the para position. This type of fingerprint is showing poor activity against HDAC9(for example compound **A119** with IC_{50} > 3.33e+4nM).

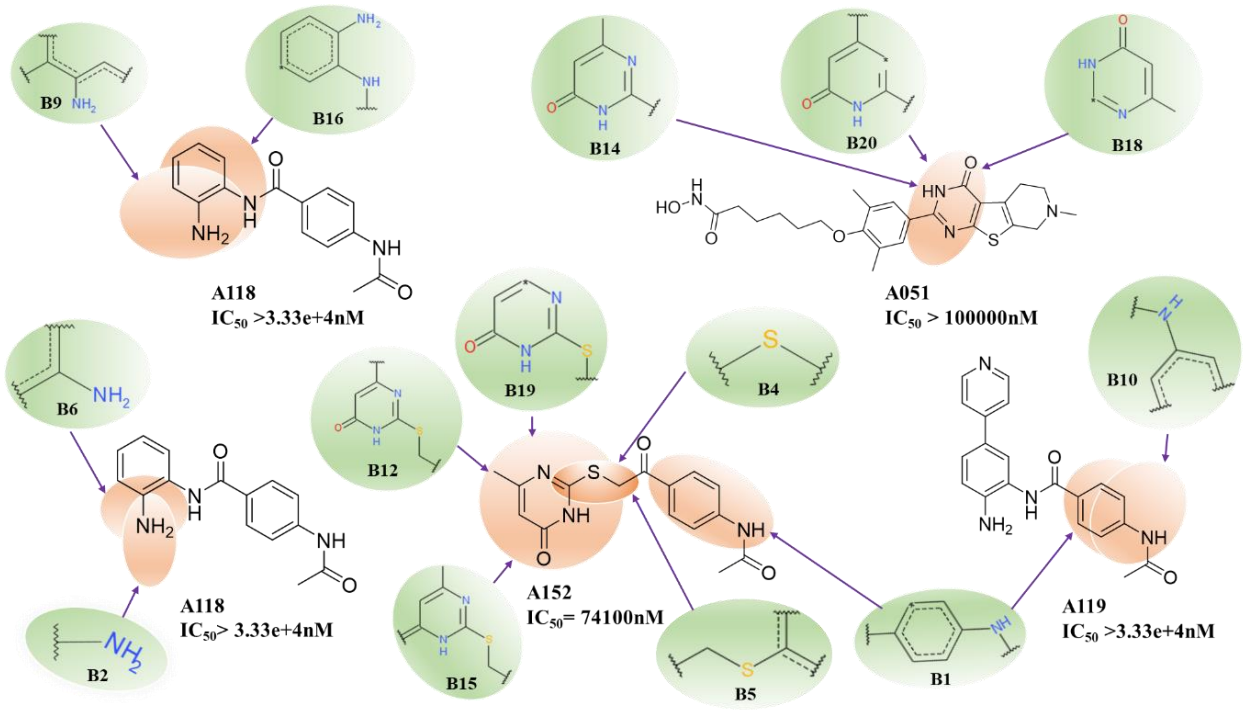

Figure 11. Some common inhibitors contain bad Bayesian fingerprints which are inactive toward the HDAC9 interaction

5.4 Recursive partitioning study

Using several MPs and combinations of MPs and fingerprint characteristics (FCFP_6) in DS 3.0, the default configuration of the RP model was developed. Before the RP model was generated, eight different types of molecular descriptors were computed, including lipophilicity, nR, nAR, nRB, AlogP, MW, nHBA, nHBD, M_FPSA, ECFP_6, and FCFP_6. The same training set was used to build the RP model with six trees. The best tree is Tree 1 with an ROC score of 0.8666, accuracy (Acc) was 0.809, sensitivity (Se) of 0.612, specificity (Sp) of 0.936, precision (Pr) of 0.860, F1 score of 0.715, and AUCb of 0.774. and a 5-fold cross-validation ($ROC_{5\text{-}CV}$) of 0.784. However, the test dataset showed an accuracy of 0.809, along with values for precision (Pr) at 0.757, sensitivity (Se) at 0.675, specificity (Sp) at 0.905, F1 score at 0.714, and AUCb of 0.790 (**Table 6**).

Based on FCFP_6, the most effective decision tree with eight leaves exported five structural fragments (FP-1 to FP-5). As a result, these fingerprint features are critical in distinguishing between active and inactive HDAC9 inhibitors.

Leaf **#1** has an **FP-1** fingerprint containing 1-(3-fluoro-2-methylphenyl)-N-hydroxy-3,4-dimethylcyclopentene with carboxamide moiety is a most important structure to find some potent molecule like compound **A210**(IC_{50} = 39nM). Leaf No. **#5** contains **FP-2** fingerprint which is in charge of adding potency to numerous molecules like compound **A015** (IC50=15nM), compound **A217** (IC_{50} =44nM), and compound **A027**(IC_{50} =27nM) respectively. Leaf **#12, #15,** and **#16** contain **FP-12** which includes an amide linker. Hydrophobicity (AlogP) and

Table 5: Results of the RP model as obtained from the training set of HDAC9 inhibitor

Tree No: Depth: Leaves	***ROC Rating***	***ROC Score***	***TP***	***FP***	***TN***	***FN***	***Acc***	***Pr***	***Se***	***Sp***	***F1***	***AUC_b***	***γ***
1:5:8	**0.784**	**0.866**	**68**	**11**	**162**	**43**	**0.809**	**0.860**	**0.612**	**0.936**	**0.715**	**0.774**	**0.548**
2:5:6	0.776	0.856	69	10	153	52	0.781	0.873	0.570	0.938	0.69	0.754	0.508
3:4:5	0.777	0.835	64	15	161	44	0.792	0.810	0.592	0.914	0.684	0.753	0.506
4:3:4	0.712	0807	58	21	169	36	0.799	0.734	0.617	0.889	0.670	0.753	0.506
5:2:3	0.691	0.753	45	34	191	14	0.830	0.569	0.762	0.848	0.652	0.805	0.610
6:1:2	0.691	0.705	36	43	196	9	0.816	0.455	0.8	0.820	0.580	0.810	0.620

Table 6: Results of the RP model as obtained from the test set of HDAC9 inhibitor

Tree No: Depth: Leaves	***ROC Rating***	***ROC Score***	***TP***	***FP***	***TN***	***FN***	***ACC***	***Se***	***Sp***	***Pr***	***F1***	***AUC_b***	***γ***
1:5:8	**0.816**	**0.816**	**25**	**8**	**77**	**12**	**0.836**	**0.675**	**0.905**	**0.757**	**0.714**	**0.790**	**0.580**
2:5:6	0.813	0.812	25	8	73	16	0.803	0.609	0.901	0.757	0.675	0.755	0.510
3:4:5	0.805	0.805	24	9	75	14	0.811	0.631	0.892	0.727	0.676	0.762	0.523
4:3:4	0.813	0.813	24	9	77	12	0.827	0.666	0.895	0.727	0.695	0.781	0.622
5:2:3	0.732	0.732	17	16	84	5	0.827	0.772	0.84	0.515	0.618	0.806	0.355
6:1:2	0.640	0.640	10	23	87	2	0.795	0.833	0.790	0.303	0.444	0.812	0.623

number of rotatable bonds(nRB) plays a significant role in HDAC9 inhibition. This type of fingerprint was identified in compound **A051**(IC_{50} >100000nM) and showed very poor HDAC9 inhibitory activity. Leaf **#13** contains an **FP-4** fingerprint, that is critical for improving the potency of compounds **A013** (IC_{50} = 12nM) and **A217** (IC_{50} = 44 nM) (shown in **Figure**

12). Leaf **#18** has an **FP-5** fingerprint containing an aromatic ring with multiple substitutions which influences the bad HDAC9 inhibitory activity (compound **A051**, **A152,** and **A119** with IC_{50} > 100000nM, > 3.33e+4nM and > 3.33e+4nM respectively). We may gain a better understanding of the fingerprints that are responsible for a compound's increased activity by using this form of classification-based model development.

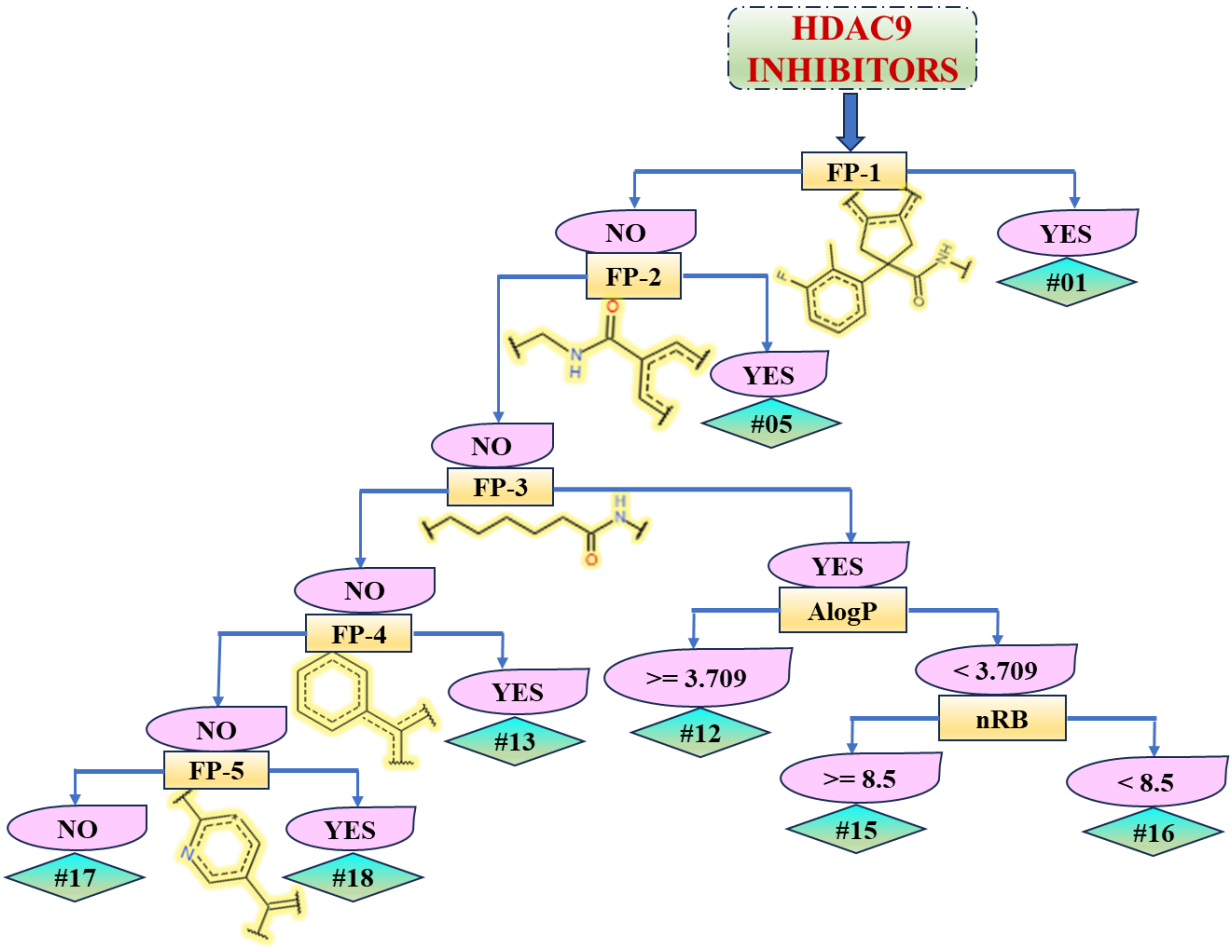

Figure 12. The decision tree generated from the recursive partitioning study, along with the important fingerprints are shown below

5.5 SARpy analysis

To identify the crucial structural signals causing powerful HDAC9 inhibition, the dataset molecules' structural analysis using SARpy was performed. The active ruleset, which has eight substructures, was created using adjustable structural alert variables such as minimum atom count: 2; maximum atom count: 18; and minimum occurrences: 3. Here, we solely took into account the training set's active classes to achieve the best possible sensitivity and specificity

results. Additionally, we used the active ruleset to confirm the outcome using a test set of chemicals. All the information is provided on the validation outcomes. The seven substructures/fingerprints *i.c* c1c2c(n(n1)c1ccccc1)CC(C2)(C(=O)NO), c12CC(Cc1n(nc2))C(=O)NO, N(c1ncc(cn1)C(=O)NO)C, c12c(sc(n1))C(CC2), c2ccc(c(c2)c2ccccc2)C with some of their representative training set (active) of compounds are given in **Table 7.**

Table 7: Seven substructures (SMARTS) with their representative molecular structure obtained from the SARpy training model

Structural alert No.	SMARTS	LR	Fragment
1	c1c2c(n(n1)c1ccccc1)CC(C2)(C(=O)NO)	41.52	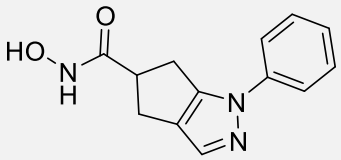
2	c12CC(Cc1n(nc2))C(=O)NO	35.03	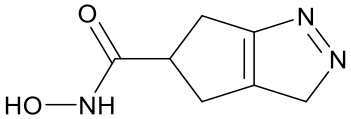
3	N(c1ncc(cn1)C(=O)NO)C	10.38	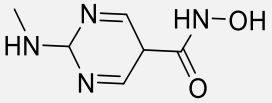
4	c12c(sc(n1))C(CC2)	6.92	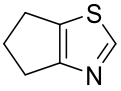
5	c2ccc(c(c2)c2ccccc2)C	5.19	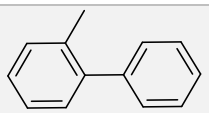
6	c1(ccc(cc1))c1ncc(cn1)C	3.89	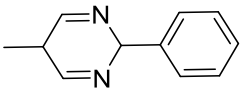
7	CCc1c[nH]c2c1cccc2	3.89	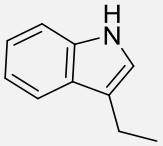

Regarding the structural warnings, it was identified that a few pieces were essential for effectively inhibiting HDAC9. The structure containing N-hydroxy-1-phenyl-1,4,5,6-tetrahydrocyclopenta[c]pyrazole-5-carboxamide moiety having an LR value of 41.52 shows

good HDAC9 inhibitory activity. The importance of N-hydroxy-3,4,5,6-tetrahydrocyclopenta[c]pyrazole-5-carboxamide fragment (LR value 35.03) for imparting effective HDAC9 inhibition. Similarly, N-hydroxy-2-(methylamino)-2,5-dihydropyrimidine-5-carboxamide (LR value 10.38), 5,6-dihydro-4H-cyclopenta[d]thiazole (LR value 6.92), 2-methyl-1,1'-biphenyl (LR value 5.19), 5-methyl-2-phenyl-2,5-dihydropyrimidine (LR value 3.89), 3-ethyl-1H-indole (LR value 3.89), for the imparting potent HDAC9 activity.

5.6 Molecular Docking Studies

The methods section explains how the homology-modeled structure of HDAC9 is produced. The structural alignment between the created model and template structure (shown in Figure **13A**) demonstrates low RMSD values (<1 Å). a Z-score of -8.2, (as seen in Figure **13B**).

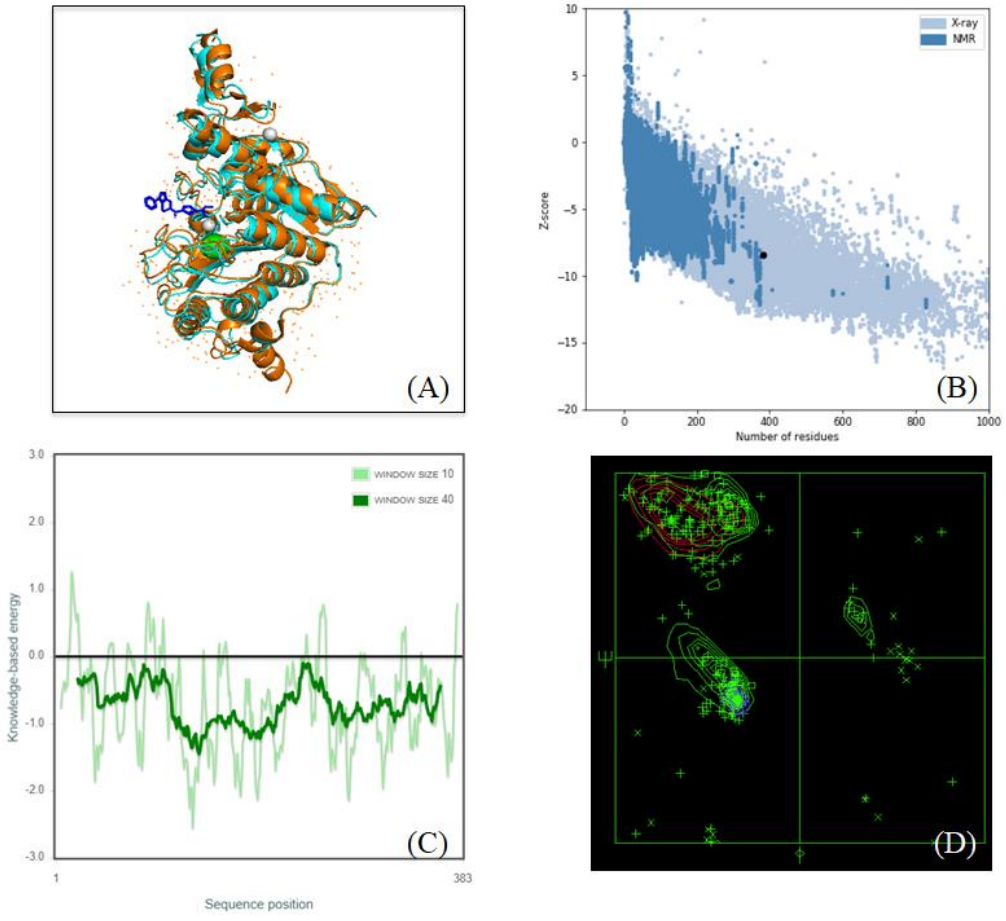

Figure 13: (A) Structural alignment of HDAC4 shown in brown color (PDB: 2VQM) with generated homology shown in Siam color. (B) Homology modeling validations. (C) ProSA analysis (D) Ramachandran plot

The Z-score value of a model indicates its quality, calculated by comparing the structure's total energy to the energy distribution of random conformations. This indicates that the model is of

acceptable quality. The molecular docking analysis of HDAC9's homology structure with four actively anticipated compounds from the Bayesian classification and RP models using LeDock yielded satisfactory results.

The molecular docking was performed for one compound (compound A240) with important fingerprints for HDAC9 inhibition, as identified by the modeling studies. **Figure 14**. depicts the docking poses of the one compound A240. Docking analysis confirmed that the compounds can bind in the same binding pocket where the inbound ligand binds. There are several interactions found to be important for the binding interactions in the case of compound A240.

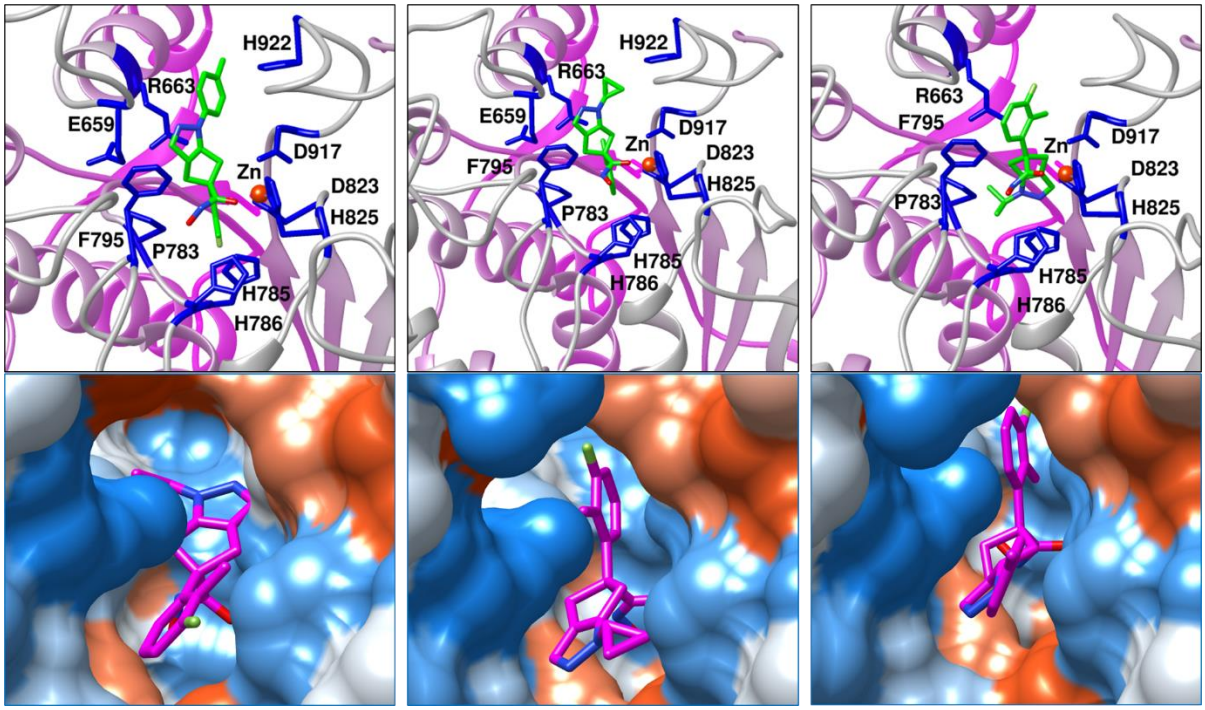

Figure 14: Protein-ligand interaction plot for compounds A210, A223 and A240

In compound **A210**, the amino acids F795 and P783 are involved in alkyl and π-alkyl interaction with hexahydrocyclopenta[c]pyrazole. Additionally, P783 also interacts with fluorobenzene via π-alkyl interaction. A π-anion interaction takes place between amino residue D823 and fluorobenzene. There is a π-π T-shaped interaction is formed between the methyl benzene and amino acid H922. For compound **A223,** the amino residue A914 interacts with the fluorine of fluorobenzene via halogen interaction whereas amino acid D823 interacts with the benzene ring through π-anion bond formation. Amino residues L926 and H922 interact with the cyclopropane ring via alkyl and π-alkyl interaction. Amino residue P783 The amino acid R663 is involved in π-cation interaction with the fluorobenzene moiety of compound **A240**. This moiety also interacts with L926 through alkyl and π-alkyl interaction. The zinc-

binding group is engaged in conventional hydrogen bond interactions with the amino acid G794. Amino acid H785 has participated in π-π stacked interactions with the ligand. Additionally, amino residues G784, C796, H786, F795, K659, P658, H922, F916 and S913 interact through Weaks van der Waals interaction with the ligand (compound **240**).

Table 8: Three best active compounds with corresponding binding affinity with HDAC9 homology protein.

SL no	Name	Binding affinity (kcal/ mol^{-1})
1	A210	-5.13
2	A223	-5.42
3	A240	-4.22

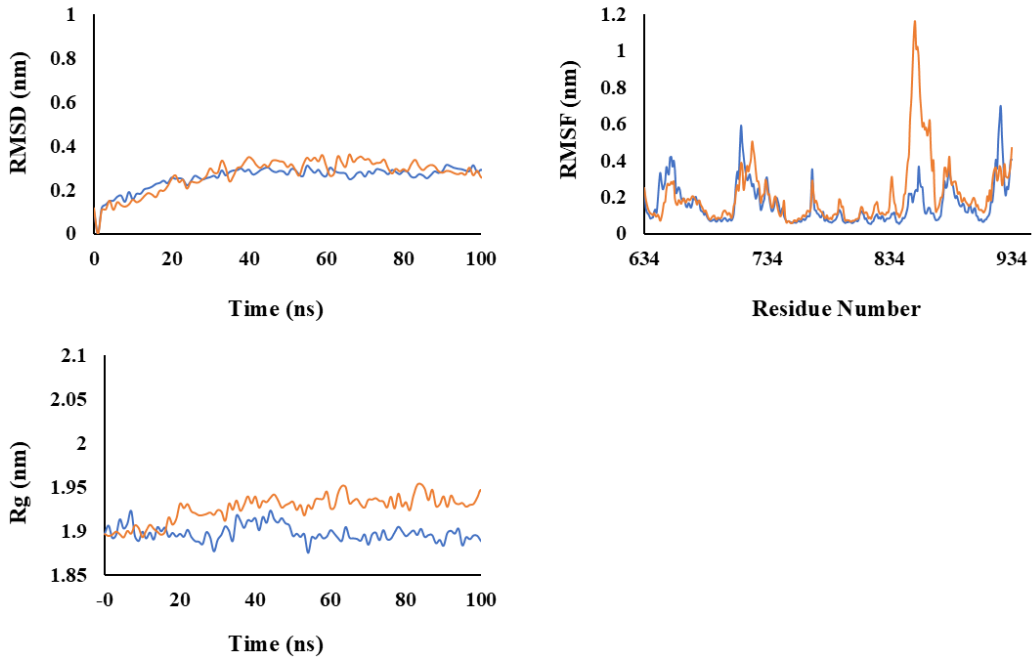

Figure 15: *RMSD, RMSF, and Rg* for the MD analysis of the apo form of HDAC9 and its complex with compound A240

5.7 Molecular Dynamics Simulation

MD simulation was performed for up to 100 ns to assess the stability of the complexes with compound 240 (shown in **Figure 15**). The average *RMSD* of the apo and its complex are found to be 0.37 (apo), and 0.45 (compound 240). The average RMSD values reflect that the complex of A 240 is slightly higher than the apo form. The corresponding average *RMSF* values of amino acid residues are found to be 0.16 (apo form), and 0.21 (compound 240).

The compactness of HDAC9 alone (apo form) and after complex with the compound 240 was determined by doing a comparative analysis of *Rg* data. The mean *Rg* values of 2.14 nm (apo form), and 0.35 nm (compound 240) were computed for the apo form and the complexes with compound 240. This result highlights that the compactness of the ligand-bound form of the complexes is lower than the apo form, indicating the decreased stability of the ligand-bound form of HDAC9.

6. Conclusion and Future Perspective

6. Conclusion and Future Perspective

The purpose of this work was to find the significant fingerprints needed for the HDAC9 protein inhibitors. This molecular modeling investigation found good and poor molecular fingerprints using machine learning (ML), Bayesian classification, and RP (single) tree approaches, with strong statistical validation metrics. The Bayesian classification and SARpy analysis provide insights into important directions and suggest that the 1,4,5,6-tetrahydrocyclopenta[c]pyrazole ring with various substitutes is important for the design of HDAC9 selective inhibitors. In addition to ligand-based drug design, this study also finds a suitable binding site where the ligand actively binds with the HDAC9 protein. Therefore, using a variety of molecular modeling approaches like molecular docking enables us to identify distinct structural fingerprints associated with HDAC9 inhibition. At last, the Molecular dynamics analysis was performed to analyze the stability of the protein along with the potent ligand. Overall, this work provides important details on the fundamental structural characteristics of HDAC9 inhibitors for medicinal research.

7. Annexture-1

SMILE format of the whole dataset of HDAC9 inhibitors

molecule_no	smiles	binary	IC50 (nM)
A001*	N(Cc1ccc(cc1)C(=O)Nc1ccccc1N)C(=O)OCc1cccnc1	1	0.5
A002*	C(CCCCNC(=O)C=C1c2c(cccc2)c2c1cccc2)C(=O)NO	1	2.3
A003*	c1(ccc2c(c1)nccc2)/C=C/C(=O)NCCCCCC(=O)NO	1	2.8
A004*	c1(ccc(cc1F)Cl)/C=C/C(=O)NCCCCCC(=O)NO	1	3.9
A005	C(CCCCNC(=O)/C=C(/C=C/c1ccccc1)\C)C(=O)NO	1	4.2
A006	[C@@H]1(CNC(=O)c2cc3C(CC(=O)Nc3cc2)(C)C)CC[C@H](CC1)/C=C/C(=O)NO	1	5.2
A007	O=C(NO)/C=C/c1ccc(CNCCc2c3c([nH]c2C)cccc3)cc1	1	5.7
A008	c1cc2n(cc(c2cc1)CNCC1CCN(CC1)c1ncc(cn1)C(=O)NO)C	1	6.7
A009	c1cc(ccc1/C=C/C(=O)NO)CN(CCO)CCc1c[nH]c2c1cccc2	1	8.2
A010*	c1cc(ccc1c1noc(n1)C(F)(F)F)C(=O)N[C@@H](CN(CCC)CCC)C	1	10
A011	C1(CCOCC1)(CNC(=O)c1cccc(c2nc(on2)C(F)(F)F)c1)c1nc(cs1)c1ccccc1	1	10
A012	c1c(c(c(cc1)F)n1ncc2c1C[C@](C2)(C(=O)NO)c1cccc(c1C)F)F	1	12
A013	n1cc2c(n1c1c(cccc1)Cl)C[C@@](C2)(c1c(c(ccc1)F)C)C(=O)NO	1	15
A014	c1c2c(n(n1)c1c(cccc1F)Cl)C[C@@](C2)(c1c(c(ccc1)F)C)C(=O)NO	1	15
A015	C(C)(C)(CNC(=O)c1cccc(c1)c1noc(C(F)(F)F)n1)c1nc(oc1)c1ccccc1	1	16
A016	c1c2c(n(n1)c1c(cccc1)F)C[C@](C2)(C(=O)NO)c1c(c(ccc1)F)C	1	17
A017*	c1(n2ncc3c2C[C@](C3)(C(=O)NO)c2c(c(ccc2)F)C)c(c(ccc1)Cl)F	1	17
A018*	c12C[C@@](Cc1cnn2c1c(cccc1C)F)(c1c(c(ccc1)F)C)C(=O)NO	1	19
A019*	N1(Cc2ccc(c(c2)c2ccccc2)C(=O)NO)C(=O)c2c(C1=O)cccc2	1	20
A020	c1cc(ccc1C(=O)/C(=C/[C@@H](C)/C=C/C(=O)NO)/C)N(C)C	1	20
A021*	c1ccccc1NC(=O)CCCCCCC(=O)NO	1	20
A022	c1c2c(n(n1)c1cc(ccc1C)C)C[C@@](C2)(c1cccc(c1C)F)C(=O)NO	1	21
A023	c1c2c(n(n1)c1c(cccc1)C)C[C@](C2)(C(=O)NO)c1c(c(ccc1)F)C	1	23
A024	C(=O)(CCCCCCC(=O)Nc1cc2CCC(=O)Nc2cc1)NO	1	25
A025*	c1(cccc([C@@]2(C(=O)NO)c3c(CC2)n(nc3)Cc2ccccc2)c1C)F	1	27
A026*	c12C[C@@](Cc1cnn2c1c(cccc1C)C)(c1cccc(c1C)F)C(=O)NO	1	27
A027	c1c2c(n(n1)c1ccccc1)C[C@](C2)(C(=O)NO)c1c(c(ccc1)F)C	1	28
A028	c1(cccc(c1C)F)[C@@]1(Cc2cnn(c2C1)c1cc(ccc1)C)C(=O)NO	1	28
A029	c1cc2c(cc1S(=O)(=O)N1CCN(CC1)c1ncc(cn1)C(=O)NO)cccc2	1	28
A030	C[C@H](/C=C/C(=O)NO)/C=C(\C)/C(=O)c1ccc(cc1)N(C)C	0	8861
A031	N1(Cc2ccc(cc2)C(=O)NO)c2c(CC[C@H]3[C@H]1CCCC3)cccc2	0	8900
A032*	c1ccc2c(c1)c(c([nH]2)C)/C=C/c1c(cccc1)c1ccc(cc1)/C=C/C(=O)NO	0	8900
A033	c1(ccc(cc1)/C=C/C(=O)NO)c1ccc(cc1)O	0	8920
A034*	C1(=O)N([C@@H](C(=O)N1c1ccc(cc1)Cl)CCC(=O)Nc1ccc(cc1)C(=O)NO)Cc1ccc(cc1)Br	0	9100
A035*	c1(ccc2c3c1cccc3c(=O)n(c2=O)CCCCCC(=O)NO)NCc1ccccc1	0	9300
A036	c1c(cccc1)c1c2c(sn1)C[C@@](C2)(c1c(c(ccc1)F)C)C(=O)NO	0	9700
A037	c1(ccc(s1)Cc1cc(c(cc1)OCC)c1nc2c(c(=O)[nH]1)n(nc2CCC)C)C(=O)NO	0	>10000
A038*	c1(c(cc2c(c1)oc(n2)Nc1cc(ccc1)C(=O)NO)Cl)Cl	0	>10000

A039	O=C(NO)c1c2c(C(C)(C)N(c3[nH]c4cc(ccc4n3)C(F)(F)F)C2)ccc1	0	>10000
A040	c1c(c(ccc1)c1[nH]c2c(n1)cc(cc2)C(=O)NO)C(F)(F)F	0	>10000
A041	OCCN(C(=O)Cc1ccc(C(=O)NO)cc1)c1ccccc1	0	>10000
A042	c1c(ccc(c1)/C=C/C(=O)NNCCC)CNCCc1c([nH]c2c1cccc2)C	0	>10000
A043*	c1(ccc2c3c1cccc3c(=O)n(c2=O)CCCCCC(=O)NO)NCCC	0	>10000
A044	c1(ccc(cc1)C(=O)Nc1cc(ccc1N)c1cccs1)NC(=O)C	0	>1.0e+4
A045	C12(C(=O)NC1)CCN(c1ccc(C(=O)Nc3cc(ccc3N)c3cccs3)cn1)CC2	0	>1.0e+4
A046	SCC/C=C/[C@@H]1CC(=O)N[C@@H](c2scc(C(=O)N/C(=C\C)/C(=O)N[C@H](C(=O)O1)C(C)C)n2)C(C)C	0	>10000
A047	SCC/C=C/[C@@H]1CC(=O)NCc2scc(C(=O)N/C(=C\C)/C(=O)N[C@H](C(=O)O1)C(C)C)n2	0	>10000
A048	S(CC/C=C/[C@@H]1CC(=O)NCc2scc(C(=O)N/C(=C\C)/C(=O)N[C@H](C(=O)O1)C(C)C)n2)C(=O)C	0	>10000
A049*	c1ccc2c(c1)c(nc(n2)C)N(c1cc(c(cc1)OC)OCCCC(=O)NO)C	0	>10000
A050	n1c([nH]c(=O)c2c1sc1c2CCN(C1)C)c1cc(c(c(c1)C)OCCCCCC(=O)NO)C	0	>10000
A051	c1(cc(cc(c1)C(F)(F)F)C(=O)N(c1ccc(cc1)C(=O)NO)C(C)C)C(F)(F)F	0	>10000
A052	c1c(cc2c(c1)ccn2Cc1ccc(cc1)OC)C(=O)NO	0	>10000
A053	O=S(=O)(c1ccc(cc1)c1cn(nc1)C)n1ccc(c1)/C=C/C(=O)Nc1ccccc1N	0	>10000
A054	c1ncccc1/C=C/C(=O)NCc1ccc(cc1)C(=O)Nc1ccc(cc1N)F	0	>10000
A055	n1c(nc2c(c1N1CCOCC1)ncn2CCCCCCC(=O)NO)c1ccc(nc1)N	0	>10000
A056	n1c(nc2c(c1N1CCOCC1)ccn2CCCCCCC(=O)NO)c1cnc(nc1)N	0	>10000
A057*	C(=O)(/C=C/c1cc2nc(n(c2cc1)CCN(CC)CC)CCCC)NO	0	>10000
A058	c1(nc2n(c1)cccc2)c1cc(ccc1)c1nc2c([nH]1)cc(cc2)C(=N)NO	0	>10000
A059	FC(F)(c1nc(c2cc3nc(c4cc(c5nc6n(c5NC(C)(C)C)ccnc6)ccc4)[nH]c3cc2)no1)F	0	>10000
A060*	[C@@H](Oc1cc(N(c2c3ccccc3nc(n2)C)C)ccc1OC)(C(=O)NO)C(C)C	0	>10000
A061	n1c2c(c3n(c1N)nc(n3)c1occc1)cnn2CCc1ccc(cc1)C(=O)Nc1ccccc1N	0	>10000
A062	N(c1c(N)cccc1)C(=O)CCCCCCC(=O)Nc1ccccc1	0	>10000
A063	c1ccc(cc1S(=O)(=O)N(c1ccccc1)C)/C=C/C(=O)NO	0	>10000
A064	c1ccc(cc1S(=O)(=O)N(CCc1ccccc1)C)/C=C/C(=O)NO	0	>10000
A065	c1c(ccc(c1)/C=C/C(=O)NO)CNC[C@]12C[C@H]3C[C@H](C[C@@H](C1)C3)C2	0	>10000
A066	c1c(cc2c(c1)C=C(CC2)C(=O)NO)CN(C[C@]12C[C@H]3C[C@H](C[C@@H](C1)C3)C2)C	0	>10000
A067	c1(/C=C/C(=O)NO)ccc(cc1)CNCC1CCCCC1	0	>10000

A068	O=C(N)c1c2c(C(C)(C)N(C2)c2cnc(cn2)C(F)(F)F)ccc1	0	>10000
A069	O=C(NO)c1c2c(C(C)(C)N(C2)c2cnc(cn2)C(F)(F)F)ccc1	0	>10000
A070	c1ccc(c(c1)CN1C[C@H](CC1)O)NC(=O)CCCCCCC(=O)NO	0	>10000
A071	C(=O)(/C=C/c1ccc(cn1)NC(=O)[C@H](Cc1ccccc1)c1ccccc1)NO	0	10600
A072*	c1(cc(on1)CN1CCOCC1)c1ccc(cc1)/C=C/C(=O)NO	0	11200
A073	c1c(ccc(c1)C(=O)COc1nc(cc(=O)[nH]1)C)NC(=O)C	0	11700
A074*	c1c(ccc(c1)/C=C/C(=O)NO)/C=N/OCc1c(c(c(c(c1F)F)F)F)F	0	12000
A075	c1ccc2c(c1)c(c1c(n2)cccc1)Nc1cccc(c1)C(=O)NO	0	12180
A076*	O=S1(=O)C[C@@H]2[C@H](N(c3c1cccc3)Cc1ccc(cc1)C(=O)NO)CCCC2	0	13000
A077	C1Cc2c(N(Cc3ccc(cc3)C(=O)NO)[C@H]3[C@H](C1)CCCC3)cccc2	0	13000
A078	c1([C@@H]2CN(C[C@H]2C(=O)Nc2ccc(cc2)Cl)C)ccc(/C=C/C(=O)Nc2c(cccc2)N)cc1	0	13000
A079*	c1c(ccc(c1)/C=C/C(=O)NO)/C=N/OCCN1CCOCC1	0	13100
A080*	c1ccc2c(c1)c(Nc1ccc(cc1)C(=O)NO)ccn2	0	13230
A081*	c1ccc2c(c1)n(cc2C)Cc1ccc(cc1)C(=O)NO	0	14500
A082	C1CC[C@H]2[C@H](C1)[C@H](C[C@@H]2C)c1ccc(cc1)C(=O)NO	0	14500
A083	c1c(ccc(c1)/C=C/C(=O)NO)CN(C[C@]12C[C@H]3C[C@H](C[C@@H](C1)C3)C2)C	0	>15000
A084	C1(=O)N([C@@H](C(=O)N1c1ccc(cc1)Cl)CCC(=O)Nc1ccc(cc1)C(=O)NO)Cc1ccccc1	0	15200
A085*	c1ccc2c(c1)CC(C2)(c1ccccc1)C(=O)NO	0	15300
A086	c1([C@H]2CN(C[C@@H]2C(=O)Nc2ccc(cc2)Cl)C)ccc(/C=C/C(=O)Nc2c(cccc2)N)cc1	0	16000
A087	C(/C=C/[C@@H]1CC(=O)NCc2scc(n2)c2n(CC(=O)N[C@H](C(=O)O1)C(C)C)nnn2)CS	0	16200
A088	C(=O)(c1ccc(cc1)CN(C(=O)Nc1ccc(cc1)CN)CCCC)NO	0	17300
A089	c12CC[C@@](Cc1cnn2c1ccccc1)(c1c(c(ccc1)F)C)C(=O)NO	0	17300
A090	C(=O)(CCCCc1nn(cc1)Cc1ccc(cc1)Nc1ccccc1)NO	0	18300
A091*	C1CC[C@@H]2[C@H](C1)[C@H]([C@@H](C2)C)c1ccc(cc1)C(=O)NO	0	18300
A092	c1ccc2c(c1)n(c(c2)C)Cc1ccc(cc1)C(=O)NO	0	18300
A093	C1(c2ncc3c(n2)CC[C@]3(C(=O)NO)c2cccc(c2C)F)CC1	0	19400
A094	c12CC[C@@](Cc1cn(n2)c1ccccc1F)(c1c(c(ccc1)F)C)C(=O)NO	0	19800
A095	C(=O)([C@H](Cc1ccccc1)n1nnc(c1C#Cc1ccccc1)c1ccccc1)NO	0	>20000
A096	C(=O)([C@H](Cc1ccccc1)n1nnc(c1C#CC1CC1)c1ccccc1)NO	0	>20000
A097	n1c(sc(c1C(=O)N[C@H](c1ccc(cc1)C(=O)NO)C)C1CC1)c1ncc(s1)c1ccccc1	0	>20000
A098	c1(CN[C@]23C[C@H]4C[C@H](C[C@@H](C2)C4)C3)cccc(c1)/C=C/C(=O)NO	0	>20000
A099*	C1(=O)N(c2c(S(=O)(=O)c3c1cc(cc3)OC)cccc2)CCCCCC(=O)NO	0	>20000
A100*	N1CCN(CC1)c1ccc2c(n1)ccc(c2)C(=O)Nc1cc(ccc1N)c1cccs1	0	>20000
A101	C1[C@H]2[C@H](N(Cc3ccc(cc3)C(=O)NO)c3c1cccc3)CCCC2	0	25000
A102*	N1(Cc2ccc(cc2)C(=O)NO)c2c(S(=O)c3c1cccc3)cccc2	0	27570
A103*	C(=C\CCC(=O)O)/C[C@H]1NC(=O)[C@H](NC(=O)[C@@H](C)NC(=O)[C@@H](C(C)C)NC(=O)[C@H]1C)Cc1ccccc1	0	28000
A104*	c1ccc2c(c1)c(c1c(n2)cccc1)Nc1ccc(cc1)CCC(=O)NO	0	28960

A105	S1c2c(N(Cc3ccc(cc3)C(=O)NO)c3c1ccc(c3)OC)cccc2	0	29700
A106	c1c(ccc(c1)C(=O)NO)CN(CCCCO)C(=O)Nc1ccccc1	0	29700
A107	c1ccc2c(c1)n(c1c2CN(CC1)C)Cc1ccc(cc1)C(=O)NO	0	>30000
A108*	c1cc(ccc1C(=O)Nc1ccc(cc1N)F)NC(=O)C	0	>30000
A109*	C1c2c(N(Cc3ccc(cc3)C(=O)NO)[C@H]3[C@H]1CCCCC3)cccc2	0	>30000
A110	C1Cc2c(N(Cc3ccc(cc3)C(=O)NO)[C@H]3[C@H](C1)CCCC3)cc(cc2)C(F)(F)F	0	>30000
A111	C(=O)(c1ccc(cc1)CCn1c(=O)c2c3c(c1=O)ccc(c3ccc2)N1CCOCC1)NO	0	>30000
A112	c1ccc(c(c1)C(=O)N)Nc1cccc(c1)OCCc1ccccc1	0	>30000
A113	c1(C(=O)N[C@H](C(=O)NO)C(N)(C)C)ccc(cc1)OCC#CC	0	>30000
A114	c1cccc(c1)NC(=O)CCCCCC[C@@H](C(=O)NC)N=O	0	30700
A115	c1(ccc2c(c1)c(c1c(n2)cccc1)Nc1ccc(cc1)C(=O)NO)OC(F)(F)F	0	31100
A116*	C(/C=C/[C@@H]1CC(=O)NCc2scc(n2)c2nnn(c2)CC(=O)N[C@H](C(=O)O1)C(C)C)CS	0	32000
A117	c1(ccc(cc1)C(=O)Nc1ccccc1N)NC(=O)C	0	>3.33e+4
A118	c1cc(ccc1C(=O)Nc1cc(ccc1N)c1ccncc1)NC(=O)C	0	>3.33e+4
A119	c1ccc(cc1)C(=O)NO	0	>33330
A120	C(=O)(NO)C1=CCCC1	0	>33330
A121	[C@@H]1(C(=O)Nc2c(ccc(c2)c2ccc(cc2)F)N)C[C@H]2CC[C@@H](C1)O2	0	>33330
A122	C(=O)(N[C@@H](C(=O)O)c1ccccc1)c1cccc(=S)n1O	0	34000
A123*	C(/C=C/[C@@H]1CC(=O)NCc2scc(n2)c2nnn(n2)CC(=O)N[C@H](C(=O)O1)C(C)C)CS	0	34600
A124	c1(ccc2c(c1)C[C@@H](CC2)Nc1nccc(n1)c1cccnc1)C(=O)NO	0	35000
A125*	N1(Cc2ccc(cc2)C(=O)NO)c2c(Sc3c1cccc3)cccc2	0	36470
A126	o1c(cc(n1)C(=O)NO)CCNC(=O)c1cc(c(cc1)Cl)Cl	0	38200
A127	c1(ccc(cc1)/C=C/C(=O)NO)c1ccc(cc1)OC	0	39000
A128*	c1c(cc2c(c1)c(c1c(n2)ccc(n1)OC)Nc1ccc(cc1)C(=O)NO)Cl	0	>40000
A129	c1ccc2c(c1)c(Nc1ccc(cc1)C(=O)NO)c1c(n2)CCCC1	0	>40000
A130	c1ccc2c(c1)N(c1c([S@@]2=O)ccc(c1)/C(=N/O)/C)Cc1ccc(cc1)C(=O)NO	0	>40000
A131	c1c(ccc(c1)/C=C/C(=O)NO)CN(C[C@]12C[C@H]3C[C@H](C[C@@H](C1)C3)C2)CCF	0	>40000
A132	c1(c(ccc(c1)c1ccc(cc1)/C=C/C(=O)NO)O)[C@]12C[C@@H]3C[C@H](C1)C[C@@H](C3)C2	0	41000
A133	c1(cc(ccc1CC#N)c1c(cc(cc1)/C=C/C(=O)NO)Cl)[C@]12C[C@@H]3C[C@H](C1)C[C@@H](C3)C2	0	42000
A134	CN1C[C@H](c2c(cc(/C=C/C(=O)Nc3c(cccc3)N)cc2)F)[C@H](C1)C(=O)Nc1ccc(cc1)Cl	0	43000
A135*	c1c(=S)n(c(cc1)C(=O)O)O	0	47000
A136*	C(=O)(CCCCc1nn(cc1)Cc1ccc(cc1)c1ccccc1)NO	0	47200
A137	C(=O)(CCCCc1nn(cc1)Cc1cc(ccc1)c1ccccc1)NO	0	48900
A138*	c1ccc2c(c1)CC[C@]2(c1ccccc1)C(=O)NO	0	>50000

A139*	C(=O)(/C=C/c1ccccc1)NO	0	>50000
A140	C(=O)(/C=C/c1cc2nc(n(c2cc1)CCN(C)C)CCCC)NO	0	>50000
A141	c1(c(ccc(c1)/C=C/C(=O)NO)CNC[C@]12C[C@H]3C[C@H](C[C@@H](C1)C3)C2)F	0	>50000
A142	c1(c(ccc(c1)/C=C/C(=O)NO)CN(C[C@]12C[C@H]3C[C@H](C[C@@H](C1)C3)C2)C)F	0	>50000
A143	[C@@H]12CC(=O)N[C@@H](C(=O)N[C@@H](C(=O)N[C@@H]([C@H](CC(=O)O1)O)[C@H](CC)C)CSSCC/C=C/2)CCCC	0	>50000
A144*	C(=O)(CCCCSc1nc(cc(=O)[nH]1)c1ccc(cc1)c1ccccc1)NO	0	>50000
A145*	C(=O)(CCCCCC(c1c[nH]c2c1cccc2)c1c[nH]c2c1cccc2)Nc1ccccc1N	0	50000
A146*	C(=O)(CCCCc1nn(cc1)c1ccccc1)NO	0	55800
A147*	Ic1c(O)c2ncccc2c(Cl)c1	0	57000
A148*	C(=O)(N[C@@H](C(=O)O)C)c1cccc(=S)n1O	0	58000
A149*	c1(ccc2c(c1)CN(CC2)Cc1ccc(o1)c1cccc(c1)[N+](=O)[O-])C(=O)NO	0	65800
A150*	c1cc(ccc1/C=C/C(=O)NO)OC	0	>70000
A151	c1c(ccc(c1)C(=O)CSc1[nH]c(=O)cc(n1)C)NC(=O)C	0	74100
A152	C(=O)(NO)C(CCC)CCC	0	91000
A153	c1ccc2c(c1)C(=O)c1c(C2=O)ccc(c1)/C=C/C(=O)NO	0	>100000
A154	C1(NC(=O)CCCCCC[C@@H](C(=O)NC)N=O)c2c(cccc2)c2c1cccc2	0	>100000
A155	c1cc(ccc1C(=O)NNCCCC)Br	0	>100000
A156	C1(=O)N([C@@H](C(=O)N1c1ccc(cc1)Cl)CCC(=O)Nc1ccc(cc1)C(=O)NO)Cc1ccc(cc1)C	0	>100000
A157	c1cc(cc(c1)NC(=O)CCCCCC[C@@H](C(=O)NC)N=O)Br	0	>100000
A158	c1c(ccc(c1)C(=O)CSc1nc(ccn1)C)NC(=O)C	0	>100000
A159	c1c(ccc(c1)C(=O)CSc1nc(cc(n1)OC)C)NC(=O)C	0	>100000
A160	c1c(ccc(c1)C(=O)CSc1nc(cc(n1)C)C)NC(=O)C	0	>100000
A161	c1c(ccc(c1)C(=O)CSc1cc(ccc1)O)NC(=O)C	0	>100000
A162	c1c(ccc(c1)C(=O)COc1cc(cc(=O)[nH]1)C)NC(=O)C	0	>100000
A163*	c1(nc(cc(=O)[nH]1)C)SCc1ccc(cc1)NC(=O)C	0	>100000
A164	c1(nc(cc(=O)[nH]1)C)SC[C@@H](c1ccc(cc1)NC(=O)C)O	0	>100000
A165	c1(nc(cc(=O)[nH]1)C)SCC(=O)c1ccccc1	0	>100000
A166	c1(nc(cc(=O)[nH]1)C)SCC(=O)c1ccc(cc1)N(C(=O)C)C	0	>100000
A167*	c1(nc(cc(=O)[nH]1)C)SCC(=O)c1ccc(cc1)NC(=O)c1ccccc1	0	>100000
A168	S(c1[nH]c(=O)cc(n1)C)CC(=O)c1ccc(OC)cc1	0	>100000
A169*	c1(nc(cc(=O)[nH]1)C)SCC(=O)c1ccc(cc1)C(C)(C)C	0	>100000
A170	c1(nc(cc(=O)[nH]1)C)SCC(=O)c1ccc(cc1)Cl	0	>100000

A171	c1(nc(cc(=O)[nH]1)C)SCC(=O)c1ccc(cc1)O	0	>100000
A172	S(CC(=O)c1cc(O)c(O)cc1)c1nc(cc(=O)[nH]1)C	0	>100000
A173*	c1(nc(cc(=O)[nH]1)C)SCC(=O)c1cc2c(cc1)OCCO2	0	>100000
A174*	c1(nc(cc(=O)[nH]1)C)SCC(=O)c1sccc1	0	>100000
A175*	c1(nc(cc(=O)[nH]1)C)SCC(=O)OC	0	>100000
A176*	c1(nc(cc(=O)[nH]1)C)SCC(=O)C	0	>100000
A177	c1(nc(cc(=O)[nH]1)C)SCC(=O)C(C)(C)C	0	>100000
A178	c1(nc(cc(=O)[nH]1)C)SCC(=O)CC(=O)OCC	0	>100000
A179	c1(nc(cc(=O)[nH]1)C)SCC(=O)NCCCCc1ccccc1	0	>100000
A180*	S(CC(=O)NCCc1ccccc1)c1nc(cc(=O)[nH]1)C	0	>100000
A181	c1(nc(cc(=O)[nH]1)C)SCC(=O)NCCCCCCc1ccccc1	0	>100000
A182	c1(nc(cc(=O)[nH]1)C)SCC(=O)c1cc2c(cc1)CC(=O)N2	0	>100000
A183	C(CCC(=O)Nc1ccccc1N)CCC(=O)Nc1ccc(cc1)C	0	>100000
A184	c1c(ccc(c1)/C=C/C=C/C(=O)NO)c1ccc(cc1)OC	0	>100000
A185	C(=O)(NO)/C=C/C=C/c1ccc(c2ccc(c(c2)[C@]23C[C@@H]4C[C@H](C2)C[C@@H](C4)C3)OC)cc1	0	>100000
A186	N(Cc1ccc(cc1)C(=O)Nc1ccccc1N)C1=N[C@@H]([C@@H](O1)c1ccccc1)c1ccccc1	0	>100000
A187	C(=O)(/C=C/c1ccc(cc1)C(F)(F)F)NO	0	>100000
A188*	c1cc(cc2c1cccc2)NC(=O)CCCCCC[C@@H](C(=O)NC)N=O	0	>100000
A189*	n1cc(cc2c1cccc2)NC(=O)CCCCCC[C@@H](C(=O)NC)N=O	0	>100000
A190	c12cc(oc1cccc2)c1nc2c(cccc2)c(c1)C(=O)NC(c1ccccc1)c1ccccc1	0	>200000
A191	[O-][N+](=O)c1c(N)cc(N2CCN(CC2)C)cc1	0	>200000
A192*	C(=O)(NO)CCCc1ccccc1	0	430000
A193	C(C)CC(=O)O	0	>2000000
A194	C(CC(CCC)C(=O)O)C	0	>2000000
A195*	[O-]C(=O)CCCc1ccccc1	0	>2000000
A196	CCCC(=O)NO	0	>2000000
A197*	c12C[C@](Cc1cnn2c1c(cc(cc1)F)F)(C(=O)NO)c1cccc(c1C)F	1	29
A198	c1c(ccc(c1)C(=O)N[C@@H](CN1[C@H](CCC1)C)C)c1noc(n1)C(F)(F)F	1	30
A199*	c1(ccc(cc1)[C@@H](c1ccccc1F)C(=O)NO)c1cnc(nc1)C	1	30
A200	c1c2c(n(n1)c1ncc(cc1)F)C[C@](C2)(C(=O)NO)c1c(c(ccc1)F)C	1	31
A201	C(=O)(CCCCCCNC(=O)c1cc2ccc(nc2cc1)OC)NO	1	34

A202*	C(=O)(CCCCCCNC(=O)c1cc2CCC(=O)Nc2cc1)NO	1	35
A203*	c1(c(cccc1[C@@]1(C(=O)NO)Cc2c(C1)cnn2c1c(cc(cc1)F)Cl)F)C	1	36
A204*	C1(n2ncc3c2C[C@](C3)(C(=O)NO)c2cccc(c2C)F)CCCC1	1	37
A205*	C(=C\C(=O)NO)/c1ccc(CNC(=O)c2cc3C(CC(=O)Nc3cc2)(C)C)cc1	1	37
A206	c1c2c(n(n1)c1nccnc1)C[C@](C2)(C(=O)NO)c1cccc(c1C)F	1	38
A207*	S1(=O)(=O)N(Cc2ccc(c(c2)c2ccccc2)C(=O)NO)C(=O)c2c1cccc2	1	38
A208	ONC(=O)/C=C/C(=C/[C@H](C(=O)c1ccc(N(C)C)cc1)C)/C	1	38
A209*	c1(n2ncc3c2C[C@@](C3)(c2c(c(ccc2)F)C)C(=O)NO)ccc(cc1)C	1	39
A210	C(=O)(CCCCCCNC(=O)c1cc2C(CC(=O)Nc2cc1)(C)C)NO	1	39
A211*	[C@H](N1CCN(CC1)c1ncc(cn1)C(=O)NO)(/C=C/c1ccc(cc1)F)CO	1	41
A212	C(=O)(CCCCCCNC(=O)c1cc2ccc(=O)n(c2cc1)C)NO	1	41
A213	N(C(=O)CCCCCCS)c1nc(cs1)c1ccc(cc1)C	1	42
A214	c1(cccc(c1C)[C@]1(C(=O)NO)Cc2c(C1)nc(s2)c1ccnn1C)F	1	44
A215*	c1c2c(n(n1)c1cc(ccc1)F)C[C@](C2)(C(=O)NO)c1c(c(ccc1)F)C	1	44
A216	c1c2c(n(n1)c1ccc(cc1C)F)C[C@@](C2)(c1c(c(ccc1)F)C)C(=O)NO	1	44
A217	C(=O)(CCCCCCC(=O)Nc1cc2C(CC(=O)Nc2cc1)(C)C)NO	1	45
A218*	C(=O)(CCCCCCNC(=O)[C@H]1C[C@@H]2CCC(=O)N[C@@H]2CC1)NO	1	46
A219*	N1(Cc2ccc(c(c2)c2ccccc2)C(=O)NO)C(=O)c2c(C1=O)c(ccc2)F	1	46
A220	c1(cccc([C@@]2(C(=O)NO)Cc3c(C2)cnn3Cc2ccccc2)c1C)F	1	48
A221	FC(F)(c1nc(c2ccc(cc2)C(=O)N[C@@H]2CN(CC2)Cc2ccccc2)no1)F	1	48
A222	c12C[C@](Cc1n(nc2)C1CC1)(c1c(c(ccc1)F)C)C(=O)NO	1	48
A223	[C@@H]1(CNC(=O)c2cc3C(CC(=O)Nc3cc2)(C)C)CC[C@@H](CC1)CCC(=O)NO	1	50
A224	c1(ccc(cc1)[C@H](c1ccccc1F)C(=O)NO)c1ncc(cn1)C(F)(F)F	1	50
A225	c12c(C[C@@](C1)(c1cccc(c1C)F)C(=O)NO)nc(s2)c1ccc(cn1)F	1	51
A226	C1[C@H]2C[C@@H]3C[C@@H](C[C@]1(C3)N(c1ncc(cn1)C(=O)NO)C)C2	1	52
A227	c1cc(c(c(c1)[C@]1(C(=O)NO)Cc2c(C1)c(n(n2)C)c1ccc(cc1)F)C)F	1	53
A228	c1c2c(n(n1)c1ccc(cc1)F)C[C@](C2)(C(=O)NO)c1c(c(ccc1)F)C	1	53
A229	C1c2c(C[C@]1(c1c(c(ccc1)F)C)C(=O)NO)cn(n2)c1ccncc1C	1	53
A230	[C@@H]1(CNC(=O)c2cc3C(CC(=O)Nc3cc2)(C)C)CC[C@H](CC1)CCC(=O)NO	1	57
A231	N(C(=O)CCCCCCS)c1nc(cs1)c1ccc(cc1)F	1	57
A232	c1cc(c(cn1)C)n1ncc2c1C[C@](C2)(C(=O)NO)c1c(c(ccc1)F)C	1	57
A233	C(=O)(CCCCCCC(=O)N[C@H]1C[C@@H]2CCC(=O)N[C@@H]2CC1)NO	1	58
A234	[nH]1c(c(cc1c1ccc(cc1)O)c1cocc1)C(=O)NCc1ccc(cc1)C(=O)NO	1	59
A235	c1c2c(n(n1)c1cc(ccc1)Cl)C[C@](C2)(C(=O)NO)c1c(c(ccc1)F)C	1	61
A236	c1(cc2cc(c1)/C=C\CO[C@H](C(=O)Nc1c(OC2)cccc1)CCCCCC(=O)NO)OC	1	61
A237	N(C(=O)CCCCCCS)c1nc(cs1)c1cc(c(cc1)C)F	1	62
A238	C1c2c(C[C@]1(c1c(c(ccc1)F)C)C(=O)NO)cn(n2)c1c(cccn1)Cl	1	65
A239	c12n(ncc1C[C@@](C2)(C(=O)NO)c1c(c(ccc1)F)C)C(C)C	1	67
A240	c1(c2sc3c(n2)C[C@](C3)(c2c(c(ccc2)F)C)C(=O)NO)cnn(c1C)C	1	68
A241	c1c(ccc(c1)C(=O)NCCN1CCCC1)c1noc(n1)C(F)(F)F	1	70
A242*	c1c(c(cc(c1)C(=O)NO)F)Cn1c(nc2c1cccc2)C	1	70
A243*	c12c([C@@](CC1)(c1c(c(ccc1)F)C)C(=O)NO)cnn2c1ccccc1	1	72
A244*	c1c2c(nn1c1cc(ccc1)C)C[C@@](C2)(c1c(c(ccc1)F)C)C(=O)NO	1	76
A245	N(C(=O)CCCCCCS)c1nc(cs1)c1cc(ccc1)F	1	78
A246*	c1c(cccc1)c1c2c(sn1)C[C@](C2)(c1c(c(ccc1)F)C)C(=O)NO	1	79

A247*	c12c(C[C@@](C1)(C(=O)NO)c1c(c(ccc1)F)C)sc(n2)c1ccc(cc1)F	1	81
A248*	C(CCCCCS)C(=O)Nc1nc(cs1)c1ccccc1	1	82
A249	c12ccc(nc1cccc2)N(CCCCCCC(=O)NO)c1ccccn1	1	90
A250	[C@@H]1(CNC(=O)c2cc3C(CC(=O)Nc3cc2)(C)C)CC[C@@H](CC1)/C=C/C(=O)NO	1	91
A251	c12c(sc(n1)C1CC1)[C@@](CC2)(c1c(c(ccc1)F)C)C(=O)NO	1	94
A252	c12c(C[C@](C1)(C(=O)NO)c1cccc(c1C)F)nc(s2)c1ccc(cn1)OC	1	95
A253	C1C[C@](c2c1n(nc2)C1CC1)(c1c(c(ccc1)F)C)C(=O)NO	1	100
A254	O=S1(=O)c2c3c(n(Cc4ccc(cc4)C(=O)NO)c2CC1)cccc3	1	100
A255	c1(cc2cc(c1)/C=C\CO[C@@H](C(=O)Nc1c(OC2)cccc1)CCCCCC(=O)NO)OC	1	100
A256	c12c([C@@](CC1)(c1c(c(ccc1)F)C)C(=O)NO)cnc(n2)c1c(cccc1)Cl	1	102
A257	C1c2c(C[C@]1(c1c(c(ccc1)F)C)C(=O)NO)cn(n2)c1c(cccn1)F	1	104
A258*	c12C[C@@](Cc1cnn2c1ccc(cc1)OC(F)F)(c1cccc(c1C)F)C(=O)NO	1	109
A259	c12c(cccc1)CC(C2)(c1c(c(ccc1)F)C)C(=O)NO	1	110
A260	n1cc2c(n1c1ccc(cc1)Cl)C[C@](C2)(C(=O)NO)c1c(c(ccc1)F)C	1	112
A261	C1C[C@](c2c1nc(s2)c1ccc(cc1)F)(c1cccc(c1C)F)C(=O)NO	1	120
A262*	c1ccc2c(c1)C(c1c2cccc1)C(=O)NO	1	120
A263	C(=O)(CCCCCCNC(=O)c1cc2C(CC(=O)N(c2cc1)C)(C)C)NO	1	120
A264*	c12c(C[C@@](C1)(C(=O)NO)c1c(c(ccc1)F)C)sc(n2)c1cc(nn1C)C	1	122
A265	c1(cc2cc(c1)CCCO[C@H](C(=O)Nc1c(OC2)cccc1)CCCCCC(=O)NO)OC	1	123
A266	C1c2c([C@@](C1)(c1c(c(ccc1)F)C)C(=O)NO)sc(n2)c1c(cccc1)C	1	143
A267	c12c(cc(nc1)N(CCCCCCC(=O)NO)c1ccccn1)cccc2	1	145
A268	c12C[C@@](Cc1cn(n2)c1ccc(cc1)OC(F)F)(c1c(c(ccc1)F)C)C(=O)NO	1	147
A269	C(=O)(CCCCCC(c1c[nH]c2c1cc(cc2)[N+](=O)[O-])c1c[nH]c2c1cc(cc2)[N+](=O)[O-])NO	1	150
A270	C1c2c(C[C@@]1(C(=O)NO)c1cccc(c1C)F)cnc(n2)c1c(cccc1)Cl	1	156
A271	c1c(c([nH]c1c1ccc(cc1)OC)C(=O)NCc1ccc(cc1)C(=O)NO)c1ccoc1	1	160
A272*	c12c(C[C@](C1)(c1c(c(ccc1)F)C)C(=O)NO)cnc(n2)C1CC1	1	160
A273	C(=O)(NCCOc1ccc(cc1)C(=O)NO)c1c(c2c(cccc2)o1)CN(C)C	1	168
A274*	c12CC[C@](Cc1sc(n2)NS(=O)(=O)c1ccccc1)(c1c(c(ccc1)F)C)C(=O)NO	1	190
A275	c1(c2sc3c(n2)C[C@](C3)(c2c(c(ccc2)F)C)C(=O)NO)ccccc1F	1	193
A276	c12c(C[C@](C1)(C(=O)NO)c1c(c(ccc1)F)C)sc(n2)c1ccc(cc1)F	1	193
A277	C1c2c(C[C@]1(c1c(c(ccc1)F)C)C(=O)NO)cn(n2)c1ccc(cc1C)F	1	197
A278	c1(C(=O)N[C@H](C(=O)Nc2ccccc2)CSCCCC(=O)NO)ccccc1	0	>200
A279*	O=S1(=O)[C@H]2c3c(N(Cc4ccc(cc4)C(=O)NO)[C@@H]2CC1)cccc3	1	200
A280	c12c(C[C@@](C1)(c1c(c(ccc1)F)C)C(=O)NO)sc(n2)c1cc(ccc1)F	0	210
A281	c12C[C@](Cc1nc(nc2)c1cnccc1)(c1cccc(c1C)F)C(=O)NO	0	220
A282	c1(c(cccc1F)[C@]1(Cc2c(C1)nc(nc2)C1CC1)C(=O)NO)C	0	220
A283	n1c(sc2c1C[C@@](C2)(C(=O)NO)c1c(c(ccc1)F)C)c1n(ncc1)C	0	240
A284	c12CC[C@](c1ccc(n2)C1CC1)(C(=O)NO)c1cccc(c1C)F	0	270
A285*	c1cc(c(cc1F)C)c1sc2c(n1)C[C@](C2)(c1c(c(ccc1)F)C)C(=O)NO	0	270
A286*	c1c(c([nH]c1c1ccc(cc1)O)C(=O)NCc1ccc(cc1)C(=O)NO)c1ccsc1	0	277
A287*	c1(c(cccc1[C@@]1(C(=O)NO)Cc2c(C1)cn(n2)c1nc(cc(n1)C)C)F)C	0	280
A288	c12C[C@@](Cc1cnc(n2)c1ccc(cc1)F)(c1c(c(ccc1)F)C)C(=O)NO	0	290
A289	O=S1(=O)Cc2c(CC1)n(c1c2cccc1)Cc1ccc(cc1)C(=O)NO	0	300
A290	c1(cc2cc(c1)/C=C\CO[C@@H](C(=O)Nc1c(OC2)cccc1)CCCCCC(=O)NO)OC	0	302
A291*	c1(cc2cc(c1)CCCO[C@@H](C(=O)Nc1c(OC2)cccc1)CCCCCC(=O)NO)OC	0	322

A292	c1(cc2cc(c1)CCCO[C@H](C(=O)Nc1c(OC2)cccc1)CCCCCC(=O)NO)OC	0	336
A293	C(=O)(CCCCCC(c1c[nH]c2c1cccc2OC)c1c[nH]c2c1cccc2OC)NO	0	340
A294	S1c2c(N(Cc3ccc(cc3)C(=O)NO)c3c1ccc(c3)Cl)cccc2	0	350
A295	n1(cc(c2c1ccc(c2)OC)CCNC(=O)C)Cc1ccc(cc1)C(=O)NO	0	362
A296	c1(c(c(cc(c1)/C=C\c1ccc(c(c1)/C=C/C(=O)Nc1ccccc1N)OC)OC)OC)OC	0	370
A297	C(=O)(NO)c1cnc(N(Cc2onc(n2)C2CCN(CC2)Cc2ccc(cc2)C)C)nc1	0	441
A298	c1c(c([nH]c1c1ccc(cc1)OC)C(=O)NCc1ccc(cc1)C(=O)NO)c1ccsc1	0	478
A299*	n1c2c(cn1CC(F)(F)F)CC[C@@](CC2)(c1c(c(ccc1)F)C)C(=O)NO	0	480
A300	c1(c(cc(cc1F)C(=O)NO)F)Cn1nc(nn1)c1ncccn1	0	480
A301*	c12c(C[C@](C1)(c1cccc(c1C)F)C(=O)NO)nc(s2)Cc1cccc(c1)C(F)(F)F	0	490
A302	c1c(cc2c(c1)n(c1c2C[S@](=O)CC1)Cc1ccc(cc1)C(=O)NO)F	0	500
A303	O=S1(=O)Cc2c(CC1)n(c1c2cc(cc1)F)Cc1ccc(cc1)C(=O)NO	0	500
A304*	c1ccc(cc1)C(C(=O)NO)c1ccccc1	0	510
A305	C(=O)(Nc1ccc(C(=O)NO)cc1)OCc1cc2c(cc(CN(CC)CC)cc2)cc1	0	512
A306	c1(ccc2c(c1)c(c1c(n2)cccc1)Nc1ccc(cc1)C(=O)NO)F	0	520
A307	c1(CNC(=O)c2cc3C(CC(=O)Nc3cc2)(C)C)cc(ccc1)/C=C/C(=O)NO	0	570
A308	c1ccc2c(c1)c(c1c(n2)cccc1)Nc1ccc(cc1)C(=O)NO	0	570
A309*	c1ccc2c(c1)N(c1c(S2)ccc(c1)C(=O)N)Cc1ccc(cc1)C(=O)NO	0	590
A310	[C@@]1(Cc2c(CC1)n(nc2)Cc1ccc(cc1)F)(C(=O)NO)c1cccc(c1C)F	0	600
A311	c12CC[C@](Cc1cn(n2)Cc1ccc(cc1)F)(c1c(c(ccc1)F)C)C(=O)NO	0	600
A312*	C(=O)(CCCCCC(c1c[nH]c2c1cccc2)c1c[nH]c2c1cccc2)NO	0	640
A313	C1c2cc(ccc2N(CC1)Cc1ccc(cc1)C(=O)NO)C(=O)N	0	650
A314	c1(cc(cc(c1Cn1c(nnn1)c1sccc1)F)C(=O)NO)F	0	658
A315	c1cccc2c1OCCCCCCCO[C@@H](C(=O)N2)CCCCCC(=O)NO	0	687
A316	ONC(=O)CCCCCn1c(=O)c2cccc3cccc(c1=O)c23	0	700
A317	[C@]1(c2c(CC1)nn(c2)Cc1c(cccc1)F)(c1c(c(ccc1)F)C)C(=O)NO	0	710
A318	c1ccc2c(c1)N(c1c([S@@]2=O)ccc(c1)SC)Cc1ccc(cc1)C(=O)NO	0	720
A319	c1ccc2c(c1)N(c1c(S2)ccc(c1)C(=O)Nc1ncccc1)Cc1ccc(cc1)C(=O)NO	0	730
A320*	c1ccc(nc1)N(CCCCCCC(=O)NO)c1ccc(cn1)OC	0	759
A321*	c1(ccc(nc1)N(CCCCCCC(=O)NO)c1ccccn1)C	0	759
A322	c1(c(cccc1F)[C@]1(CCc2c(C1)sc(n2)C1CC1)C(=O)NO)C	0	770
A323	S1Cc2c(CC1)n(c1c2cc(cc1)F)Cc1ccc(cc1)C(=O)NO	0	800
A324*	c12CC[C@](c1cn(n2)Cc1ccccc1)(c1c(c(ccc1)F)C)C(=O)NO	0	820
A325	c1c2c(nc(n1)C(F)(F)F)C[C@@](C2)(c1c(c(ccc1)F)C)C(=O)NO	0	880
A326*	c1ccc2c(c1)N(c1c(S2)ccc(c1)C(=O)Nc1ncc(cc1)C)Cc1ccc(cc1)C(=O)NO	0	900
A327*	C(/C(=C/c1ccc(cc1)/C=C/C(=O)NO)/c1ccc(cc1)F)NC1CC1	0	927
A328*	C1(=O)[C@@H](C(C)C)NC(=O)C[C@H]2OC(=O)[C@H](C(C)C)NC(=O)/C(=C/C)/NC(=O)[C@@H](CSSCC/C=C/2)N1	0	>1000
A329	C1c2c(C[C@@]1(c1cccc(c1C)F)C(=O)NO)cnn2c1ccccc1	0	1000
A330	C(=O)(c1c(c(c(c(c1F)F)F)F)F)NCc1ccc(cc1)C(=O)NO	0	>1000
A331*	c12c(c(ccc1)C(=O)OC)CN(C2(C)C)c1ncc(nc1)C(F)(F)F	0	>1000
A332	c1cc(ccc1NC(=O)c1ccc(cc1)C(C)(C)C)C(=O)NO	0	>1000
A333	c12CC[C@@](Cc1scn2)(c1c(c(ccc1)F)C)C(=O)NO	0	1000
A334	c1cccc2c1OCCCCCCCCO[C@H](C(=O)N2)CCCCCC(=O)NO	0	1040
A335	c12CC[C@@](Cc1cnn2c1ccccc1C)(C(=O)NO)c1c(c(ccc1)F)C	0	1100
A336*	c1c(cccc1)COc1ccc2c(c1)c(c1c(n2)cccc1)Nc1ccc(cc1)C(=O)NO	0	1250

A337	n1c(nc2c(c1N1CCOCC1)ncn2CCCCCCC(=O)NO)c1cc(ccc1)CO	0	1282
A338*	CC(C)(Nc1n2ccccc2nc1c1cc(ccc1)C(=O)Nc1c(cc(cc1)F)N)C	0	1300
A339	C1[C@@](CCc2c(C1)cnc(n2)C1CC1)(C(=O)NO)c1cccc(c1C)F	0	1300
A340	c1(ccc(cc1)C(=O)NO)Cn1c(nnn1)c1cccs1	0	1439
A341	C1(=O)N(c2c(Sc3c1cc(cc3)OC)cccc2)CCCCCC(=O)NO	0	1470
A342	C(=O)(c1ccc(cc1)CNc1cccc2cccnc12)NO	0	1530
A343	[C@]1(C(=O)NO)(c2c(c(ccc2)F)C)Cc2c(CC1)nc(cn2)C1CC1	0	1600
A344*	[C@@H]12CC[C@](C[C@@H]1C(=O)N[C@@H](N2)C1CC1)(c1c(c(ccc1)F)C)C(=O)NO	0	1600
A345*	c1(nc2c(cn1)C[C@@](CC2)(C(=O)NO)c1c(c(ccc1)F)C)C1CC1	0	1600
A346	c1c(cc2c(c1)c(cn2Cc1ccc(cc1)C(=O)NO)C(=O)c1cc(c(c(c1)OC)OC)OC)OC	1	1.7
A347	[C@@]1(Cc2c(CC1)n(nc2)CC(F)(F)F)(C(=O)NO)c1cccc(c1C)F	0	1700
A348	c1(c(cccc1[C@@]1(CCc2c(C1)cn(n2)CC(F)(F)F)C(=O)NO)F)C	0	1700
A349	c1(ccc(cc1)C(=O)NO)Cn1nc(nn1)c1ncccn1	0	1705
A350	Clc1cc([C@H](N2CCN(CC2)CC)c2cccnc2)c(O)c2ncccc12	0	1880
A351*	c1(c(cccc1F)[C@]1(CCc2c(C1)sc(n2)c1cncnc1)C(=O)NO)C	0	1900
A352*	c1cccc2c1OCCCCCO[C@@H](C(=O)N2)CCCCCC(=O)NO	0	1900
A353	C(=O)(c1ccc(cc1)CNc1c2cccnc2ccc1)NO	0	1915
A354	c1ccc2c(c1)N(c1c([S@@]2=O)ccc(c1)Cl)Cc1ccc(cc1)C(=O)NO	0	1960
A355	C(=O)(c1ccc(cc1)CN(C(=O)Nc1ccccc1)CCCC)NO	0	2000
A356	FC(F)(c1nc(c2ccc(c3nc4n(c3NC(C)(C)C)cccc4)cc2)no1)F	0	2311
A357*	c1c(ccc(c1)/C=C/C(=O)NO)/C=N/OCc1ccc(cc1)[N+](=O)[O-]	0	2470
A358	N1(Cc2ccc(cc2)C(=O)NO)c2c(Sc3c1cc(cc3)C(F)(F)F)cccc2	0	2580
A359	S(=O)(=O)(c1c(c(c(c(c1)F)F)F)F)N(Cc1ccc(cc1)C(=O)NO)Cc1cnccc1	0	2750
A360	c1(cc(ccc1Cl)C(=O)NCc1ccc(cc1)C(=O)NO)Cl	0	3070
A361*	[C@]1(C(=O)NO)(c2c(c(ccc2)F)C)Cc2c(CC1)nc(cn2)c1ccccc1	0	3200
A362	c1(ccccc1)c1ncc2c(n1)CC[C@@](C2)(c1c(c(ccc1)F)C)C(=O)NO	0	3200
A363	c1ccc2c(c1)N(c1c(S2)ccc(c1)SC)Cc1ccc(cc1)C(=O)NO	0	3260
A364	C(c1c[nH]c2c1cccc2)(c1c[nH]c2c1cccc2)c1ccc(cc1)/C=C/C(=O)NO	0	3300
A365*	C1c2c(N(CC1)Cc1ccc(cc1)C(=O)NO)ccc(c2)Cl	0	3400
A366*	c1cccc(c1)[C@@H]1[C@H](C1)NCC1CCN(CCCc2ccc(cc2)C(=O)NO)CC1	0	3430
A367	[se]1n(c(=O)c2c1cccc2)c1ccccc1	0	3700
A368*	c1(c(cccc1[C@]1(CCc2c(C1)cncn2)C(=O)NO)F)C	0	3700
A369	c1ccc(cc1)NC(=O)CCCCCC(=O)NO	0	3800
A370	n1(Cc2ccc(cc2)C(=O)NO)sc2c(c1=O)cccc2	0	3800
A371*	c1ccc2c(c1)N(c1c([S@@]2=O)ccc(c1)C(F)(F)F)Cc1ccc(cc1)C(=O)NO	0	3820
A372	c1ccc2c(c1)N(c1c([S@@]2=O)ccc(c1)C(=O)N)Cc1ccc(cc1)C(=O)NO	0	4200
A373*	O=c1c2cc(NCc3ccc(cc3)/C=C/C(=O)NO)ccc2nc2n1CCCCC2	0	4320
A374	c1ccc2c(c1)N(c1c(S2)ccc(c1)/C(=N/O)/C)Cc1ccc(cc1)C(=O)NO	0	4340
A375	c12CC[C@](Cc1c(n(n2)CC(F)(F)F)C1CC1)(c1c(c(ccc1)F)C)C(=O)NO	0	4400
A376	C[C@@H](/C=C/C(=O)NO)/C=C(\C)/C(=O)c1ccc(cc1)N(C)C	0	4824
A377*	c12n(cc(c1cccc2)CCNCc1ccc(cc1)/C=C/C(=O)NO)C	0	4849
A378	c1(c(cc2c(c1OC)c(c1c(n2)cccc1)Nc1ccc(cc1)C(=O)NO)OC)OC	0	4950
A379*	c1c(c([nH]c1c1ccc(cc1)O)C(=O)NCc1ccc(cc1)C(=O)Nc1c(cccc1)N)c1ccoc1	0	>5000
A380	c1ccc(CCNC(=O)CCCNC(=O)OCC)cc1	0	5000
A381	N(C(=O)CCCC(=O)NCCc1ccccc1)O	0	5000

A382	C\1(=C\2/C(=O)Nc3c2cccc3)/C(=N/OCCCC(=O)NO)/c2c(N1)cccc2	0	>5000
A383	C\1(=C\2/C(=O)Nc3c2cccc3)/C(=N/OCCCC(=O)O)/c2c(N1)cccc2	0	>5000
A384*	c1c(ccc(c1)C(=O)NNCCC)CNC(=O)c1cc2c([nH]1)cccc2	0	>5000
A385	C(=O)(NCc1ccc(cc1)C(=O)NNCCC)/C=C/c1ccccc1	0	>5000
A386	O=C(NNCC)c1ccc(cc1)CN1c2ccccc2C=Cc2c1cncc2	0	>5000
A387	C(=O)([C@H](/C=C(/C=C/C(=O)NO)\C)C)c1ccc(N(C)C)cc1	0	5100
A388	C1[C@@H]2C[C@@H]3C[C@H]1C[C@](C2)(C3)CN(Cc1c(cc(cc1)C(=O)NO)F)C	0	5200
A389*	c1ccc(cc1)CC(=O)N(CCO)Cc1ccc(cc1)C(=O)NO	0	5300
A390	C(=O)(Cc1ccccc1)N(CCO)C(=O)Cc1ccc(cc1)C(=O)NO	0	5334
A391	C(=O)(/C=C/c1cc(ccc1)S(=O)(=O)n1c2c(cccn2)cc1)NO	0	5340
A392	c1(ccc2c(c1)c(c1c(n2)cccc1)Nc1ccc(cc1)C(=O)NO)Br	0	5510
A393*	C(=O)(/C=C/c1c(=O)n(ccc1)CCCc1cc2c(cc1)cccc2)NO	0	5580
A394	c1ccc2c(c1)CC[C@@]2(c1ccccc1)C(=O)NO	0	5670
A395*	C(=O)(c1ccc(cc1)CN(C(=O)Nc1ccc(cc1)CN)CCCCO)NO	0	6270
A396	c1ccc2c(c1)c(c1c(n2)cccc1)Nc1ccc(cc1)CC(=O)NO	0	6420
A397	c1c(ccc(c1)/C=C/C(=O)NO)/C=N/OCc1ccc(cc1)C(=O)OC	0	6430
A398*	c1ccc2c(c1)N(c1c([S@@]2=O)ccc(c1)OC)Cc1ccc(cc1)C(=O)NO	0	6560
A399	c1c(c(c(cc1O)C)c1[nH]c2c(n1)cc(cc2)C(=O)NO)C	0	6900
A400	c1ccc2c(c1)C(=O)c1c(C2=O)ccc(c1)C(=O)NO	0	7782
A401	O=S1(=O)c2ccccc2N([C@@H]2[C@H](C1)CCCC2)Cc1ccc(cc1)C(=O)NO	0	>8000
A402	c1ccc2c(c1)n(cc2)Cc1ccc(cc1)C(=O)NO	0	8160
A403*	C1CC[C@@H]2[C@H](C1)[C@H](CC2)c1ccc(cc1)C(=O)NO	0	8160
A404	n1(cc2c(n1)CC[C@](CC2)(c1ccccc1)C(=O)NO)CC(F)(F)F	0	8200
A405	c1ccc2c(c1)N(c1c(S2)ccc(c1)C(=O)N)Cc1ccc(cc1)/C=C/C(=O)NO	0	8270
A406	C(=O)(CCCCC[C@H](C)n1ncc(c1)c1c2c(ncn1)[nH]cc2)NO	0	8500

*Denotes the Test molecule.

8. Reference

8. Reference

Abraham MJ, Murtola T, Schulz R, Páll S, Smith JC, Hess B, Lindahl E. GROMACS: High-performance molecular simulations through multi-level parallelism from laptops to supercomputers. SoftwareX. 2015 Sep 1;1:19-25. doi: https://doi.org/10.1016/j.softx.2015.06.001

Ambure P, Aher RB, Gajewicz A, Puzyn T, Roy K. "NanoBRIDGES" software: open access tools to perform QSAR and nano-QSAR modeling. Chemometrics and Intelligent Laboratory Systems. 2015 Oct 15;147:1-3. doi: https://doi.org/10.1016/j.chemolab.2015.07.007

Amin SA, Nandi S, Kashaw SK, Jha T, Gayen S. A critical analysis of urea transporter B inhibitors: molecular fingerprints, pharmacophore features for the development of next-generation diuretics. Molecular Diversity. 2022 Oct 1:1-1. doi: https://doi.org/10.1007/s11030-021-10353-w

Asare Y, Campbell-James TA, Bokov Y, Yu LL, Prestel M, El Bounkari O, Roth S, Megens RT, Straub T, Thomas K, Yan G. Histone deacetylase 9 activates IKK to regulate atherosclerotic plaque vulnerability. Circulation research. 2020 Aug 28;127(6):811-23. doi: https://doi.org/10.1161/CIRCRESAHA.120.316743

Asfaha Y, Schrenk C, Avelar LA, Hamacher A, Pflieger M, Kassack MU, Kurz T. Recent advances in class IIa histone deacetylases research. Bioorganic & medicinal chemistry. 2019 Nov 15;27(22):115087. doi: https://doi.org/10.1016/j.bmc.2019.115087

Azghandi S, Prell C, Van Der Laan SW, Schneider M, Malik R, Berer K, Gerdes N, Pasterkamp G, Weber C, Haffner C, Dichgans M. Deficiency of the stroke-relevant HDAC9 gene attenuates atherosclerosis in accord with allele-specific effects at 7p21. 1. Stroke. 2015 Jan;46(1):197-202. doi: https://doi.org/10.1161/STROKEAHA.114.007213

Banerjee A, Kar S, Pore S, Roy K. Efficient predictions of cytotoxicity of TiO2-based multi-component nanoparticles using a machine learning-based q-RASAR approach. Nanotoxicology. 2023 Jan 2;17(1):78-93. doi: https://doi.org/10.1080/17435390.2023.2186280

Banerjee A, Roy K. Machine-learning-based similarity meets traditional QSAR:"q-RASAR" for the enhancement of the external predictivity and detection of prediction confidence

outliers in an hERG toxicity dataset. Chemometrics and Intelligent Laboratory Systems. 2023 Jun 15;237:104829. doi: https://doi.org/10.1016/j.chemolab.2023.104829

Banerjee S, Amin SA, Jha T. A fragment-based structural analysis of MMP-2 inhibitors in search of meaningful structural fragments. Computers in Biology and Medicine. 2022 May 1;144:105360. doi: https://doi.org/10.1016/j.compbiomed.2022.105360

Bera A, Russ E, Srinivasan M, Eidelman O, Eklund M, Hueman M, Pollard HB, Hu H, Shriver CD, Srivastava M. Proteomic analysis of inflammatory biomarkers associated with breast cancer recurrence. Military medicine. 2020 Jan 7;185(Supplement_1):669-75. doi: https://doi.org/10.1093/milmed/usz254

Bradbury CA, Khanim FL, Hayden R, Bunce CM, White DA, Drayson MT, Craddock C, Turner BM. Histone deacetylases in acute myeloid leukaemia show a distinctive pattern of expression that changes selectively in response to deacetylase inhibitors. Leukemia. 2005 Oct;19(10):1751-9. doi: https://doi.org/10.1038/sj.leu.2403910

Brancolini C, Di Giorgio E, Formisano L, Gagliano T. Quis custodiet ipsos custodes (who controls the controllers)? Two decades of studies on HDAC9. Life. 2021 Jan 27;11(2):90. doi: https://doi.org/10.3390/life11020090

Breccia M, Alimena G. NF-κB as a potential therapeutic target in myelodysplastic syndromes and acute myeloid leukemia. Expert opinion on therapeutic targets. 2010 Nov 1;14(11):1157-76. doi: https://doi.org/10.1517/14728222.2010.522570

Cacabelos R. Epigenetics and pharmacoepigenetics of neurodevelopmental and neuropsychiatric disorders. In Pharmacoepigenetics 2019 Jan 1 (pp. 609-709). Academic Press. doi: https://doi.org/10.1016/B978-0-12-813939-4.00022-X

Cao Q, Rong S, Repa JJ, Clair RS, Parks JS, Mishra N. Histone deacetylase 9 represses cholesterol efflux and alternatively activated macrophages in atherosclerosis development. Arteriosclerosis, thrombosis, and vascular biology. 2014 Sep;34(9):1871-9. doi: https://doi.org/10.1161/ATVBAHA.114.303393

Chatterjee TK, Basford JE, Knoll E, Tong WS, Blanco V, Blomkalns AL, Rudich S, Lentsch AB, Hui DY, Weintraub NL. HDAC9 knockout mice are protected from adipose tissue dysfunction and systemic metabolic disease during high-fat feeding. Diabetes. 2014 Jan 1;63(1):176-87. doi: https://doi.org/10.2337/db13-1148

Chatterjee TK, Basford JE, Yiew KH, Stepp DW, Hui DY, Weintraub NL. Role of histone deacetylase 9 in regulating adipogenic differentiation and high fat diet-induced metabolic disease. Adipocyte. 2014 Oct 2;3(4):333-8. doi: https://doi.org/10.4161/adip.28814

Chatterjee TK, Idelman G, Blanco V, Blomkalns AL, Piegore MG, Weintraub DS, Kumar S, Rajsheker S, Manka D, Rudich SM, Tang Y. Histone deacetylase 9 is a negative regulator of adipogenic differentiation. Journal of Biological Chemistry. 2011 Aug 5;286(31):27836-47. doi: https://doi.org/10.1074/jbc.M111.262964

Chen J, Zhang Z, Wang N, Guo M, Chi X, Pan Y, Jiang J, Niu J, Ksimu S, Li JZ, Chen X. Role of HDAC9-FoxO1 axis in the transcriptional program associated with hepatic gluconeogenesis. Scientific reports. 2017 Jul 21;7(1):6102. doi: https://doi.org/10.1038/s41598-017-06328-3

Chen JQ, Russo J. ERα-negative and triple negative breast cancer: molecular features and potential therapeutic approaches. Biochimica et Biophysica Acta (BBA)-Reviews on Cancer. 2009 Dec 1;1796(2):162-75. doi: https://doi.org/10.1016/j.bbcan.2009.06.003

Chen Y, Yang H, Wu Z, Liu G, Tang Y, Li W. Prediction of farnesoid X receptor disruptors with machine learning methods. Chemical Research in Toxicology. 2018 Oct 29;31(11):1128-37. doi: https://doi.org/10.1021/acs.chemrestox.8b00162

Cho Y, Cavalli V. HDAC signaling in neuronal development and axon regeneration. Current opinion in neurobiology. 2014 Aug 1;27:118-26. doi: https://doi.org/10.1016/j.conb.2014.03.008

Clark MD, Marcum R, Graveline R, Chan CW, Xie T, Chen Z, Ding Y, Zhang Y, Mondragón A, David G, Radhakrishnan I. Structural insights into the assembly of the histone deacetylase-associated Sin3L/Rpd3L corepressor complex. Proceedings of the National Academy of Sciences. 2015 Jul 14;112(28):E3669-78. doi: https://doi.org/10.1073/pnas.1504021112

Claveria-Cabello A, Colyn L, Arechederra M, Urman JM, Berasain C, Avila MA, Fernandez-Barrena MG. Epigenetics in liver fibrosis: could HDACs be a therapeutic target?. Cells. 2020 Oct 19;9(10):2321. doi: https://doi.org/10.3390/cells9102321

Clocchiatti A, Florean C, Brancolini C. Class IIa HDACs: from important roles in differentiation to possible implications in tumorigenesis. Journal of cellular and molecular

medicine. 2011 Sep;15(9):1833-46. doi: https://doi.org/10.1111/j.1582-4934.2011.01321.x

Cohen TJ, Waddell DS, Barrientos T, Lu Z, Feng G, Cox GA, Bodine SC, Yao TP. The histone deacetylase HDAC4 connects neural activity to muscle transcriptional reprogramming. Journal of Biological Chemistry. 2007 Nov 16;282(46):33752-9. doi: https://doi.org/10.1074/jbc.M706268200

Damić AM, Jelena S. Plant products in the prevention of diabetes mellitus. Mini-Reviews in Medicinal Chemistry. 2022 Jun 1;22(10):1395-419. doi: https://doi.org/10.2174/1389557521666211116122232

Das S, Natarajan R. HDAC9: An inflammatory link in atherosclerosis. Circulation research. 2020 Aug 28;127(6):824-6. doi: https://doi.org/10.1161/CIRCRESAHA.120.317723

Das T, Bhattacharya A, Jha T, Gayen S. Exploration of Fingerprints and Data Mining-based Prediction of Some Bioactive Compounds from Allium sativum as Histone Deacetylase 9 (HDAC9) Inhibitors. Current Computer-aided Drug Design. 2024 Feb 6. doi: 10.2174/0115734099282303240126061624

Dehghani P, Rad ME, Zarepour A, Sivakumar PM, Zarrabi A. An insight into the polymeric nanoparticle's applications in diabetes diagnosis and treatment. Mini-Reviews in Medicinal Chemistry. 2023 Feb 1;23(2):192-216. doi: https://doi.org/10.2174/1389557521666211116123002

Di Giorgio E, Gagliostro E, Brancolini C. Selective class IIa HDAC inhibitors: myth or reality. Cellular and molecular life sciences. 2015 Jan;72:73-86. doi: https://doi.org/10.1007/s00018-014-1727-8

Dinakar YH, Kumar H, Mudavath SL, Jain R, Ajmeer R, Jain V. Role of STAT3 in the initiation, progression, proliferation and metastasis of breast cancer and strategies to deliver JAK and STAT3 inhibitors. Life Sciences. 2022 Nov 15;309:120996. doi: https://doi.org/10.1016/j.lfs.2022.120996

Discovery Studio 3.0 (DS 3.0), Accelrys Inc., CA, USA, 2015. Available at www.accelrys. com.

Duan YC, Jin LF, Ren HM, Zhang SJ, Liu YJ, Xu YT, He ZH, Song Y, Yuan H, Chen SH, Guan YY. Design, synthesis, and biological evaluation of novel dual inhibitors targeting

lysine specific demethylase 1 (LSD1) and histone deacetylases (HDAC) for treatment of gastric cancer. European journal of medicinal chemistry. 2021 Aug 5;220:113453. doi: https://doi.org/10.1016/j.ejmech.2021.113453

Elmezayen AD, Yelekçi K. Homology modeling and in silico design of novel and potential dual-acting inhibitors of human histone deacetylases HDAC5 and HDAC9 isozymes. Journal of Biomolecular Structure and Dynamics. 2021 Nov 22;39(17):6396-414. doi: https://doi.org/10.1080/07391102.2020.1798812

Freese K, Seitz T, Dietrich P, Lee SM, Thasler WE, Bosserhoff A, Hellerbrand C. Histone deacetylase expressions in hepatocellular carcinoma and functional effects of histone deacetylase inhibitors on liver cancer cells in vitro. Cancers. 2019 Oct 18;11(10):1587. doi: https://doi.org/10.3390/cancers11101587

Garmpis N, Damaskos C, Dimitroulis D, Kouraklis G, Garmpi A, Sarantis P, Koustas E, Patsouras A, Psilopatis I, Antoniou EA, Karamouzis MV. Clinical Significance of the Histone Deacetylase 2 (HDAC-2) Expression in Human Breast Cancer. Journal of Personalized Medicine. 2022 Oct 8;12(10):1672. doi: https://doi.org/10.3390/jpm12101672

Glaser KB. HDAC inhibitors: clinical update and mechanism-based potential. Biochemical pharmacology. 2007 Sep 1;74(5):659-71. doi: https://doi.org/10.1016/j.bcp.2007.04.007

Greim H, Kaden DA, Larson RA, Palermo CM, Rice JM, Ross D, Snyder R. The bone marrow niche, stem cells, and leukemia: impact of drugs, chemicals, and the environment. Annals of the New York Academy of Sciences. 2014 Mar;1310(1):7-31. doi: https://doi.org/10.1111/nyas.12362

Guan JS, Haggarty SJ, Giacometti E, Dannenberg JH, Joseph N, Gao J, Nieland TJ, Zhou Y, Wang X, Mazitschek R, Bradner JE. HDAC2 negatively regulates memory formation and synaptic plasticity. Nature. 2009 May 7;459(7243):55-60. doi: https://doi.org/10.1038/nature07925

Guan Y, Yang J, Liu X, Chu L. Long noncoding RNA CBR3 antisense RNA 1 promotes the aggressive phenotypes of non-small-cell lung cancer by sponging microRNA-509-3p and competitively upregulating HDAC9 expression. Oncology Reports. 2020 Oct 1;44(4):1403-14. doi: https://doi.org/10.3892/or.2020.7719

Guan YJ, Yang X, Wei L, Chen Q. MiR-365: a mechanosensitive microRNA stimulates chondrocyte differentiation through targeting histone deacetylase 4. The FASEB Journal. 2011 Dec;25(12):4457. doi: https://doi.org/10.1096%2Ffj.11-185132

Haberland M, Montgomery RL, Olson EN. The many roles of histone deacetylases in development and physiology: implications for disease and therapy. Nature Reviews Genetics. 2009 Jan;10(1):32-42. doi: https://doi.org/10.1038/nrg2485

Hashimoto H, Tsugeno Y, Sugita K, Inamura K. Mesenchymal tumors of the lung: diagnostic pathology, molecular pathogenesis, and identified biomarkers. Journal of Thoracic Disease. 2019 Jan;11(Suppl 1):S9. doi: https://doi.org/10.21037%2Fjtd.2018.12.04

Hervouet E, Cartron PF, Jouvenot M, Delage-Mourroux R. Epigenetic regulation of estrogen signaling in breast cancer. Epigenetics. 2013 Mar 1;8(3):237-45. doi: https://doi.org/10.4161/epi.23790

Hess B, Holm C, van der Vegt N. Osmotic coefficients of atomistic NaCl (aq) force fields. The Journal of chemical physics. 2006 Apr 28;124(16). doi: https://doi.org/10.1063/1.2185105

Hu S, Cho EH, Lee JY. Histone deacetylase 9: its role in the pathogenesis of diabetes and other chronic diseases. Diabetes & Metabolism Journal. 2020 Apr 1;44(2):234-44. doi: https://doi.org/10.4093/dmj.2019.0243

Hu Y, Sun L, Tao S, Dai M, Wang Y, Li Y, Wu J. Clinical significance of HDAC9 in hepatocellular carcinoma. Cellular and Molecular Biology. 2019 Apr 30;65(4):23-8. doi: https://doi.org/10.14715/10.14715/cmb/2019.65.4.4

Huang L, Wu RL, Xu AM. Epithelial-mesenchymal transition in gastric cancer. American journal of translational research. 2015;7(11):2141.

Jannat Ali Pour N, Meshkani R, Toolabi K, Mohassel Azadi S, Zand S, Emamgholipour S. Adipose tissue mRNA expression of HDAC1, HDAC3 and HDAC9 in obese women in relation to obesity indices and insulin resistance. Molecular Biology Reports. 2020 May;47:3459-68. doi: https://doi.org/10.1007/s11033-020-05431-5

Jin Q, He W, Chen L, Yang Y, Shi K, You Z. MicroRNA-101-3p inhibits proliferation in retinoblastoma cells by targeting EZH2 and HDAC9. Experimental and Therapeutic Medicine. 2018 Sep 1;16(3):1663-70. doi: https://doi.org/10.3892/etm.2018.6405

Jin Z, Wei W, Huynh H, Wan Y. HDAC9 inhibits osteoclastogenesis via mutual suppression of PPARγ/RANKL signaling. Molecular Endocrinology. 2015 May 1;29(5):730-8. doi: https://doi.org/10.1210/me.2014-1365

Kanki K, Watanabe R, Nguyen Thai L, Zhao CH, Naito K. HDAC9 is preferentially expressed in dedifferentiated hepatocellular carcinoma cells and is involved in an anchorage-independent growth. Cancers. 2020 Sep 23;12(10):2734. doi: https://doi.org/10.3390/cancers12102734

Khatun S, Amin SA, Banerjee S, Gayen S, Jha T. Modeling Inhibitors of Gelatinases. InModeling Inhibitors of Matrix Metalloproteinases 2023 Dec 29 (pp. 368-398). CRC Press.

Kumari S, Gupta R, Ambasta RK, Kumar P. Emerging trends in post-translational modification: Shedding light on Glioblastoma multiforme. Biochimica et Biophysica Acta (BBA)-Reviews on Cancer. 2023 Nov 1;1878(6):188999. doi: https://doi.org/10.1016/j.bbcan.2023.188999

Lang B, Alrahbeni TM, St Clair D, Blackwood DH, McCaig CD, Shen S, International Schizophrenia Consortium. HDAC9 is implicated in schizophrenia and expressed specifically in post-mitotic neurons but not in adult neural stem cells. American journal of stem cells. 2012;1(1):31.

Lapierre M, Linares A, Dalvai M, Duraffourd C, Bonnet S, Boulahtouf A, Rodriguez C, Jalaguier S, Assou S, Orsetti B, Balaguer P. Histone deacetylase 9 regulates breast cancer cell proliferation and the response to histone deacetylase inhibitors. Oncotarget. 2016 Apr 4;7(15):19693. doi: https://doi.org/10.18632%2Foncotarget.7564

Lee C, Kim JK. Chromatin regulators in retinoblastoma: Biological roles and therapeutic applications. Journal of Cellular Physiology. 2021 Apr;236(4):2318-32. doi: https://doi.org/10.1002/jcp.30022

Lee J, Cheng X, Jo S, MacKerell AD, Klauda JB, Im W. CHARMM-GUI input generator for NAMD, GROMACS, AMBER, OpenMM, and CHARMM/OpenMM simulations using the CHARMM36 additive force field. Biophysical journal. 2016 Feb 16;110(3):641a. doi: https://doi.org/10.1016/j.bpj.2015.11.3431

Lee MH. Harness the functions of gut microbiome in tumorigenesis for cancer treatment. Cancer Communications. 2021 Oct;41(10):937-67. doi: https://doi.org/10.1002/cac2.12200

Lenis AT, Lec PM, Chamie K. Bladder cancer: a review. Jama. 2020 Nov 17;324(19):1980-91. doi: 10.1001/jama.2020.17598

Li H, Duann P, Li Z, Zhou X, Ma J, Rovin BH, Lin PH. The cell membrane repair protein MG53 modulates transcription factor NF-κB signaling to control kidney fibrosis. Kidney international. 2022 Jan 1;101(1):119-30. doi: https://doi.org/10.1016/j.kint.2021.09.027

Li L, Liu W, Wang H, Yang Q, Zhang L, Jin F, Jin Y. Mutual inhibition between HDAC9 and miR-17 regulates osteogenesis of human periodontal ligament stem cells in inflammatory conditions. Cell death & disease. 2018 Apr 24;9(5):480. doi: https://doi.org/10.1038/s41419-018-0480-6

Li Y, Li J, Yu H, Liu Y, Song H, Tian X, Liu D, Yan C, Han Y. HOXA5-miR-574-5p axis promotes adipogenesis and alleviates insulin resistance. Molecular Therapy-Nucleic Acids. 2022 Mar 8;27:200-10. doi: https://doi.org/10.1016/j.omtn.2021.08.031

Li, C.J., Cheng, P., Liang, M.K., Chen, Y.S., Lu, Q., Wang, J.Y., Xia, Z.Y., Zhou, H.D., Cao, X., Xie, H. and Liao, E.Y., 2015. MicroRNA-188 regulates age-related switch between osteoblast and adipocyte differentiation. *The Journal of clinical investigation*, *125*(4), pp.1509-1522. doi: 10.1172/JCI77716.

Lian B, Pei YC, Jiang YZ, Xue MZ, Li DQ, Li XG, Zheng YZ, Liu XY, Qiao F, Sun WL, Ling H. Truncated HDAC9 identified by integrated genome-wide screen as the key modulator for paclitaxel resistance in triple-negative breast cancer. Theranostics. 2020;10(24):11092. doi: https://doi.org/10.7150%2Fthno.44997

Liang Z, Mu X, Liang X, Hu K, Chen M. HDAC9 associates with distant metastasis and predicts poor prognosis in clear cell renal cell cancer. Int. J. Clin. Exp. Pathol. 2017 Jan 1;10:4647-53.

Liu W, Dai J, Chen X, Du N, Hu J. Integrated Network Pharmacology and In-silico Approaches to Decipher the Pharmacological Mechanism of Dioscorea septemloba Thunb in Treating Gout and Its Complications. Combinatorial Chemistry & High Throughput Screening. 2023 Nov 10. doi: https://doi.org/10.2174/0113862073258523231025095117

Liu Y. Renal fibrosis: new insights into the pathogenesis and therapeutics. Kidney international. 2006 Jan 2;69(2):213-7. doi: https://doi.org/10.1038/sj.ki.5000054

Lu Y, Tan L, Wang X. Circular HDAC9/microRNA-138/Sirtuin-1 pathway mediates synaptic and amyloid precursor protein processing deficits in Alzheimer's disease. Neuroscience bulletin. 2019 Oct;35:877-88. doi: https://doi.org/10.1007/s12264-019-00361-0

Lucca I, Hofbauer SL, Haitel A, Susani M, Shariat SF, Klatte T, De Martino M. Urinary expression of genes involved in DNA methylation and histone modification for diagnosis of bladder cancer in patients with asymptomatic microscopic haematuria. Oncology letters. 2019 Jul 1;18(1):57-62. doi: https://doi.org/10.3892/ol.2019.10330

Lumachi F, Santeufemia DA, Basso SM. Current medical treatment of estrogen receptor-positive breast cancer. World journal of biological chemistry. 2015 Aug 8;6(3):231. doi: https://doi.org/10.4331%2Fwjbc.v6.i3.231

Ma P, Pan H, Montgomery RL, Olson EN, Schultz RM. Compensatory functions of histone deacetylase 1 (HDAC1) and HDAC2 regulate transcription and apoptosis during mouse oocyte development. Proceedings of the National Academy of Sciences. 2012 Feb 21;109(8):E481-9. doi: https://doi.org/10.1073/pnas.1118403109

Mannaerts I, Eysackers N, Onyema OO, Van Beneden K, Valente S, Mai A, Odenthal M, Van Grunsven LA. Class II HDAC inhibition hampers hepatic stellate cell activation by induction of microRNA-29. PloS one. 2013 Jan 31;8(1):e55786. doi: https://doi.org/10.1371/journal.pone.0055786

Markus HS, Mäkelä KM, Bevan S, Raitoharju E, Oksala N, Bis JC, O'Donnell C, Hainsworth A, Lehtimäki T. Evidence HDAC9 genetic variant associated with ischemic stroke increases risk via promoting carotid atherosclerosis. Stroke. 2013 May;44(5):1220-5. doi: https://doi.org/10.1161/STROKEAHA.111.000217

Marzo M, Kulkarni S, Manganaro A, Roncaglioni A, Wu S, Barton-Maclaren TS, Lester C, Benfenati E. Integrating in silico models to enhance predictivity for developmental toxicity. Toxicology. 2016 Aug 31;370:127-37. doi: https://doi.org/10.1016/j.tox.2016.09.015

Masters CL, Bateman R, Blennow K, Rowe CC, Sperling RA, Cummings JL. Alzheimer's disease. Nature reviews disease primers. 2015 Oct 15;1(1):1-8.

Mejat A, Ramond F, Bassel-Duby R, Khochbin S, Olson EN, Schaeffer L. Histone deacetylase 9 couples neuronal activity to muscle chromatin acetylation and gene expression. Nature neuroscience. 2005 Mar 1;8(3):313-21. doi: https://doi.org/10.1038/nn1408

Milazzo G, Mercatelli D, Di Muzio G, Triboli L, De Rosa P, Perini G, Giorgi FM. Histone deacetylases (HDACs): evolution, specificity, role in transcriptional complexes, and pharmacological actionability. Genes. 2020 May 15;11(5):556. doi: https://doi.org/10.3390/genes11050556

Moinul M, Amin SA, Kumar P, Patil UK, Gajbhiye A, Jha T, Gayen S. Exploring sodium glucose cotransporter (SGLT2) inhibitors with machine learning approach: A novel hope in anti-diabetes drug discovery. Journal of Molecular Graphics and Modelling. 2022 Mar 1;111:108106. doi: https://doi.org/10.1016/j.jmgm.2021.108106

Moresi V, Williams AH, Meadows E, Flynn JM, Potthoff MJ, McAnally J, Shelton JM, Backs J, Klein WH, Richardson JA, Bassel-Duby R. Myogenin and class II HDACs control neurogenic muscle atrophy by inducing E3 ubiquitin ligases. Cell. 2010 Oct 1;143(1):35-45. doi: https://doi.org/10.1016/j.cell.2010.09.004

Morrison BE, D'Mello SR. Polydactyly in mice lacking HDAC9/HDRP. Experimental biology and medicine. 2008 Aug;233(8):980-8. doi: https://doi.org/10.3181/0802-RM-48

Nicolas E, Yamada T, Cam HP, FitzGerald PC, Kobayashi R, Grewal SI. Distinct roles of HDAC complexes in promoter silencing, antisense suppression and DNA damage protection. Nature structural & molecular biology. 2007 May;14(5):372-80. doi: https://doi.org/10.1038/nsmb1239

Ning Y, Ding J, Sun X, Xie Y, Su M, Ma C, Pan J, Chen J, Jiang H, Qi C. HDAC9 deficiency promotes tumor progression by decreasing the CD8+ dendritic cell infiltration of the tumor microenvironment. Journal for immunotherapy of cancer. 2020;8(1). doi: https://doi.org/10.1136%2Fjitc-2020-000529

Okudela K, Mitsui H, Suzuki T, Woo T, Tateishi Y, Umeda S, Saito Y, Tajiri M, Masuda M, Ohashi K. Expression of HDAC9 in lung cancer–potential role in lung carcinogenesis. International journal of clinical and experimental pathology. 2014;7(1):213.

Omuro A, DeAngelis LM. Glioblastoma and other malignant gliomas: a clinical review. Jama. 2013 Nov 6;310(17):1842-50. doi: 10.1001/jama.2013.280319

Pandey SK, Roy K. Development of a read-across-derived classification model for the predictions of mutagenicity data and its comparison with traditional QSAR models and expert systems. Toxicology. 2023 Dec 1;500:153676. doi: https://doi.org/10.1016/j.tox.2023.153676

Parra M, Verdin E. Regulatory signal transduction pathways for class IIa histone deacetylases. Current opinion in pharmacology. 2010 Aug 1;10(4):454-60. doi: https://doi.org/10.1016/j.coph.2010.04.004

Patra R, Chakraborty J, Das NC, Mukherjee S. An integrated omics study on the role of HDAC9 gene in the oncogenic events of human gastrointestinal-tract associated cancers. Human Gene. 2023 Sep 1;37:201189. doi: https://doi.org/10.1016/j.humgen.2023.201189

Potthoff MJ, Olson EN. MEF2: a central regulator of diverse developmental programs. doi: https://doi.org/10.1242/dev.008367

Puche JE, Saiman Y, Friedman SL. Hepatic stellate cells and liver fibrosis. Compr Physiol. 2013 Oct 22;3(4):1473-92. doi: https://doi.org/10.1242/dev.008367

Rahmani G, Sameri S, Abbasi N, Abdi M, Najafi R. The clinical significance of histone deacetylase-8 in human breast cancer. Pathology-Research and Practice. 2021 Apr 1;220:153396. doi: https://doi.org/10.1016/j.prp.2021.153396

Ramani J, Shah H, Vyas VK, Sharma M. A review on the medicinal chemistry of sodium glucose co-transporter 2 inhibitors (SGLT2-I): Update from 2010 to present. European Journal of Medicinal Chemistry Reports. 2022 Dec 1;6:100074. doi: https://doi.org/10.1016/j.ejmcr.2022.100074

Rippe RA, Brenner DA. From quiescence to activation: gene regulation in hepatic stellate cells. Gastroenterology. 2004 Oct 1;127(4):1260-2.

Rogers D, Hahn M. Extended-connectivity fingerprints. Journal of chemical information and modeling. 2010 May 24;50(5):742-54. doi: https://doi.org/10.1021/ci100050t

Salgado E, Bian X, Feng A, Shim H, Liang Z. HDAC9 overexpression confers invasive and angiogenic potential to triple negative breast cancer cells via modulating microRNA-206. Biochemical and biophysical research communications. 2018 Sep 5;503(2):1087-91. doi: https://doi.org/10.1016/j.bbrc.2018.06.120

Sanford JA, O'Neill AM, Zouboulis CC, Gallo RL. Short-chain fatty acids from Cutibacterium acnes activate both a canonical and epigenetic inflammatory response in human sebocytes. The Journal of Immunology. 2019 Mar 15;202(6):1767-76. doi: https://doi.org/10.4049/jimmunol.1800893

Sanford JA, Zhang LJ, Williams MR, Gangoiti JA, Huang CM, Gallo RL. Inhibition of HDAC8 and HDAC9 by microbial short-chain fatty acids breaks immune tolerance of the epidermis to TLR ligands. Science immunology. 2016 Oct 28;1(4):eaah4609. doi: https://doi.org/10.1126/sciimmunol.aah4609

Sardar S, Jyotisha, Amin SA, Khatun S, Qureshi IA, Patil UK, Jha T, Gayen S. Identification of structural fingerprints among natural inhibitors of HDAC1 to accelerate nature-inspired drug discovery in cancer epigenetics. Journal of Biomolecular Structure and Dynamics. 2024 Jul 23;42(11):5642-56. doi: https://doi.org/10.1080/07391102.2023.2227710

Sher G, Salman NA, Khan AQ, Prabhu KS, Raza A, Kulinski M, Dermime S, Haris M, Junejo K, Uddin S. Epigenetic and breast cancer therapy: promising diagnostic and therapeutic applications. InSeminars in cancer biology 2022 Aug 1 (Vol. 83, pp. 152-165). Academic Press. doi: https://doi.org/10.1016/j.semcancer.2020.08.009

Soltani A, Hashemy SI. Homology modeling, virtual screening, molecular docking, and ADME approaches to identify a potent agent targeting NK2R protein. Biotechnology and Applied Biochemistry. 2024 Feb;71(1):213-22. doi: https://doi.org/10.1002/bab.2533

Strepkos D, Markouli M, Papavassiliou KA, Papavassiliou AG, Piperi C. Emerging roles for the YAP/TAZ transcriptional regulators in brain tumor pathology and targeting options. Neuropathology and Applied Neurobiology. 2022 Feb;48(2):e12762. doi: https://doi.org/10.1111/nan.12762

Tang H, Goldman D. Activity-dependent gene regulation in skeletal muscle is mediated by a histone deacetylase (HDAC)-Dach2-myogenin signal transduction cascade. Proceedings of the National Academy of Sciences. 2006 Nov 7;103(45):16977-82. doi: https://doi.org/10.1073/pnas.0601565103

Tao R, De Zoeten EF, Özkaynak E, Chen C, Wang L, Porrett PM, Li B, Turka LA, Olson EN, Greene MI, Wells AD. Deacetylase inhibition promotes the generation and function of regulatory T cells. Nature medicine. 2007 Nov;13(11):1299-307.Tickle C, Towers M.

Sonic hedgehog signaling in limb development. Frontiers in cell and developmental biology. 2017 Feb 28;5:14. doi: https://doi.org/10.1038/nm1652

Vaissière T, Sawan C, Herceg Z. Epigenetic interplay between histone modifications and DNA methylation in gene silencing. Mutation Research/Reviews in Mutation Research. 2008 Jul 1;659(1-2):40-8. doi: https://doi.org/10.1016/j.mrrev.2008.02.004

Valanciute A, Nygaard L, Zschach H, Jepsen MM, Lindorff-Larsen K, Stein A. Accurate protein stability predictions from homology models. Computational and Structural Biotechnology Journal. 2023 Jan 1;21:66-73. doi: https://doi.org/10.1016/j.csbj.2022.11.048

Verdin E. NAD+ in aging, metabolism, and neurodegeneration. Science. 2015 Dec 4;350(6265):1208-13. doi: https://doi.org/10.1126/science.aac4854

Volpatti JR, Ghahramani-Seno MM, Mansat M, Sabha N, Sarikaya E, Goodman SJ, Chater-Diehl E, Celik A, Pannia E, Froment C, Combes-Soia L. X-linked myotubular myopathy is associated with epigenetic alterations and is ameliorated by HDAC inhibition. Acta neuropathologica. 2022 Sep;144(3):537-63. doi: https://doi.org/10.1007/s00401-022-02468-7

Wakabayashi KI, Okamura M, Tsutsumi S, Nishikawa NS, Tanaka T, Sakakibara I, Kitakami JI, Ihara S, Hashimoto Y, Hamakubo T, Kodama T. The peroxisome proliferator-activated receptor γ/retinoid X receptor α heterodimer targets the histone modification enzyme PR-Set7/Setd8 gene and regulates adipogenesis through a positive feedback loop. Molecular and cellular biology. 2009 Jul 1. doi: https://doi.org/10.1128/MCB.01856-08

Wang B, Gong S, Han L, Shao W, Li Z, Xu J, Lv X, Xiao B, Feng Y. Knockdown of HDAC9 inhibits osteogenic differentiation of human bone marrow mesenchymal stem cells partially by suppressing the MAPK signaling pathway. Clinical Interventions in Aging. 2022 May 12:777-87.

Wang W, Liu Z, Zhang X, Liu J, Gui J, Cui M, Li Y. miR-211-5p is down-regulated and a prognostic marker in bladder cancer. The journal of gene medicine. 2020 Dec;22(12):e3270. doi: https://doi.org/10.1002/jgm.3270

Wong RH, Chang I, Hudak CS, Hyun S, Kwan HY, Sul HS. A role of DNA-PK for the metabolic gene regulation in response to insulin. Cell. 2009 Mar 20;136(6):1056-72. doi: https://doi.org/10.1016/j.cell.2008.12.040

Xie L, Zhang Y, Qu Y, Chai L, Li X, Wang H. Effects of nitrate on development and thyroid hormone signaling pathway during Bufo gargarizans embryogenesis. Chemosphere. 2019 Nov 1;235:227-38. doi: https://doi.org/10.1016/j.chemosphere.2019.06.177

Xiong H, Du W, Zhang YJ, Hong J, Su WY, Tang JT, Wang YC, Lu R, Fang JY. Trichostatin A, a histone deacetylase inhibitor, suppresses JAK2/STAT3 signaling via inducing the promoter-associated histone acetylation of SOCS1 and SOCS3 in human colorectal cancer cells. Molecular carcinogenesis. 2012 Feb;51(2):174-84. doi: https://doi.org/10.1002/mc.20777

Xu G, Li N, Zhang Y, Zhang J, Xu R, Wu Y. MicroRNA-383-5p inhibits the progression of gastric carcinoma via targeting HDAC9 expression. Brazilian Journal of Medical and Biological Research. 2019 Jul 29;52:e8341. doi: https://doi.org/10.1590/1414-431X20198341

Xu L, Wang J, Liu B, Fu J, Zhao Y, Yu S, Shen L, Yan X, Su J. HDAC9 Contributes to Serous Ovarian Cancer Progression through Regulating Epithelial–Mesenchymal Transition. Biomedicines. 2022 Feb 3;10(2):374. doi: https://doi.org/10.3390/biomedicines10020374

Xu WS, Parmigiani RB, Marks PA. Histone deacetylase inhibitors: molecular mechanisms of action. Oncogene. 2007 Aug;26(37):5541-52. doi: https://doi.org/10.1038/sj.onc.1210620

Yan K, Cao Q, Reilly CM, Young NL, Garcia BA, Mishra N. Histone deacetylase 9 deficiency protects against effector T cell-mediated systemic autoimmunity. Journal of Biological Chemistry. 2011 Aug 19;286(33):28833-43. doi: https://doi.org/10.1074/jbc.M111.233932

Yang C, Croteau S, Hardy P. Histone deacetylase (HDAC) 9: versatile biological functions and emerging roles in human cancer. Cellular Oncology. 2021 Oct;44:997-1017. doi: https://doi.org/10.1007/s13402-021-00626-9

Yang C, Rathman JF, Mostrag A, Ribeiro JV, Hobocienski B, Magdziarz T, Kulkarni S, Barton-Maclaren T. High throughput read-across for screening a large inventory of related structures by balancing artificial intelligence/machine learning and human knowledge.

Chemical Research in Toxicology. 2023 Jul 3;36(7):1081-106. doi: https://doi.org/10.1021/acs.chemrestox.3c00062

Yang JD, Hainaut P, Gores GJ, Amadou A, Plymoth A, Roberts LR. A global view of hepatocellular carcinoma: trends, risk, prevention and management. Nature reviews Gastroenterology & hepatology. 2019 Oct;16(10):589-604. doi: https://doi.org/10.1038/s41575-019-0186-y

Yang XJ, Grégoire S. Class II histone deacetylases: from sequence to function, regulation, and clinical implication. Molecular and cellular biology. 2005 Apr 1. doi: https://doi.org/10.1128/MCB.25.8.2873-2884.2005

Yang Y, Bae M, Park YK, Lee Y, Pham TX, Rudraiah S, Manautou J, Koo SI, Lee JY. Histone deacetylase 9 plays a role in the antifibrogenic effect of astaxanthin in hepatic stellate cells. The Journal of nutritional biochemistry. 2017 Feb 1;40:172-7. doi: https://doi.org/10.1016/j.jnutbio.2016.11.003

Yang Z, Zhang L, Liu J, Yang L, Xue H, Bai S, Wang K. PD-L1 combined with HDAC9 is a useful prognostic predictor in hepatocellular carcinoma. Translational Cancer Research. 2021 May;10(5):2305. doi: http://dx.doi.org/10.21037/tcr-20-3415

Zhang CL, McKinsey TA, Chang S, Antos CL, Hill JA, Olson EN. Class II histone deacetylases act as signal-responsive repressors of cardiac hypertrophy. Cell. 2002 Aug 23;110(4):479-88. doi: https://doi.org/10.1016/S0092-8674(02)00861-9

Zhang CL, McKinsey TA, Olson EN. The transcriptional corepressor MITR is a signal-responsive inhibitor of myogenesis. Proceedings of the National Academy of Sciences. 2001 Jun 19;98(13):7354-9. doi: https://doi.org/10.1073/pnas.131198498

Zhang J, Liang Y, Huang X, Guo X, Liu Y, Zhong J, Yuan J. STAT3-induced upregulation of lncRNA MEG3 regulates the growth of cardiac hypertrophy through miR-361-5p/HDAC9 axis. Scientific Reports. 2019 Jan 24;9(1):460. doi: https://doi.org/10.1038/s41598-018-36369-1

Zhang L, Qi M, Chen J, Zhao J, Li L, Hu J, Jin Y, Liu W. Impaired autophagy triggered by HDAC9 in mesenchymal stem cells accelerates bone mass loss. Stem cell research & therapy. 2020 Dec;11:1-6. doi: https://doi.org/10.1186/s13287-020-01785-6

Zhang Y, Yang Y, Yang F, Liu X, Zhan P, Wu J, Wang X, Wang Z, Tang W, Sun Y, Zhang Y. HDAC9-mediated epithelial cell cycle arrest in G2/M contributes to kidney fibrosis in male mice. Nature Communications. 2023 May 25;14(1):3007. doi: https://doi.org/10.1038/s41467-023-38771-4

Zhao J, Gray SG, Greene CM, Lawless MW. Unmasking the pathological and therapeutic potential of histone deacetylases for liver cancer. Expert Review of Gastroenterology & Hepatology. 2019 Mar 4;13(3):247-56. doi: https://doi.org/10.1080/17474124.2019.1568870

Zheng Y, Chen H, Yin M, Ye X, Chen G, Zhou X, Yin L, Zhang C, Ding B. MiR-376a and histone deacetylation 9 form a regulatory circuitry in hepatocellular carcinoma. Cellular Physiology and Biochemistry. 2015 Jan 1;35(2):729-39. doi: https://doi.org/10.1159/000369733

Zhou Y, Peng J, Jiang S. Role of histone acetyltransferases and histone deacetylases in adipocyte differentiation and adipogenesis. European journal of cell biology. 2014 Apr 1;93(4):170-7. doi: https://doi.org/10.1016/j.ejcb.2014.03.001

Zou Y, Gong N, Cui Y, Wang X, Cui A, Chen QI, Jiao T, Dong X, Yang H, Zhang S, Fang F. Forkhead box P1 (FOXP1) transcription factor regulates hepatic glucose homeostasis. Journal of Biological Chemistry. 2015 Dec 18;290(51):30607-15. doi: https://doi.org/10.1074/jbc.M115.681627

9. Publications

List of publications:

1. **Das, T**., Khatun, S., Jha, T., & Gayen, S. (2024). HDAC9 as a Privileged Target: Reviewing its Role in Different Diseases and Structure-activity Relationships (SARs) of its Inhibitors. Mini-Reviews in Medicinal Chemistry (Vol. 24, Issue 7, pp. 767–784). https://doi.org/10.2174/0113895575267301230919165827 (**IF: 3.6**)
2. **Das, T**., Bhattacharya, A., Jha, T., & Gayen, S. (2024). Exploration of Fingerprints and Data Mining-based Prediction of Some Bioactive Compounds from Allium sativum as Histone Deacetylase 9 (HDAC9) Inhibitors. Current Computer-Aided Drug Design (Vol. 20).
   https://doi.org/10.2174/0115734099282303240126061624 (**IF: 1.7)**
3. Dawn, S., Manna, P., **Das, T**., Kumar, P., Ray, M., Gayen, S., & Amin, SA. (2024). Exploring fingerprints for novel antidiabetes therapeutics related to Peroxisome Proliferator-Activated Receptor Gamma (PPARγ) modulators: Machine learning-based chemometric modeling. Computational Biology and Chemistry. (Vol. 112, pp. 108142).
   https://doi.org/10.1016/j.compbiolchem.2024.108142 (**IF: 2.6)**
4. Dasgupta, I., **Das, T**., Das, B., & Gayen, S. (2024). Identification of structural features of engineered nano metal oxides for their uptake in human cell lines through ML Based Classification QSAR study. The Beilstein Journal of Nanotechnology. (Vol. 15, pp. 909-924).
   https://doi.org/10.3762/bjnano.15.75 (**IF: 2.6)**

Publication-1

Send Orders for Reprints to reprints@benthamscience.net

Mini-Reviews in Medicinal Chemistry, 2024, *24*, 767-784

REVIEW ARTICLE

HDAC9 as a Privileged Target: Reviewing its Role in Different Diseases and Structure-activity Relationships (SARs) of its Inhibitors

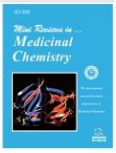

Totan Das[1,#], Samima Khatun[1,#], Tarun Jha[2,*] and Shovanlal Gayen[1,*]

[1]*Department of Pharmaceutical Technology, Laboratory of Drug Design and Discovery, Jadavpur University, Kolkata, 700032, India;* [2]*Department of Pharmaceutical Technology, Natural Science Laboratory, Division of Medicinal and Pharmaceutical Chemistry, Jadavpur University, Kolkata, 700032, India*

ARTICLE HISTORY

Received: June 15, 2023
Revised: July 17, 2023
Accepted: August 11, 2023

DOI:
10.2174/0113895575267301230919165827

Abstract: HDAC9 is a histone deacetylase enzyme belonging to the class IIa of HDACs which catalyses histone deacetylation. HDAC9 inhibit cell proliferation by repairing DNA, arresting the cell cycle, inducing apoptosis, and altering genetic expression. HDAC9 plays a significant part in human physiological system and are involved in various type of diseases like cancer, diabetes, atherosclerosis and CVD, autoimmune response, inflammatory disease, osteoporosis and liver fibrosis. This review discusses the role of HDAC9 in different diseases and structure-activity relationships (SARs) of various hydroxamate and non-hydroxamate-based inhibitors. SAR of compounds containing several scaffolds have been discussed in detail. Moreover, structural requirements regarding the various components of HDAC9 inhibitor (cap group, linker and zinc-binding group) has been highlighted in this review. Though, HDAC9 is a promising target for the treatment of a number of diseases including cancer, a very few research are available. Thus, this review may provide useful information for designing novel HDAC9 inhibitors to fight against different diseases in the future.

Keywords: Epigenetic, cancer, HDAC9 inhibitor, selectivity, structure-activity relationships, SARs.

1. INTRODUCTION

An enzyme class known as histone deacetylases (HDACs) eliminate acetyl groups from histone's N-acetyl lysine amino acid enabling the DNA to be more tightly wrapped by the histones [1]. These epigenetic regulators control different cellular activities like cell division, migration, proliferation, and differentiation and cell death [2, 3]. They work by reversing the open state of chromatin when they interact with histones. Due to their ability to change DNA and histone structures, epigenetic alterations play a crucial part in gene regulation. HDACs are primarily implicated in gene silencing because their activity causes condensation of chromatin into a transcriptionally suppressed shape [4-6]. To regulate a number of biological processes, HDACs interact with both histone and non-histone targets [7]. HDACs can be divided into five main groups based on how closely their sequences resemble the original yeast enzymes. Class I HDACs include HDAC1, HDAC2, HDAC3 and HDAC8; class IIa HDACs include HDAC4, HDAC5, HDAC7, and HDAC9; and class IIb HDACs include HDAC6, HDAC10 [8-10]. Class III HDACs include sirtuins 1-7 that are NAD+ dependent. The only HDAC in class IV is HDAC11 [11, 12].

Out of all the aforementioned categories of HDACs, Class IIa HDACs standout from other HDACs due to their distinct features [13]. The interaction with the myocyte enhancer-binding factor 2 (MEF2) is required for Class IIa HDACs to be recruited to specific genomic loci [14-16]. The N-terminus of Class IIa HDACs comprises of conserved serine residues that are phosphorylated in response to signals, causing the enzymes to be exported into the nucleus and releasing their substrates. Class IIa HDACs serve as vital enzyme for the development and differentiation of particular tissues and organs inside the organism, which is one of their most significant characteristics [13]. Currently, HDAC9 has no crystal structure. However, the crystal structure of HDAC9/MEF2/DNA complex has been solved (Pdb id 1TQE) [17]. According to the crystal structure, HDAC9 binds to the MEF2 dimer's hydrophobic groove and inhibit their transcriptional activity [18]. The absence of a suitable and appropriate crystal structure of HDAC9 in inhibitor bound form is impeding the generation of HDAC9 isoform-specific inhibitors [19].

Human HDAC9 is extensively expressed in the myocardium [20]. It is generally found in the skeletal muscles and

*Address correspondence to these authors at the Department of Pharmaceutical Technology, Laboratory of Drug Design and Discovery, Jadavpur University, Kolkata, 700032, India; E-mail: shovanlal.gayen@gmail.com and Department of Pharmaceutical Technology, Natural Science Laboratory, Division of Medicinal and Pharmaceutical Chemistry, Jadavpur University, Kolkata 700032; E-mail: tjupharm@yahoo.com
#*These authors contributed equally to this work.*

1875-5607/24 $65.00+.00

Publication-2

Send Orders for Reprints to reprints@benthamscience.net

Current Computer-Aided Drug Design, XXXX, XX, 0-0

RESEARCH ARTICLE

Exploration of Fingerprints and Data Mining-based Prediction of Some Bioactive Compounds from *Allium sativum* as Histone Deacetylase 9 (HDAC9) Inhibitors

Totan Das[1], Arijit Bhattacharya[1], Tarun Jha[2] and Shovanlal Gayen[1,*]

[1]*Laboratory of Drug Design and Discovery, Department of Pharmaceutical Technology, Jadavpur University, Kolkata 700032, India;* [2]*Natural Science Laboratory, Division of Medicinal and Pharmaceutical Chemistry, Department of Pharmaceutical Technology, Jadavpur University, Kolkata 700032, India*

ARTICLE HISTORY

Received: October 03, 2023
Revised: January 12, 2024
Accepted: January 18, 2024

DOI:
10.2174/0115734099282303240126061624

Abstract: ***Background*:** Histone deacetylase 9 (HDAC9) is an important member of the class IIa family of histone deacetylases. It is well established that over-expression of HDAC9 causes various types of cancers including gastric cancer, breast cancer, ovarian cancer, liver cancer, lung cancer, lymphoblastic leukaemia, *etc*. The important role of HDAC9 is also recognized in the development of bone, cardiac muscles, and innate immunity. Thus, it will be beneficial to find out the important structural attributes of HDAC9 inhibitors for developing selective HDAC9 inhibitors with higher potency.

***Methods*:** The classification QSAR-based methods namely Bayesian classification and recursive partitioning method were applied to a dataset consisting of HADC9 inhibitors. The structural features strongly suggested that sulphur-containing compounds can be a good choice for HDAC9 inhibition. For this reason, these models were applied further to screen some natural compounds from *Allium sativum*. The screened compounds were further accessed for the ADME properties and docked in the homology-modelled structure of HDAC9 in order to find important amino acids for the interaction. The best-docked compound was considered for molecular dynamics (MD) simulation study.

***Results*:** The classification models have identified good and bad fingerprints for HDAC9 inhibition. The screened compounds like ajoene, 1,2 vinyl dithiine, diallyl disulphide and diallyl trisulphide had been identified as compounds having potent HDAC9 inhibitory activity. The results from ADME and molecular docking study of these compounds show the binding interaction inside the active site of the HDAC9. The best-docked compound ajoene shows satisfactory results in terms of different validation parameters of MD simulation study.

***Conclusion*:** This *in-silico* modelling study has identified the natural potential lead (s) from *Allium sativum*. Specifically, the ajoene with the best *in-silico* features can be considered for further *in-vitro* and *in-vivo* investigation to establish as potential HDAC9 inhibitors.

Keywords: Histone deacetylase 9 (HDAC9), bayesian classification, recursive partitioning tree, *Allium sativum*, molecular docking, molecular dynamics simulation.

1. INTRODUCTION

The histone deacetylase (HDAC) family is linked to a wide range of epigenetic diseases and disorders *via* the deacetylation of nucleosomal histone proteins [1]. Epigenetic modifications are important in gene regulation [2]. The HDACs, also known as lysine deacetylases or 'remover enzymes', are Zn^{2+} or NAD^{+} dependent enzymes that are responsible for the N-terminal lysine deacetylation of nuclear histone proteins. The HDAC enzymes are classified into four major classes based on structural and functional properties: class I (HDAC1, HDAC2, HDAC3, and HDAC8), class IIa (HDAC4, HDAC5, HDAC7 and HDAC9), class IIb (HDAC6, and HDAC10), class III (SIRT1-7) and class IV (HDAC11) [3].

HDAC9 comes under the class IIa of the HDACs family [4]. There are several alternatively spliced isoforms of HDAC9. One of these isoforms is histone deacetylase-related protein or myocyte enhancer-binding factor 2-interacting transcriptional repressor (MITR), which lacks an

*Address correspondence to this author at the Laboratory of Drug Design and Discovery, Department of Pharmaceutical Technology, Jadavpur University, Kolkata 700032, India; E-mails: shovanlal.gayen@gmail.com and sgayen.pharmacy@jadavpuruniversity.in

1573-4099/XX $65.00+.00

Publication-3

BEILSTEIN JOURNAL OF NANOTECHNOLOGY

Identification of structural features of surface modifiers in engineered nanostructured metal oxides regarding cell uptake through ML-based classification

Indrasis Dasgupta, Totan Das, Biplab Das and Shovanlal Gayen*

Full Research Paper

Open Access

Address:
Laboratory of Drug Design and Discovery, Department of Pharmaceutical Technology, Jadavpur University, Kolkata 700032, India

Email:
Shovanlal Gayen* - shovanlal.gayen@gmail.com

* Corresponding author

Keywords:
Bayesian classification; cellular uptake; machine learning; nanoparticles (NPs)

Beilstein J. Nanotechnol. **2024,** *15,* 909–924.
https://doi.org/10.3762/bjnano.15.75

Received: 22 March 2024
Accepted: 01 July 2024
Published: 22 July 2024

This article is part of the thematic issue "Nanoinformatics: spanning scales, systems and solutions".

Guest Editor: I. Lynch

Abstract

Nanoparticles (NPs) are considered as versatile tools in various fields including medicine, electronics, and environmental science. Understanding the structural aspects of surface modifiers in nanoparticles that govern their cellular uptake is crucial for optimizing their efficacy and minimizing potential cytotoxicity. The cellular uptake is influenced by multiple factors, namely, size, shape, and surface charge of NPs, as well as their surface functionalization. In the current study, classification-based ML models (i.e., Bayesian classification, random forest, support vector classifier, and linear discriminant analysis) have been developed to identify the features/fingerprints that significantly contribute to the cellular uptake of ENMOs in multiple cell types, including pancreatic cancer cells (PaCa2), human endothelial cells (HUVEC), and human macrophage cells (U937). The best models have been identified for each cell type and analyzed to detect the structural fingerprints/features governing the cellular uptake of ENMOs. The study will direct scientists in the design of ENMOs of higher cellular uptake efficiency for better therapeutic response.

Introduction

In recent years, the rapid advancement of nanotechnology has led to the widespread utilization of engineered nanostructured metal oxides (ENMOs) in various industrial and biomedical applications [1]. Nanoparticles (NPs) are described by the International Organization for Standardization as structures characterized by one, two, or three dimensions within the range of 1 to 100 nm [2]. The diminutive size of nanoparticles contributes to a significantly high surface area with respect to volume, resulting in enhanced reactivity, improved stability, and augmented functionality. In the field of nanomaterials, ENMOs are a notable subset. These nanoparticles consist of metal elements bonded with oxygen in intricate structures [3,4]. They exhibit

Publication-4

Computational Biology and Chemistry 112 (2024) 108142

Contents lists available at ScienceDirect

Computational Biology and Chemistry

journal homepage: www.elsevier.com/locate/cbac

Exploring fingerprints for antidiabetic therapeutics related to peroxisome proliferator-activated receptor gamma (PPARγ) modulators: A chemometric modeling approach

Subham Dawn [a], Prabir Manna [a], Totan Das [b], Prabhat Kumar [c], Moumita Ray [a], Shovanlal Gayen [b,*], Sk Abdul Amin [a,*]

[a] Department of Pharmaceutical Technology, JIS University, 81, Nilgunj Road, Agarpara, Kolkata, West Bengal 700109, India
[b] Laboratory of Drug Design and Discovery, Department of Pharmaceutical Technology, Jadavpur University, Kolkata, West Bengal 700032, India
[c] Jagtarni Upgraded Senior Secondary School, Khamhar, Samastipur, Bihar 851128, India

ARTICLE INFO

Keywords:
Diabetes mellitus
PPARγ modulators
Recursive partitioning
Molecular docking
MD simulation
Fingerprint

ABSTRACT

This study demonstrated the correlation of molecular structures of Peroxisome proliferator-activated receptor gamma (PPARγ) modulators and their biological activities. Bayesian classification, and recursive partitioning (RP) studies have been applied to a dataset of 323 PPARγ modulators with diverse scaffolds. The results provide a deep insight into the important sub-structural features modulating PPARγ. The molecular docking analysis again confirmed the significance of the identified sub-structural features in the modulation of PPARγ activity. Molecular dynamics simulations further underscored the stability of the complexes formed by investigated modulators with PPARγ. Overall, the integration of many computational approaches unveiled key structural motifs essential for PPARγ modulatory activity that will shed light on the development of effective modulators in the future.

1. Introduction

Diabetes mellitus (DM) is a metabolic as well as hormonal disorder in our body due to rising glucose levels in the blood. This condition may arises because the pancreatic beta cells unable to produce substantial amounts of insulin (American Diabetes Association, 2009; Carpenter and Coustan, 1982). To improve glucose metabolism and achieve normalization of blood glucose levels, individuals with diabetes may require insulin, which can be administered either through direct injection of recombinant peptides or through the body's endogenous production (Wilcox, 2005). A comprehensive approach involving lifestyle adjustments and pharmacological interventions is essential to effectively manage diabetes and mitigate the long-term risks of both macrovascular and microvascular complications. Oral hypoglycemic agents play a crucial role in enhancing glycemic control through diverse mechanisms, such as insulin secretagogues by promoting insulin secretion and insulin sensitizers by modifying insulin sensitivity and reducing the need for insulin by inhibiting glucose absorption (Sheehan, 2003).

Recently, the peroxisome proliferator-activated receptor (PPAR) subfamily of nuclear receptors has emerged as a significant target in pharmacology. Activation of these receptors has shown promise in normalizing metabolic dysfunctions and mitigating certain cardiovascular issues associated with type 2 diabetes (Jay and Ren, 2007) PPARα agonists like fibrates are effective in addressing dyslipidemia, while PPARγ agonists namely thiazolidinediones serve as insulin sensitizers, enhancing insulin resistance management in type 2 diabetes patients. However, due to limitations in potency and potential side effects associated with PPAR agonists, coupled with the rising incidence of type 2 diabetes, there is an urgent need for the advancement of selective PPAR modulators that offer better clinical effectiveness (Gross and Staels, 2007). Over the past decade, there has been significant research attention directed towards the peroxisome proliferator-activated receptor gamma (PPARγ), as its ligands have proven to be potent insulin sensitizers utilized in type 2 diabetes therapy. Elevated levels of circulating free fatty acids and non-adipose tissue lipid accumulation are linked to insulin resistance development. PPARγ activating ligands do this by promoting fatty acid storage in adipose depots and regulating the expression of adipocyte-secreted hormones (Fig. 1) that play a role in glucose homeostasis (Rangwala and Lazar, 2004).

In humans, three subtypes of PPAR (PPARα, PPARδ, and PPARγ)

* Corresponding authors.
E-mail addresses: shovanlal.gayen@gmail.com (S. Gayen), pharmacist.amin@gmail.com (S.A. Amin).

https://doi.org/10.1016/j.compbiolchem.2024.108142
Received 7 May 2024; Received in revised form 28 June 2024; Accepted 30 June 2024
Available online 2 July 2024